THE ROLE OF SULFONATED STEROIDS AND PHARMACEUTICAL COMPOUNDS IN STEROID HORMONE BIOSYNTHESIS

kumulative Dissertation zur Erlangung des Grades Doktor der Naturwissenschaften (Dr. rer. nat.)
der Naturwissenschaftlich-Technischen Fakultät III
Chemie, Pharmazie, Bio- und Werkstoffwissenschaften
der Universität des Saarlandes

Diplom Biologe
Jens Neunzig
Saarbrücken im Juni 2014

Tag des Kolloquiums:	04.12.2014
Dekan:	Prof. Dr. Dirk Bähre
Berichterstatter:	Prof. Dr. Rita Bernhardt
	Prof. Dr. Stefan A. Wudy
Vorsitz:	Prof. Dr. Uli Müller
Akad. Mitarbeiter:	Dr. Björn Becker

“An einem kleinen Muster können wir oft das ganze Stück beurteilen.”

Miguel de Cervantes-Saavedra (1547 – 1616)

Die Arbeiten für diese Dissertation wurden in der Arbeitsgruppe Biochemie der Universität des Saarlandes unter der Leitung von Prof. Dr. Rita Bernhardt von Juni 2010 bis April 2014 durchgeführt

Mein besonderer Dank gilt:

..Frau Prof. Dr. Rita Bernhardt für die Möglichkeit, in ihrem Institut an diesem interessanten Thema zu forschen. Sie stand mir stets mit großer Geduld und Verständnis beratend zur Seite

..Herrn Prof. Dr. Stefan Wudy für die freundliche Übernahme des Zweitgutachtens und die Kooperation mit seinem Analytiklabor

..Herrn Dr. Frank Hannemann für die gute Arbeitsatmosphäre und seine große Diskussionsbereitschaft zu fachlichen Themen

..Herrn Dipl. Biol. Adrian Gerber für das Korrekturlesen, die Bereitschaft seine exzellenten Englischkenntnisse mit mir zu teilen, sowie für die vielen interessanten Gespräche

..Herrn Azzam Mosa für seine Unterstützung bei den Proteinreinigungen

außerdem möchte ich mich für die massenspektrometrischen Messungen bei Alberto Sánchez Guijo bedanken, sowie für seine ausführlichen Erklärungen zu diesem Thema

weiter möchte ich mich bedanken bei:

..der gesamten Arbeitsgruppe des Instituts für Biochemie an der Universität des Saarlandes für das nette Arbeitsumfeld und gegenseitige Unterstützung

..dem DFG FOR1369 Forscherteam, für die Kooperationsbereitschaft und den vielen Sitzungen aus denen hochinteressante wissenschaftliche Ideen herauskamen

ganz herzlich bedanke ich mich bei:

..meiner Frau Ina für ihre nicht enden wollende Geduld mit mir, für die vielen fachlichen Gespräche und Ratschläge und nicht zuletzt für ihre große Hilfe bei dem Erstellen dieser Arbeit

..meinen Kindern Luana und Elina für ihre Fähigkeit, mir meinen Kopf frei zu machen und mir das Gefühl zu geben wichtig zu sein

..meinen Schwiegereltern Maria und Frank Kielinger und meiner Schwägerin Laura für ihre stete Bereitschaft, da einzuspringen wo Not am Manne ist

..meiner Mutter Ursel, für ihre große Unterstützung mit Haus, Hund und Kind

Scientific contributions

This work is based on 3 original publications, which are reproduced in chapter 2. They are printed with kind permission of PLoSONE (2.1: Neunzig et al., 2014), JSBMB (2.2: Neunzig et al., 2014) and Wolters Kluwer Health Lippincott Williams & Wilkins (2.3: Shanmugasundararaj et al., 2013).

2.1: Neunzig et al. (2014)

The author has expressed and purified CYP11A1 used in this study and has conducted all of the laboratory work and data interpretation for the generation of the published results (HPLC analyses, spectroscopic studies, bia-core experiments and interpretation of the data). The author also contributed to writing the manuscript.

2.2: Neunzig et al. (2014)

The author has expressed and purified CYP17A1 used in this study and has conducted all of the laboratory work and data interpretation for the generation of the published results (HPLC analyses, spectroscopic studies and interpretation of the data) except for the mass-spectrometry which was carried out by Alberto Sanchez-Guijo in the Steroid Research & Mass Spectrometry Unit (Prof. Wudy) in Giessen. The author also contributed to writing the manuscript.

2.3: Shanmugasundararaj et al. (2013)

The author planned and conducted the spectrometric experiments and contributed to the methodological section reported in this publication. The results obtained from these experiments revealed that etomidate and carboetomidate differentially bind to CYP11B1, elucidating the distinct inhibitory effects of these two anesthetic compounds.

CONTENT

ABSTRACT

This work provides new insights into the effects of sulfonated steroids and pharmaceutical compounds on cytochromes P450 involved in the steroid hormone biosynthesis.

At first, the CYP11A1 dependent side-chain cleavage of cholesterol was examined under the influence of DHEAS. An augmentation of the catalytic efficiency (75%) of CYP11A1 in the presence of DHEAS was demonstrated, which was shown to be a result of a tighter binding of CYP11A1 with its redox partner Adx and of a better affinity for its substrate.

Further, it was investigated whether pregnenolone sulfate (PregS) constitutes a starting compound for a potential steroidogenic pathway for sulfonated steroids. The authors provide evidence that CYP17A1 hydroxylates PregS at position C17, although no subsequent lyase-reaction could be induced in the presence of cytochrome b_5.

Taken together, these findings provide evidence that sulfonated steroids play a more important role in the steroid metabolism of mammals than previously assumed.

In addition, it was possible to elucidate the underlying mechanism of the unequal inhibitory effect of the anesthetic compounds etomidate and carboetomidate on the cortisol producing enzyme CYP11B1 at a molecular level. Both were shown to interact differently with CYP11B1, which was demonstrated by spectroscopic and docking studies, as well as substrate conversion experiments.

ZUSAMMENFASSUNG

Diese Arbeit gewährt neue Einblicke in die Wirkungsweise sulfonierter Steroide und pharmazeutischer Substanzen auf Cytochrome P450, die an der Steroidhormonbiosynthese beteiligt sind.

Zunächst wurde die CYP11A1-abhängigen Seitenkettenspaltung von Cholesterin unter Einfluss von DHEAS untersucht. Es konnte eine Steigerung der katalytischen Effizienz (75%) des CYP11A1 in Anwesenheit von DHEAS nachgewiesen werden, die auf eine stärkere Bindung des CYP11A1 mit seinem Redoxpartner Adx, sowie einer erhöhten Affinität des Enzyms zu seinem Substrat zurückzuführen war.

Des Weiteren wurde untersucht, ob Pregnenolonsulfat (PregS) eine Ausgangssubstanz für einen Stoffwechselweg für sulfonierte Steroide darstellt. Es konnte gezeigt werden, dass CYP17A1 PregS an Position C17 hydroxyliert, wobei auch in Anwesenheit von Cytochrom b_5 keine Lyaseaktivität induziert werden konnte.

Zusammengefasst zeigen diese Ergebnisse, dass sulfonierte Steroide eine bedeutendere Rolle im Steroidmetabolismus spielen als bisher angenommen.

Ferner wurde der zugrundeliegende Mechanismus für den unterschiedlichen inhibitorischen Effekt der Anesthetika Etomidat und Carboetomidat auf das Kortisol bildende Enzym CYP11B1 auf molekularer Ebene aufgeklärt. Es konnte durch spektroskopische Versuche, Dockingstudien, sowie Substratumstatzexperimente gezeigt werden, dass beide Substanzen mit dem CYP11B1 auf unterschiedliche Weise interagieren.

1 GENERAL PART

1.1 INTRODUCTION

CYTOCHROMES P450

Cytochromes P450 (CYPs) are heme-containing proteins, which can be found virtually ubiquitous in organisms from all biological kingdoms. They are extremely versatile enzymes catalyzing a huge variety of reactions, such as hydroxylations, N-, O- and S-dealkylations, sulphoxidations, epoxidations, deaminations, desulphurations, dehalogenations, peroxidations, and N-oxide reductions [1]. CYPs are involved in many biological processes. They contribute to the biotransformation of drugs and xenobiotics, are involved in the synthesis of steroid hormones, fatty acids, eicosanoids and bile acids, are essential for the metabolism of vitamin D, convert alkanes, terpenes and aromatic compounds, and participate in the biodegradation of herbicides and insecticides [2]. So far (July 2014), 21,039 CYP sequences have been identified[1]. To classify the huge number of CYPs, a systematic nomenclature was introduced by Nebert *et al.* in 1989 [3]: the abbreviation CYP stands for **cy**tochrome **P**450. The number after the CYP indicates the membership to a family (>40 % identity of amino acid sequence is required to belong to the same family). The subfamiliy (>55% identity of amino acid sequence is required to belong to the same subfamily) is displayed by a letter. Then, again a number indicates the corresponding isoenzyme, as shown in Figure 1.

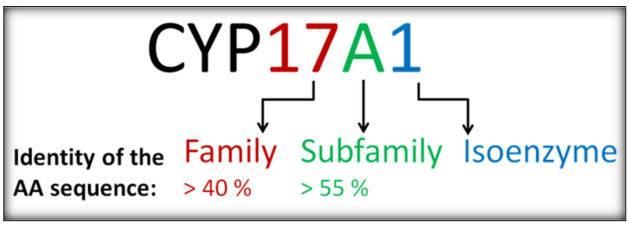

FIGURE 1: NOMENCLATURE OF CYPS EXEMPLIFIED BY *CYP17A1*.

CYPs were first discovered independently by Klingenberg and Garfinkel in the late 1950s [4,5]. They examined liver microsomes from rats and pigs, observing a red pigment with an absorption peak at 450 nm in the CO-difference spectrum. But not until 1964 these pigments were identified as heme-containing proteins by Omura and Sato [6], with an iron(III)-ion bound protoporphyrin XI as prosthetic group. Due to their characteristic absorption maximum, they were aptly termed 'Cytochromes P450'. This particular absorbance property results from the binding of the fifth ligand of the heme-iron [7], which is the thiolate group of a conserved cysteine. Thus, CYPs are categorized as heme-thiolate proteins [8]. The general reaction catalyzed by cytochromes P450 is shown in Figure 2.

[1] http://drnelson.uthsc.edu/CytochromeP450.html

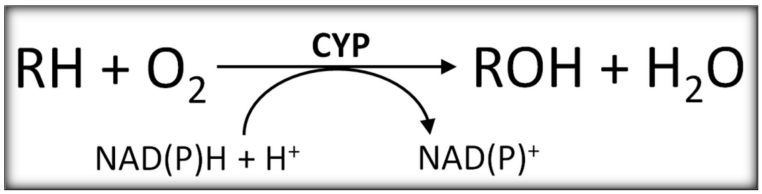

FIGURE 2: GENERAL REACTION MECHANISM OF CYPS.

An oxygen atom, delivered from molecular oxygen, is inserted into an aliphatic or aromatic compound, while the second oxygen atom is reduced to water. CYPs are classified as external monooxygenases, as they require electrons commonly provided by NAD(P)H via electron transfer partners to catalyze this reaction. Depending on their cellular localization and the type of electron transfer chain, CYPs are assigned to different classes of which ten have been described so far [2]. In mammals only two exist: the mitochondrial class I and the microsomal class II cytochrome P450 systems (Figure 3). The mitochondrial CYPs are arranged at the inner mitochondrial membrane. The electrons needed to carry out their hydroxylation reactions are transferred from NADPH via a FAD containing ferredoxin/adrenodoxin reductase (AdR) and an iron-sulphur containing ferredoxin/adrenodoxin (Adx). In case of the microsomal CYPs, which are attached to the endoplasmatic reticulum (ER), the electrons are delivered from NADPH through a FAD and FMN containing NADPH-dependent oxidoreductase (CPR).

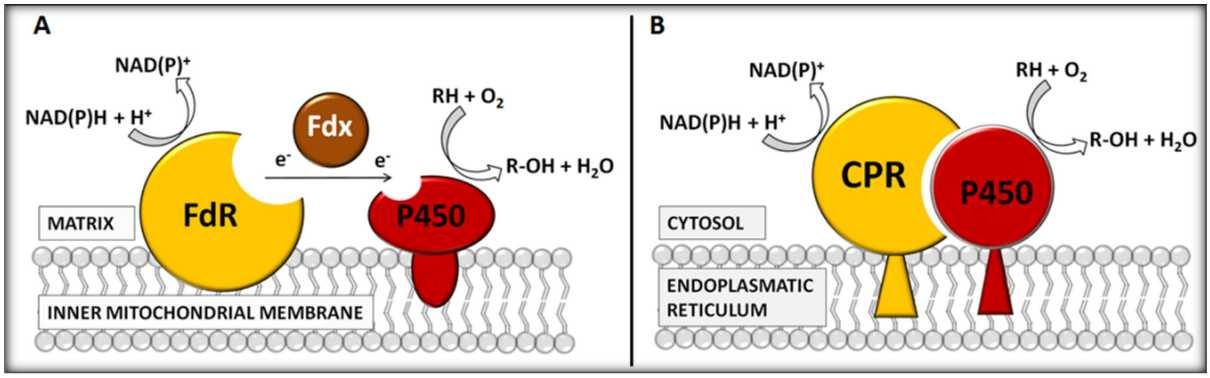

FIGURE 3: SCHEME OF MITOCHONDRIAL AND MICROSOMAL CYOTOCHROME P450 REDOX SYSTEMS. A: CLASS I MITOCHONDRIAL SYSTEM TRANSFERRING ELECTRONS FROM NADPH VIA ADR AND ADX TO THE CYPS. B: CLASS II MICROSOMAL SYSTEM TRANSFERRING ELECTRONS FROM NADPH VIA CPR TO THE CYPS.

Although the sequence homology between different CYPs can be less than 20 %, their three-dimensional structure remains strongly conserved. The variable regions are formed by the flexible substrate recognition sites and enable CYPs to utilize an extreme diverse range of different substrates and to catalyze a big variety of reactions [9].

STEROID HORMONE BIOSYNTHESIS

In mammals steroid hormones carry out multiple physiological actions and are indispensable for a normal development and reproduction. Their synthesis takes place in steroidogenic organs or tissues like the gonads, testes, adrenal gland or the brain. In a series of enzymatic

reactions involving six CYPs and three hydroxysteroid dehydrogenases (HSDs), mineralo- and glucocorticoids as well as sex hormones are generated (Figure 4).

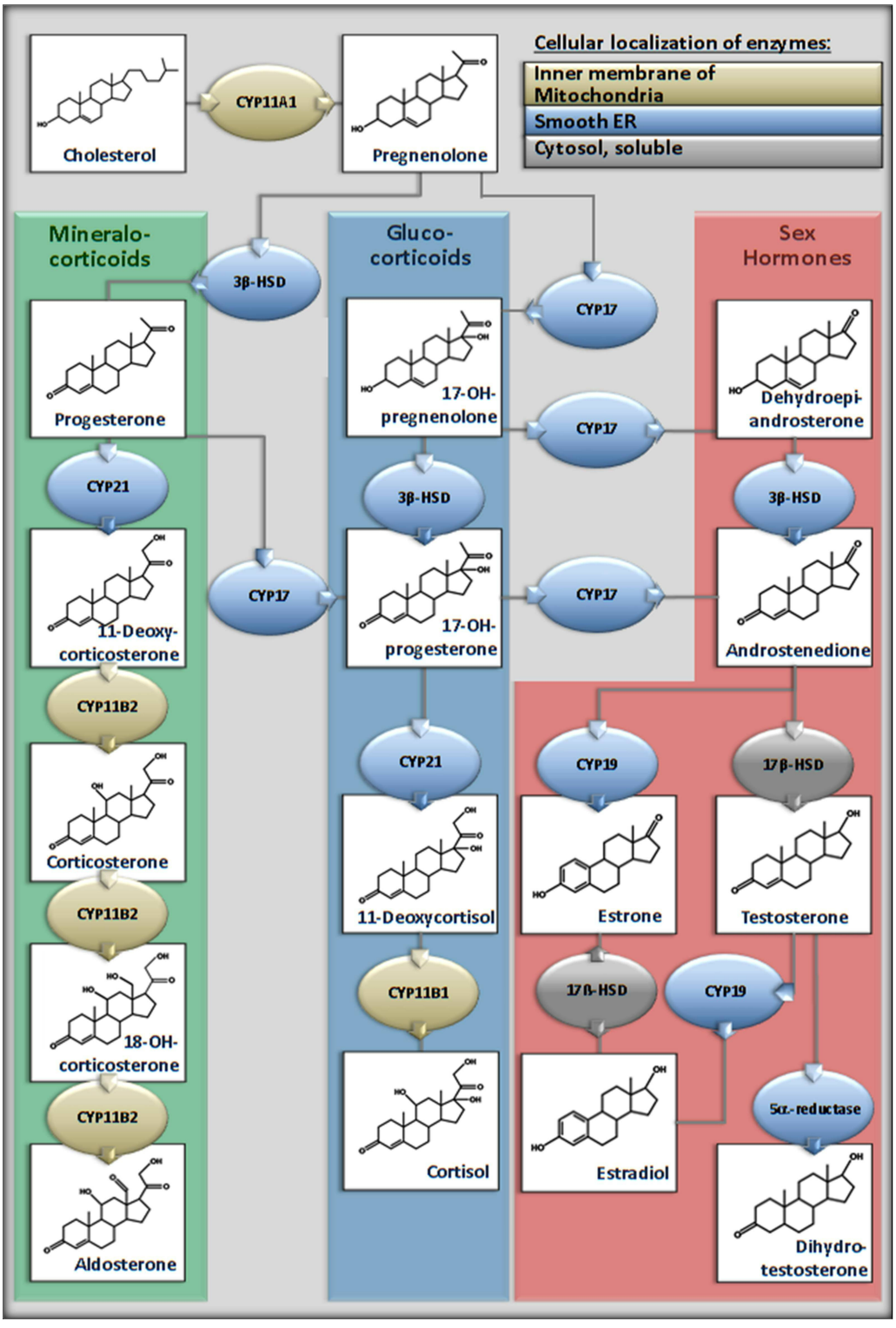

FIGURE 4: STEROID HORMONE BIOSYNTHESIS. IN A CASCADE OF REACTIONS, WHERE SIX CYPS AND THREE HSDS PARTICIPATE, MINERALOCORTICOIDS, GLUCOCORTICOIDS AND SEX HORMONES ARE FORMED.

In the steroidogenesis, mitochondrial (CYP11A1, CYP11B1 and CYP11B2) as well as microsomal (CYP17A1, CYP21A2 and CYP19) CYPs participate. The significance of this compartmentalization on the rate of steroid production and the balance of different steroids is not fully understood so far. In 2012 Nguyen et al. used mathematical modeling to

demonstrate that this localization in different organelles of a cell generates a cellular steroid gradient and can influence the balance of the different steroid products [10], thus providing a regulatory mechanism.
The first enzymatic and rate-limiting step of the steroid hormone biosynthesis constitutes the CYP11A1 dependent side-chain cleavage of cholesterol (C), yielding pregnenolone (Preg), which is the precursor of mineralo- and glucocorticoids, as well as the sex hormones.

MINERALOCORTICOIDS

The mineralocorticoid pathway is initiated by the conversion of Preg by 3β-HSD, which oxidizes the 3-hydroxyl group to a keto group and moves the double bond from C5 to C4 through an isomerase reaction. The formed product progesterone (Prog) is an important progestagen involved in embryogenesis, female menstrual cycle and pregnancy and, moreover, it serves as substrate for CYP21A2, which hydroxylates Prog at position C21 yielding 11-deoxycorticosterone (DOC). Via the two intermediates, corticosterone (B) and 18OH-corticosterone (18OH-B), DOC is converted to aldosterone (Aldo) through two hydroxylation and one oxidation steps. Aldo, the main mineralocorticoid, regulates the blood- and water-homeostasis through modification of the sodium channels in the kidney. Thereby, uptake of sodium and water in the kidney and secretion of potassium occurs, leading to an increased blood volume and thus to an increased blood pressure. The production of mineralocorticoids is regulated via the renin-angiotensin-aldosterone-system (RAAS), as shown in Figure 5 [11].

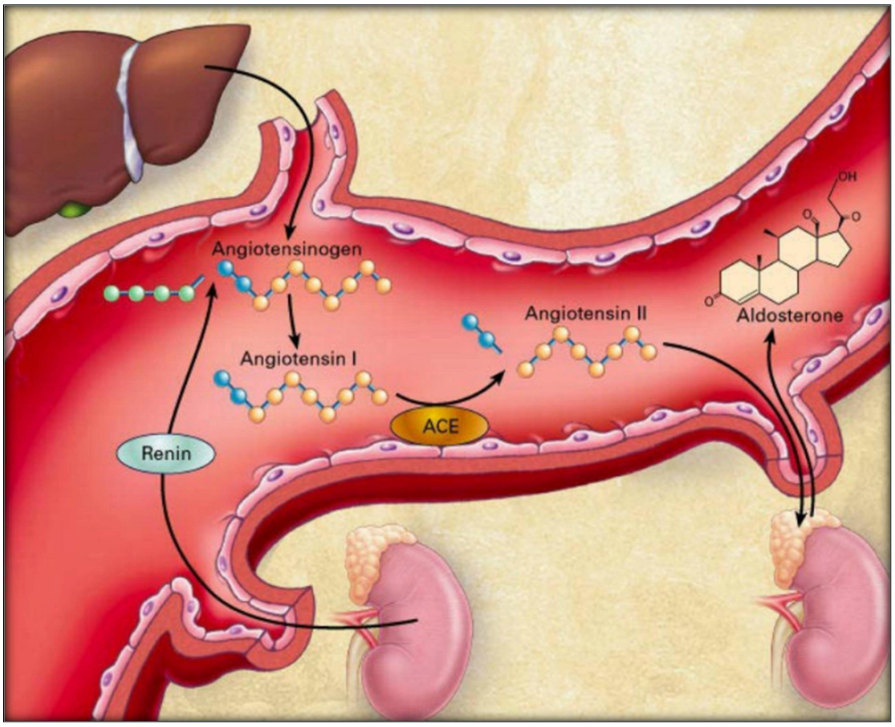

FIGURE 5: SCHEMATIC OVERVIEW OF THE RAAS: RENIN IS RELEASED BY THE KIDNEY. ANGIOTENSINOGEN IS CLEAVED BY RENIN, YIELDING ANGIOTENSIN I, WHICH IS CONVERTED TO ANGIOTENSIN II BY ANGIOTENSIN-CONVERTING ENZYME. ANGIOTENSIN II STIMULATES THE ADRENAL GLAND TO RELEASE ALDOSTERONE [11].

In mammals, low blood volume stimulates the kidney to release renin directly into the circulation. This enzyme converts the peptide hormone angiotensinogen, which is secreted by the liver, into angiotensin I. Subsequently, angiotensin I, which serves as substrate for the angiotensin-converting enzyme (ACE), is converted to angiotensin II. The latter acts on the adrenal cortex, stimulating Aldo secretion and, thus, increasing blood volume.

GLUCOCORTICOIDS

The pathway for the synthesis of glucocorticoids starts with the CYP17A1-dependent hydroxylation of Preg at position C17 (Figure 4). The resulting product 17OH-pregnenolone (17OH-Preg) is further metabolized to 17OH-progesterone (17OH-Preg) by 3β-HSD. 17OH-Prog can also be formed from Prog via a 17-hydroxylation by CYP17A1. Afterwards, this steroid metabolite is converted to 11-deoxycortisol (RSS) through a hydroxylation at C21 by CYP21A2, which is then transformed into cortisol (F) by CYP11B1, catalyzing a hydroxylation at position C11. F, the main glucocorticoid is released in response to stress in mammals and possesses a wide spectrum of functions. It is involved in the stimulation of the gluconeogenesis in the liver to increase the blood sugar and has a catabolic effect on fat and protein metabolism. Cortisol availability is regulated through the hypothalamic-pituitary-adrenal (HPA) axis as shown in Figure 6.

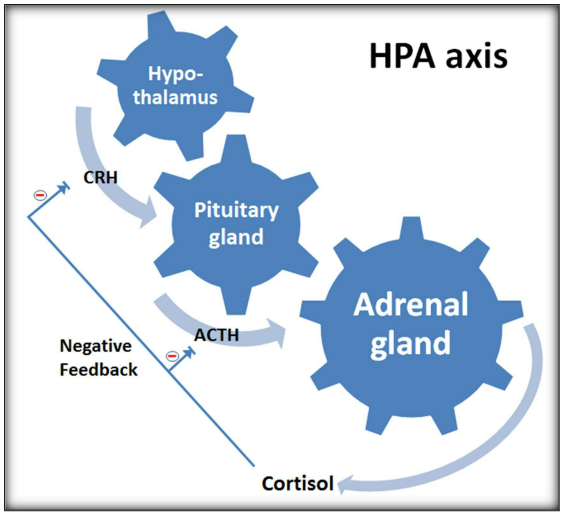

FIGURE 6: SCHEME OF THE HPA AXIS: STRESS INDUCES THE RELEASE OF THE *CORTICOTROPIN RELEASING* HORMONE (CRH) FROM THE HYPOTHALAMUS. CRH STIMULATES THE PITUITARY GLAND TO SECRETE THE ADRENOCORTICOTROPIC HORMONE (ACTH), WHICH STIMULATES THE ADRENAL GLAND TO PRODUCE CORTISOL.

Stress, illness, physical activity, low cortisol levels and the circadian rhythm stimulate the hypothalamus to secrete corticotropin-releasing hormone (CRH). CRH is transported to the pituitary gland, where it induces the secretion of the adrenocorticotropic hormone (ACTH). The latter enters the blood circulation to reach the adrenal cortex. There, ACTH interacts with its corresponding receptors, inducing cholesterol delivery into mitochondria and expression of CYP11A1, CYP11B1 and their corresponding electron transfer partners Adx and AdR [12]. As a consequence, F production and release are enhanced.

SEX HORMONES

The formation of sex hormones commences with the synthesis of dehydroepiandrosterone (DHEA). CYP17A1 is capable to catalyze a lyase reaction utilizing 17OH-Preg as substrate, yielding DHEA. Multiple beneficial properties are ascribed to DHEA, such as prevention of osteoporosis, anti-obesity action, prevention of atherosclerosis, anti-carcinogenic properties and more [13]. In addition, DHEA represents the precursor of androgens and estrogens, which can be metabolized to androstenedione (Andro) by 3β-HSD. Andro can also be formed from 17OH-Prog via a lyase reaction by CYP17A1. This intermediate serves as substrate for CYP19, which eliminates the methyl group at C19 through three consecutive hydroxylations at this position, yielding estrone (E1). E1 can further be metabolized to estradiol (E2) by 17β-HSD, which reduces the keto group at position C17 to a hydroxyl group. E1 and E2 are the main estrogens in mammals. They are present in both genders but in significant higher concentrations in female. Principally, they induce the development of the female secondary sexual characteristics and regulate the female menstrual cycle. In addition, they are important for the maturation of sperm in male [14]. Moreover, Andro can be converted into testosterone (T) by 17β-HSD, and then, after reduction by 5α-reductase to dihydro-testosterone. T and dihydrotestosterone are the main androgens with higher concentrations in male. They are crucial for the development of male secondary sexual characteristics like increased muscle and bone mass, as well as the growth of body hair.

Similar to the HPA-axis for cortisol regulation, androgen availability is controlled by the hypothalamic-pituitary-gonadal (HPG)-axis. The hypothalamus secretes gonadotropin-releasing hormone (GnRH), which stimulates the pituitary gland to release luteinizing hormone (LH) and follicle-stimulating hormone (FSH). LH induces testicular T production, which causes a negative feedback loop resulting in GnRH and LH inhibtion [15].

The action of T is further enhanced by the effect of FSH, which stimulates cells to express androgen receptors. In female, the feedback effect of different steroid hormones changes depending on the stage of the menstrual cycle. Progesterone and estradiol, which are released during the *postovulatory phase*, inhibit LH and FSH secretion. In the *late luteal phase*, FSH and FH levels increase, as progesterone and estrogen production decrease, leading to the recruitment of a new follicle. The growing follicle starts to release increasing amounts of estrogens in the *follicular growth phase*, which slightly inhibit LH and FSH secretion. Afterwards, in the *preovulatory surge phase*, preparing for ovulation, increased amounts of LH and FSH are released. It is thought that further elevation of estrogens results in a switch from inhibitory feedback to activatory effect of estrogens onto LH and FSH production. When the egg is released, increasing amounts of progesterone are produced, leading to inhibition of LH and FSH release. During conception, the fetus takes over progesterone production, preventing a new ovulation.

COMPARTMENTALIZATION OF STEROID HORMONE SYNTHESIS

The production of mineralo- and glucocorticoids, as well as sex hormones, takes place in different zones in steroidogenic tissues of different organs, supporting the regulation of the production of distinct steroid hormones [10]. The most striking example is the adrenal gland, consisting of different zones, each producing different steroid hormones (Figure 7). The *zona glomerulosa* expresses CYP11A1, CYP21A2 and CYP11B2, but lacks to express CYP17A1, which is essential for glucocorticoid and sex hormone production. Thus, this zone is solely designated to synthesize mineralocorticoids. As this adrenal area possesses angiotensin II receptors, the aldosterone production is under control of the renin-angiotensin system (Figure 5).

Further, in the *zona fasciculata,* CYP17A1, CYP21A2 and CYP11B1 are found, whereas CYP11A1 and cytochrome b_5, which is essential to induce the lyase activity of CYP17A1, are not expressed. In addition, ACTH receptors are synthesized in this zona. The presence of CYP17A1 and the absence of cytochrome b_5 lead on to the production of glucocorticoids, like cortisol, which is regulated by the HPA-axis (Figure 6).

The androgens DHEA and androstenedione are produced in the *zona reticularis* of the adrenal gland. Here, CYP21A2 and CYP11B1 are expressed in very small quantities, in contrast to CYP17A1 and cytochrome b5, which are synthesized in large amounts increasing the capability of CYP17A1 to scissor the 17,20 carbon carbon bond of 17OH-Preg, yielding DHEA. As 3β-HSD is also produced there in small quantities, androstenedione can be synthesized from DHEA in a small extend.

Further metabolism to estrogens and androgens takes place in reproductive tissues like the gonads or the testes.

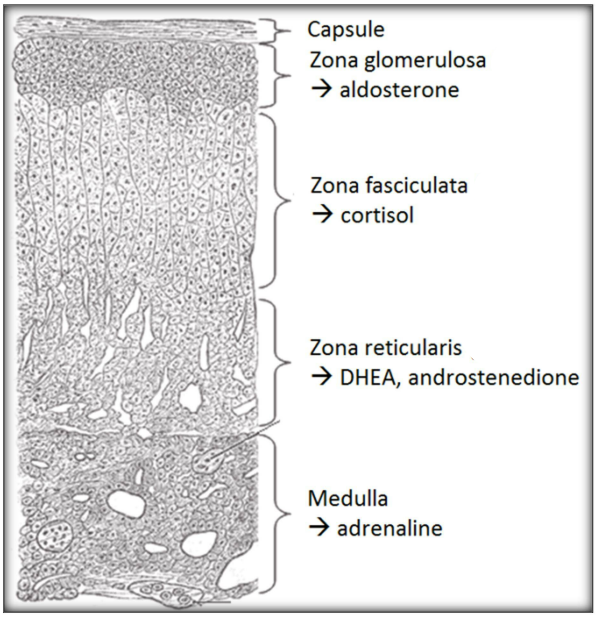

FIGURE 7: ADRENAL GLAND HISTOLOGY DIAGRAM: PRODUCTION OF STEROID *HORMONES TAKES PLACE* IN THE THREE DIFFERENT ZONES OF THE ADRENAL GLAND[2].

[2] http://www.normalhistology.com/wp-content/uploads/Adrenal-Gland-Histology-Diagram.gif

EFFECT OF STEROID HORMONE METABOLISM DISORDERS

Steroid hormones are very important endogenous compounds indispensable for mammalian vitality. Their concentrations in organisms are strictly controlled at different levels. Alterations in the activities of steroidogenic CYPs leading to changed steroid hormone levels often cause severe diseases. One of the most common steroid metabolism disorder in humans is the congenital adrenal hyperplasia (CAH). The symptoms of affected persons vary depending on the altered steroidogenic CYP. In over 90 % of cases the deficiency of CYP21A2 is responsible for causing CAH. This enzyme is crucial for the synthesis of mineralocorticoids and glucocorticoids. For this reason, aldosterone and cortisol production are reduced and thus the control of salt balance and body fluid volume as well as the glycemic control and stress response are altered [16]. In the case of a complete loss of CYP21A2 activity, patients suffer from salt-wasting, absence of mineralo- and glucocorticoids as well as an increased level of androgens resulting in virilization of females and enlarged genitalia in males. Moreover, ACTH release is strongly increased due to a loss of the feedback inhibition by cortisol. The permanent stimulation of the adrenal gland to express steroidogenic CYPs provokes growth of this organ, resulting in a hyperplasia. The range of these symptoms depends on the degree of CYP21A2 activity alteration and it reaches from the described severe forms to mild forms with slight virilization in females and nearly no symptoms in males, without reduced aldosterone and cortisol levels in both genders. In many cases the fertility of females is reduced.

CYP11B1 catalyzes the last step in the cortisol production. It hydroxylates 11-deoxycortisol at position C11, yielding cortisol. Deficiencies of the CYP11B1 enzyme account for 5-8 % of patients suffering from CAH. A decreased cortisol production leads to elevated androgen and aldosterone levels, resulting in virilization and hypertension. Further, glucocorticoid-dependent biological functions such as delivery of sugar to the blood and regulation of the immune system might be altered.

An impairment of CYP11B2 activity, which is essential for aldosterone synthesis, provokes severe salt loss and patients suffer from vomiting and failure to thrive. There are two different CYP11B2 deficiencies described: corticosterone methyl oxidase (CMO) deficiency type I and type II. Their classification depends on the altered activity of CYP11B2. This enzyme catalyzes three distinct reactions, hydroxylation at position C11, followed by hydroxylation at position C18 and, finally, oxidation at C18. Patients with an altered hydroxylase activity are categorized to CMO-deficiency type I, in contrast to CMO type II, where the patients have an impaired oxidase activity of CYP11B2.

CYP17A1 catalyzes two different reactions: a 17α-hydroxylation, yielding 17α-hydroxy-pregnenolone or 17α-hydroxy-progesterone, and a 17,20 lyase reaction, yielding DHEA and androstenedione. Deficiencies of both CYP17A1 activities cause decreased levels of cortisol and androgens, leading to an elevated level of mineralocorticoids. As a consequence, patients suffer from hypertension, hypercalemia and hyponatremia. Furthermore, males exhibit intersexual genitalia after birth and females develop a primary amenorrhea. In the

case of CYP17A1 lyase activity deficiency, only decreased levels of androgens are registered, without impact on the level of glucocorticoids.
Deficiencies of CYP19A1 result in a decreased production of estrogens. Males are nearly not affected, but females are virilized after birth and exhibit amenorrhea. Moreover, patients of both genders suffering from CYP19A1 deficiency grow tall, as estrogen is crucial to close the epiphyseal lines.
Relationships between testosterone and prostate cancer as well as estrogens and breast cancer are well documented. Therefore, CYP17A1 and CYP19A1 are targets in anti-cancer therapy and the development of specific inhibitors of these enzymes are of great importance. One challenge to create such inhibitors is to avoid cross-reactivity with other steroidogenic CYPs. As x-ray structures of both human CYP17A1 [17] and human CYP19A1 [18] have been recently obtained, new improved inhibitors for prostate and breast cancer treatment might be developed.

SULFONATED STEROIDS

In mammalian organisms, sulfonated steroids often exist in notably higher concentrations than unconjugated steroids [19-21]. As the classical endocrine dogma suggests that steroids must be available in an unconjugated form in order to interact with their corresponding receptor to induce a biological response, sulfonated steroids were regarded for a long time to be inactive and to be solely designated for renal or biliary excretion [22-26]. Interestingly, especially during pregnancy, human and other mammals exhibit highly elevated levels of estrone sulfate (E1S) [19,21] and pregnenolone sulfate (PregS) [27] indicating a crucial role of these conjugated steroids in reproduction, which still has to be elucidated. In the last decades, sulfonated steroids were considered to act as precursors for unconjugated steroids, as they can be hydrolyzed by steroid sulfatases [28]. In 2008, Schuler and colleagues discovered that estrogen receptors, sulfotransferases and steroid sulfatases are expressed in the same tissue, strengthening the hypothesis that sulfonated steroids are an important alternative source for the local formation of biologically active steroids [29]. This demonstrates that the supply of active steroid hormones is not solely regulated by a superior system such as the RAAS or the HPA axis for aldosterone and cortisol supply. Due to the existence of steroid sulfatases (StS) in certain tissues, a secondary system monitoring the availability of unbound, active steroids on a cellular level might exist. In order to be hydrolyzed, sulfonated steroids first have to enter cells expressing StS. As their negatively charged sulfate moiety hinders a passive diffusion across cell membranes, steroid sulfates need to be actively transported by carriers. Transporters of the SLC or SLCO family [30-32] were identified to possess high specificity towards steroid sulfates, proving the existence of such a secondary system that controls the availability of biologically active steroids. The transport and metabolism of steroid sulfates is displayed in Figure 8. Free steroids enter the cell by a passive diffusion across the cell membrane or are synthesized endogenously from cholesterol. Afterwards, they are able to interact with their receptor and, thus, either induce a biological answer or they can be sulfonated by SULTs. Further, these sulfonated steroids

can be actively transported out of the cell by carriers or be hydrolyzed by StS, again yielding unbound steroids.

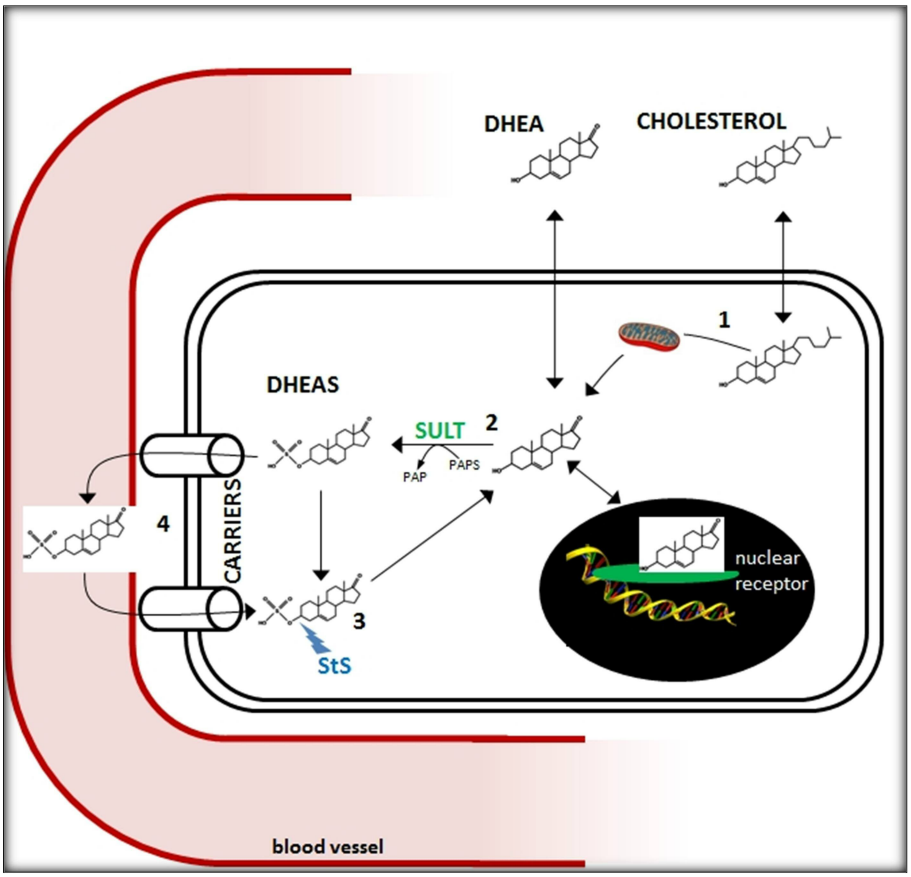

FIGURE 8: METABOLISM AND TRANSPORT OF STEROID SULFATES. (1) CHOLESTEROL IS TRANSPORTED INTO THE MITOCHONDRIA INITIATING THE STEROID HORMONE BIOSYNTHESIS. (2) FREE STEROIDS ARE SULFONATED VIA SULFOTRANSFERASES (SULT). (3) SULFONATED STEROIDS ARE HYDROLYZED VIA STEROID SULFATASES. (4) STEROID SULFATES ARE TRANSPORTED INTO CELLS VIA TRANSPORTERS SUCH AS THE SODIUM DEPENDENT ANION TRANSPORTER (SOAT).

While the knowledge about physiological features of sulfonated steroids is still sparse, research on their biological role has increased in the last years, demonstrating that they are versatile compounds involved in many different biological processes. Cholesterol sulfate (CS) activates protein kinase C in differentiating keratinocytes, thus being essential for the keratinization [33,34].

PregS displays extremely varying concentrations in humans, with highest levels during birth and pregnancy, indicating an important role in mammalian reproduction, which is not clear yet. Nevertheless, it was shown that PregS modulates a big diversity of ion channels, transporters, and enzymes [27].

DHEAS, one of the most abundant steroids in human, was shown to inhibit thrombin-dependent platelet aggregation and thrombin-dependent activation of Akt, ERK1/2, and p38 MAP kinase. Thus, DHEAS could possibly be of physiological relevance when functionality of the vascular endothelium is compromised, as Bertoni et al. suggested [35]. In addition, DHEAS stimulates the proliferation of bovine chromaffin cells, acting through a receptor other than the classical steroid receptors, as demonstrated by Sicard *et al.* [36]. Recently, Shihan et al. were able to reveal a non-classical signaling pathway in spermatogenic cells

induced by DHEAS [37]. These findings put sulfonated steroids into a new focus of interest. From an inactive compound, determined for excretion, to a reservoir for biologically active steroids, the functions of these compounds in mammalian organisms had to be completely reassessed.

SULFOTRANSFERASES AND STEROID SULFATASES

Steroid sulfates are generated via a sulfonation reaction catalyzed by three distinct sulfotransferases (SULT1E, SULT2B1, SULT2A1). The general reaction mechanism exemplified by the sulfonation of DHEA is shown in Figure 9.

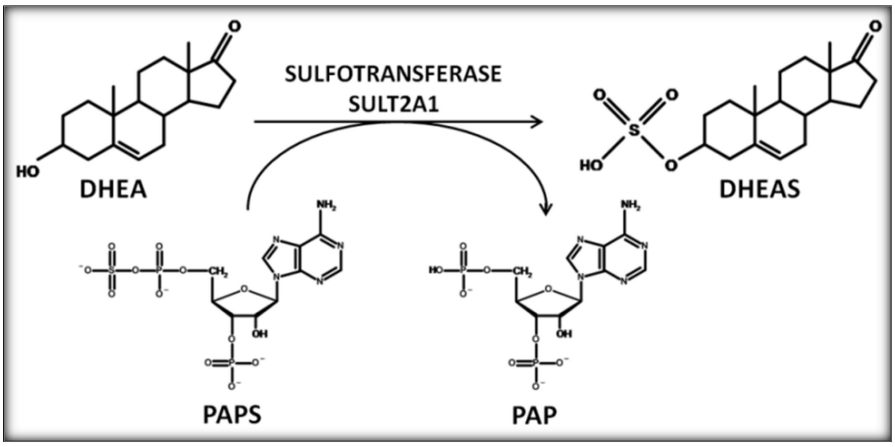

FIGURE 9: REACTION OF A STEROID SULFONATION. *DHEA IS SULFONATED BY SULT2A1 AT THE 3-HYDROXYL GROUP. THE* SULFONATE MOIETY IS PROVIDED BY 3'-PHOSPHOADENOSINE-5'-PHOSPHOSULFATE (PAPS).

Sulfonation describes the transfer of a sulfonate group (SO_3^-), which is provided by the universal sulfonate donor 3'-phosphoadenosine 5'-phosphosulfate (PAPS). The SO_3^- group-transfer to the 3β-hydroxyl group of steroids generates an SO_4 moiety. For this reason, sulfonated products have been incorrectly named "sulfates", a nomenclature often used in literature [38].

SULT1E1 exhibits high affinity for estrogens [39], but was also shown to sulfonate DHEA and Preg [40]. It was detected at protein level in the liver [41], endometrium [40], jejenum [42] and mammary epithelial cells [43].

There are two isoforms of SULT2B1: SULT2B1a and SULT2B1b. They are formed through alternative splicing, resulting in differences at the N-terminus of the synthesized proteins. These differences of the SULT2B1 isoforms lead to distinct substrate selectivities. SULT2B1a shows a high specificity towards Preg, whereas SULT2B1b is highly selective for C. RNAs encoding SULT2B1 enzymes have been detected in the placenta, trachea, prostate [44], skin, vagina, oral mucosa, colorectal mucosa [45] and other tissues [27].

SULT2A1 is the best examined human SULT, as its cDNA from liver was already cloned and expressed in the early 1990s [46,47]. It favors to sulfonate DHEA, which is considered to be the major substrate of SULT2A1, but there a many other steroids serving as substrates, such as Preg, C, E1 and E2 (3β-hydroxyl group is sulfonated), as well as T and E2 (17β-hydroxyl

groups are sulfonated). SULT2A1 was found to be expressed in the liver, adrenal gland, jejunum [48] and ovary [49] in large quantities.

The equilibration between sulfonated and unbound steroids is on one hand, regulated by the SULT enzymes, which catalyze a sulfonate transfer to free steroid hormones, and, on the other hand, by steroid sulfatases (StS), which hydrolyze sulfonated steroids, yielding unbound steroids. StSs are considered to be almost ubiquitously present in small quantities in mammals. In contrast to the cytosolic SULTs, the StSs are attached to the endoplasmatic reticulum. The putative mechanism of StS for the hydrolysis of E1S to E1 is illustrated in Figure 10.

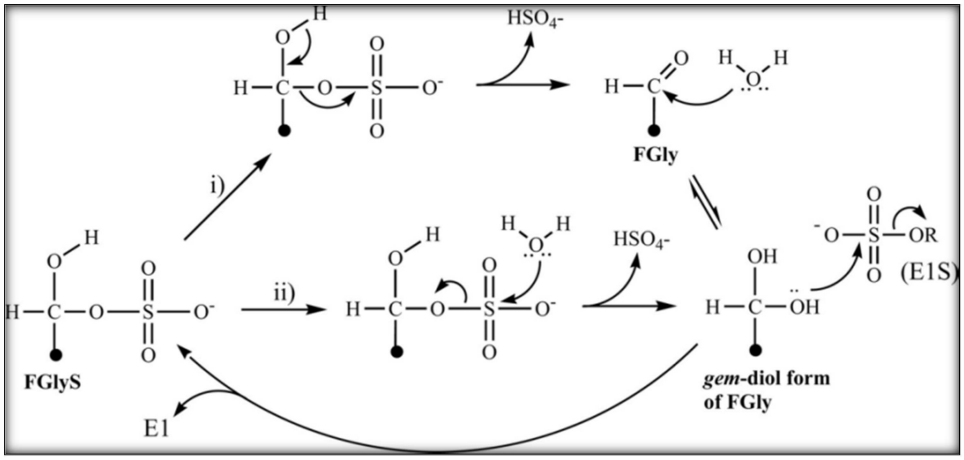

FIGURE 10: SUGGESTED REACTION FOR HYDROLYSIS OF ESTRONE SULFATE BY STS VIA: I) DESULFATION, CATALYZED BY THE NON-ESTERIFIED HYDROXYL GROUP, FOLLOWED BY THE ATTACK OF A MOLECULE OF WATER ON FORMYLGYCINE (FGLY); AND II) A DIRECT ATTACK OF A MOLECULE OF WATER ON THE SULFUR ATOM OF FGLYS [28].

In a first step, the *gem*-diol form of formylgycine (FGly) from FGlyS is regenerated via desulfation (i), catalyzed by the non-esterified hydroxyl group, followed by the attack of a water molecule on the FGly intermediate; or by a direct attack of a water molecule on the sulfur atom of FGlyS (ii). One of the hydroxyl groups of ·-CH(OH)OH then attacks the sulfur atom of estrone sulfate, yielding estrone and regenerating FGlyS as a consequence [28]. The formylglycine residue is unique in StS and other sulfatases and is generated through a posttranslational modification of a conserved cysteine residue [50].

1.2 AIMS AND SCOPE

Recombinantly expressed and purified steroidogenic CYPs allow investigations of the impact of diverse compounds on their activities, such as inhibitors or endogenous substances, on a molecular level. Although the expression of functional steroidogenic CYPs in bacteria still remains challenging, the six CYPs participating in steroid hormone biosynthesis were reported to be successfully expressed and purified [51-56]. Global aim of this work is the expression of high yields of functional steroidogenic CYPs and their redox partners for investigating the impact of sulfonated steroids and pharmaceutical compounds on the respective reactions. Therefore, bacterial expression, purification and reaction conditions for CYP11A1, CYP17A1, CYP11B1, cytochrome b_5 and their respective reaction partners had to be established and/or optimized.

Several steroid hormones exist in a sulfo-conjugated form, often in concentrations exceeding the unbound form manifold. Investigations on their biological function increased in the last decades, but, so far, it has not been considered that sulfonated steroids might interact with enzymes involved in steroidogenesis. Thus, their possible contribution to the regulation of the production of steroid hormones on the cellular level has not been investigated. In order to elucidate their impact, the influence of sulfonated DHEA on the activity of mitochondrial CYP11A1 was investigated in a reconstituted *in-vitro* system utilizing purified CYP11A1 and its electron transfer partners, Adx and AdR. Experiments were performed to clarify whether DHEAS binds to the enzyme and competes with the natural substrate cholesterol, acting as an inhibitor. Further, it had to be elucidated, whether the interaction between CYP11A1 and its redox partner, Adx, is influenced in the presence of DHEAS, due to its amphipathic structure.

In terms of the metabolism of sulfonated steroids, it is known that CS is converted to PregS in a CYP11A1-dependent reaction [57]. Further metabolism of PregS has not been studied so far in detail. Therefore, the subsequent conversion of PregS was explored in a reconstituted *in-vitro* system using purified CYP17A1 and its electron transfer partner, CPR. We aimed to determine the kinetics and binding parameters as well as the effect of cytochrome b_5, which is known to enhance the CYP17A1 dependent lyase reaction. Furthermore, to reveal a putative physiological relevance of PregS metabolism, a human cell culture system, recombinantly expressing CYP17A1 and CPR, was applied.

In addition, interference of pharmaceutical substances with the endocrine system, in particular with the cortisol production, has been investigated. The anesthetic agent etomidate is known to inhibit cortisol production, whereas its derivative carboetomidate only slightly alters cortisol synthesis. In this work, the hypothesis was proved, whether etomidate and carboetomidate differentially bind to CYP11B1, the cortisol producing enzyme. Therefore, cell culture experiments as well as kinetic and binding studies with purified CYP11B1 were conducted to elucidate this issue.

2 PUBLICATION OF THE RESULTS

The results produced during the present work are published in the articles listed below

2.1 NEUNZIG ET AL., 2014

DHEAS STIMULATES THE FIRST STEP IN STEROID HORMONE BIOSYNTHESIS

Jens Neunzig, Rita Bernhardt

Plos One, Feb. 2014, DOI: 10.1371/journal.pone.008972

OPEN ACCESS Freely available online

PLOS ONE

Dehydroepiandrosterone Sulfate (DHEAS) Stimulates the First Step in the Biosynthesis of Steroid Hormones

Jens Neunzig, Rita Bernhardt*

Department of Biochemistry, Faculty of Technical and Natural Sciences III, Saarland University, Saarbrücken, Germany

Abstract

Dehydroepiandrosterone sulfate (DHEAS) is the most abundant circulating steroid in human, with the highest concentrations between age 20 and 30, but displaying a significant decrease with age. Many beneficial functions are ascribed to DHEAS. Nevertheless, long-term studies are very scarce concerning the intake of DHEAS over several years, and molecular investigations on DHEAS action are missing so far. In this study, the role of DHEAS on the first and rate-limiting step of steroid hormone biosynthesis was analyzed in a reconstituted *in vitro* system, consisting of purified CYP11A1, adrenodoxin and adrenodoxin reductase. DHEAS enhances the conversion of cholesterol by 26%. Detailed analyses of the mechanism of DHEAS action revealed increased binding affinity of cholesterol to CYP11A1 and enforced interaction with the electron transfer partner, adrenodoxin. Difference spectroscopy showed K_d-values of 40±2.7 µM and 24.8±0.5 µM for CYP11A1 and cholesterol without and with addition of DHEAS, respectively. To determine the K_d-value for CYP11A1 and adrenodoxin, surface plasmon resonance measurements were performed, demonstrating a K_d-value of 3.0±0.35 nM (with cholesterol) and of 2.4±0.05 nM when cholesterol and DHEAS were added. Kinetic experiments showed a lower K_m and a higher k_{cat} value for CYP11A1 in the presence of DHEAS leading to an increase of the catalytic efficiency by 75%. These findings indicate that DHEAS affects steroid hormone biosynthesis on a molecular level resulting in an increased formation of pregnenolone.

Citation: Neunzig J, Bernhardt R (2014) Dehydroepiandrosterone Sulfate (DHEAS) Stimulates the First Step in the Biosynthesis of Steroid Hormones. PLoS ONE 9(2): e89727. doi:10.1371/journal.pone.0089727

Editor: Jean-Marc A. Lobaccaro, Clermont Université, France

Received December 13, 2013; **Accepted** January 22, 2014; **Published** February 21, 2014

Funding: This work is funded by the "Deutsche Forschungsgemeinschaft DFG-FOR1369" (URL: http://www.dfg.de). The funders had no role in study design, data collection and analysis, decision to publish, or preparation of the manuscript.

Competing Interests: The authors have declared that no competing interests exist.

* E-mail: ritabern@mx.uni-saarland.de

Introduction

In mammalian organisms, steroid hormones are indispensable for a normal development. Considering their action, these steroids are classified into three main groups. Mineralocorticoids, with aldosterone as the most important representative, regulate the salt household and hence the blood pressure. Cortisol belongs to the glucocorticoids and provides the organism with energy stimulating the gluconeogenesis. Finally, the sexual hormones, with androgens and estrogens, are fundamental for the formation of the sexual characteristics and the estrous cycle. Biosynthesis of all steroid hormones (Fig. 1) is initiated by CYP11A1 with the side chain cleavage of cholesterol yielding pregnenolone [1,2]. This rate-limiting step of the steroid hormone biosynthesis is carried out in the inner mitochondrial membrane and displays three hydroxylation reactions. In the first step, carbon C22 of cholesterol is hydroxylated followed by an oxidative attack at C20, forming the intermediate 20,22-dihdroxycholesterol. The cleavage of the side chain of cholesterol is initiated by a third hydroxylation. The electrons necessary oxygen activation and substrate hydroxylation are transferred from NAD(P)H via a NAD(P)H-depending ferredoxin reductase, adrenodoxin reductase, and a ferredoxin, adrenodoxin [3]. The product pregnenolone serves as precursor for mineralocorticoids, glucocorticoids, as well as DHEA and its derived sexual hormones.

To induce their biological activities, according to recent hypothesis steroid hormones have to be available in an unconjugated form to interact with their corresponding receptors. Conjugated steroids with sulfate groups have been regarded for a long time to be exclusively designated for excretion [4], although many mammalian species produce, predominantly during pregnancy, huge amounts of sulfonated steroids [5–7]. Besides their function as an inactive reservoir for steroid hormones [8], their physiological role still needs to be elucidated. So far cholesterol sulfate (CS) represents the only sulfonated steroid, which is rather well investigated: as a compound of cell membranes CS possesses a stabilizing role, CS is involved in regulating the activity of serine proteases and it is important for keratinocyte differentiation [9]. Moreover, Tuckey could demonstrate the ability of CYP11A1 to metabolize CS yielding pregnenolone sulfate [10], which can enter the "sulfatase pathway" or be metabolized to further sulfonated steroids [11]. In addition, CS was shown to have an inhibitory effect on the CYP11A1 dependent side chain cleavage of cholesterol [12,13]. These findings show the direct involvement of sulfonated steroids in the steroid hormone biosynthesis and since the discovery of the co-localization of estrogen receptors, steroid sulfatases and estrogen sulfotransferases in the same tissue [14], new hypotheses on the role of sulfonated steroids and a system that controls the availability of free steroids arose. However, detailed investigations about the interplay between steroid biosynthesis and steroid conjugation are missing so far.

In contrast to unconjugated steroids, sulfonated steroids need to be actively transported through cell membranes. Sodium depen-

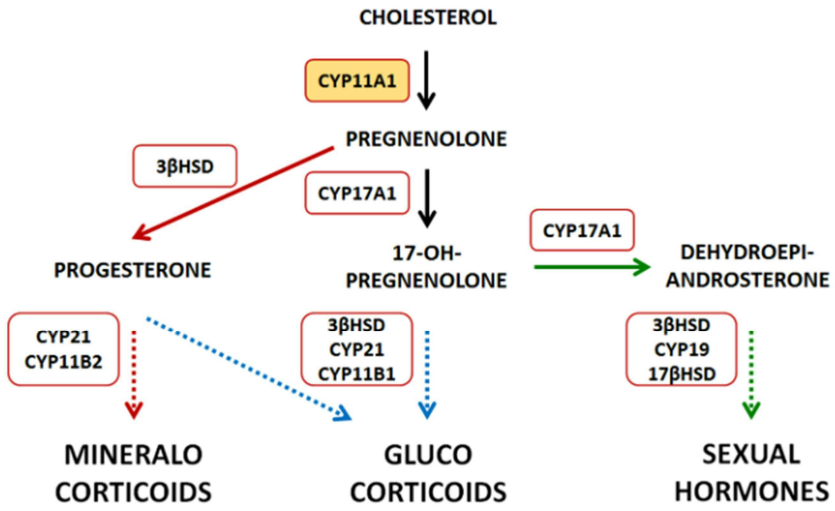

Figure 1. Schematic overview of the steroid hormone biosynthesis.
doi:10.1371/journal.pone.0089727.g001

dent organic anion transporters (SOAT) were found to possess a high sensitivity towards sulfonated steroids [15], although it has not been investigated so far whether these transporters are localized in mitochondrial membranes allowing sulfonated steroids to enter. On the other hand, sulfonated cholesterol has been found to be an endogenous compound of mitochondria in rats [16] and to be converted by CYP11A1 in isolated mitochondria [10]. This suggests that sulfonated steroids are able to pass the mitochondrial membranes and thus have direct contact with CYP11A1.

We focused here on the impact of sulfonated DHEA on CYP11A1 activity, as this steroid is the predominant circulating one in humans [17,18]. The naturally occurring concentrations of DHEAS and DHEA have been determined to be around 10 µM and 10 nM, respectively, in young adults [19]. Moreover, the DHEAS level is increased in some adrenocortical disorders: people suffering from Cushing's syndrome due to adrenal hyperplasia display very high levels of serum DHEAS [20]. Furthermore, in Western countries, dietary supplements reach a major significance in nutrition, especially when anti-aging effects are ascribed to them. One very popular dietary supplement is DHEA or DHEAS, to which multiple beneficial implications, such as anti-diabetic effect, prevention of osteoporosis, anti-obesity action, prevention of atherosclerosis, anti-carcinogenic action and anti-aging effects are attributed [21]. Normally, 50 mg per day are administrated [22], but also up to 200 mg per day were reported to be taken [23]. However, the direct action of DHEAS on the steroid hormone biosynthesis has not been studied so far and remains an enigma.

Therefore, in this study, the influence of DHEAS on reactions catalyzed by CYP11A1 is investigated on a molecular level in a reconstituted *in vitro* system. It could be demonstrated that DHEAS but not DHEA increases the CYP11A1-dependent pregnenolone formation caused by improved cholesterol and redox partner binding.

Experimental Procedure

Protein expression and purification

Heterologous expression of bovine adrenodoxin reductase (AdR) and bovine adrenodoxin (Adx) was performed and the proteins were purified as previously described [24,25]. Recombinant CYP11A1 was expressed in *E. coli* C43(DE3) cells, which were co- transformed with a plasmid encoding for groEL/groES chaperones [26].

The subsequent CYP11A1 expression was performed as described elsewhere [27]. The obtained cell pellet was suspended in 5 ml/g wet mass buffer, consisting of 50 mM potassium phosphate, pH 7.4, 500 mM sodium acetate, 20% glycerol, 1.5% sodium cholate, 1.5% Tween20, 0.1 mM EDTA, 0.1 mM DTT, 0.1 mM PMSF and 10 µM cholesterol. The disruption of the cells was carried out by sonication for 15 min with 15 s intervals, utilizing Bandelin Sonoplus with the sonotrode TT13 (Bandelin electronic, Berlin; Germany) at an amplitude of 15 Hz in an ice water bath under uninterrupted stirring. To remove cell derbis and unsoluble proteins, the homogenate was centrifuged at 30000 rpm (Himac CP75b, rotor P45, Hitachi, Tokio; Japan) for 30 min at 4°C. The supernatant was applied to an IMAC Ni-NTA column, equilibrated with buffer A, containing 50 mM potassium phosphate, pH 7.4, 500 mM sodium acetate, 20% glycerol, 1% sodium cholate, 1% Tween 20, 0.1 mM EDTA, 0.1 mM DTT, 0.1 mM PMSF and 10 µM cholesterol. Unspecific binding of proteins were removed using a washing buffer similar to buffer A, but with additional 40 mM imidazole. Elution of CYP11A1 was performed with buffer A and 200 mM imidazole. As the presence of imidazole in buffers changes the pH, acetic acid was used for readjustment to pH 7.4. Afterwards, the eluate was concentrated to a final volume of 5 ml by centricons with a size exclusion of 30 kDa. The eluate was diluted 1:3 with buffer B (20% glycerol, 0.1 mM EDTA, 0.1 mM DTT and 10 µM cholesterol) and loaded onto an ion exchange SP- sepharose column, which was equilibrated with buffer C (20 mM potassium phosphate, pH 7.4, 20% glycerol, 10 mM imidazole, 0.1 mM EDTA, 0.1 mM DTT, 0.1 mM PMSF and 10 µM cholesterol). Weakly bound proteins were removed with a washing step using buffer C. Then CYP11A1 was eluted with 0–150 mM NaCl gradient in buffer C. The red fractions containing CYP11A1 were concentrated and diluted several times utilizing a centrifugal device to substitute the buffer C with buffer D (50 mM potassium phosphate, pH 7.4, 20% glycerol, 0.1 mM EDTA, 0.1 mM dithiothreitol, 1% sodiumcholate, 0.05% Tween 20).

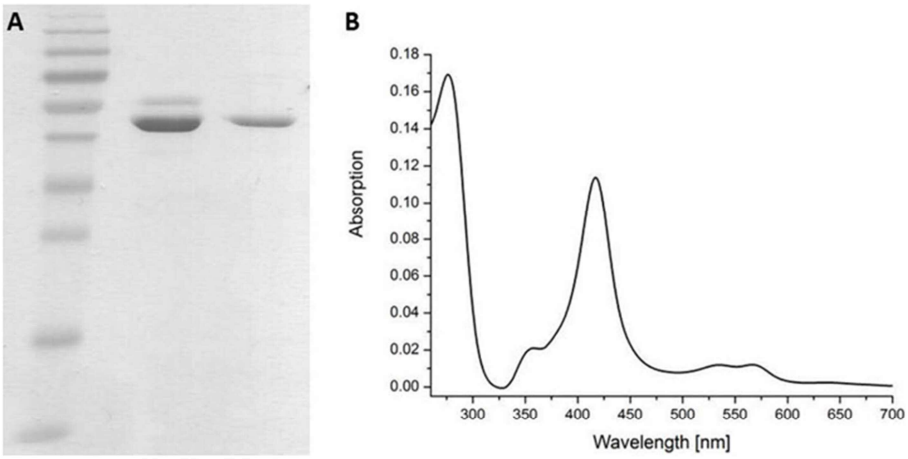

Figure 2. A) SDS-Polyacrylamid gel electrophoresis. Lane 1: protein marker IV (peqlab), lane 2: CYP11A1 after Ni-NTA purification, lane 3: CYP11A1 after Ni-NTA and Sp-sepharose purification. B) Absolute spectrum of purified CYP11A1 in the range of 260–700 nm.
doi:10.1371/journal.pone.0089727.g002

UV/Vis spectroscopy

The protein concentration of the redox partners were determined using $\varepsilon_{450} = 11.3$ (mM cm)$^{-1}$ for AdR and $\varepsilon_{414} = 9.8$ (mM cm)$^{-1}$ for Adx [28,29]. CYP11A1 concentration was defined, performing a reduced carbon-monoxide difference spectroscopy according to Omura and Sato [30] with $\varepsilon_{448} = 91$ (mM cm)$^{-1}$. Binding of cholesterol was investigated using difference spectroscopy, which was carried out in tandem cuvettes according to Schenkman [31]. The tandem cuvettes consist of two chambers. The first chamber of the cuvette was filled with buffer and 2 µM of CYP11A1, whereas to the second chamber only buffer was added. For reference, a second tandem cuvette was used, which was filled equally. To the first chamber of the cuvette increasing amounts of cholesterol were added with or without 5-fold excess of DHEAS. The same amount of these compounds was added to the second chamber of the reference cuvette. Cholesterol, as well as DHEAS, were dissolved in DMSO. The buffer utilized was composed of 50 mM potassium phosphate (pH 7.4), 20% glycerol, 0.5% sodium cholate and 0.05% Tween 20. Difference spectra were recorded from 370 to 450 nm. To determine the dissociation constant (K_d), the values from five titrations were averaged and the resulting plots were fitted with hyperbolic regression.

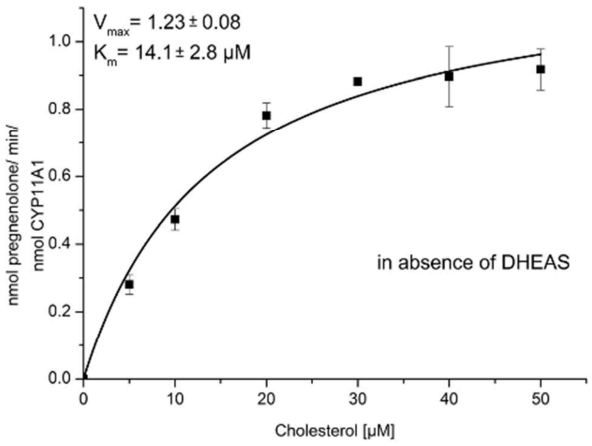

Figure 3. Kinetics of CYP11A1. Determination of kinetic parameters for the conversion of cholesterol to pregnenolone catalyzed by CYP11A1 using Adx and AdR as redox partners. The product formation analyzed by HPLC is represented as mean ± standard deviation of four individual experiments.
doi:10.1371/journal.pone.0089727.g003

Enzyme activity assay

In vitro substrate conversion assays were performed as described elsewhere [32] with slight modifications. The conversion buffer (50 mM HEPES, pH 7.4, 0.05% Tween20) contained 1 µM CYP11A1, 0.5 µM AdR, 20 µM Adx, 1 mM $MgCl_2$, 5 mM glucose-6-phosphate, 1 U glucose-6-phosphate dehydrogenase and 15 µM substrate or 15 µM substrate and 75 µM DHEA(S). After starting the reaction with 1 mM NADPH at 37°C for 7 min, the conversion was stopped in a boiling water bath for 5 min. Cholesterol and the resulting product pregnenolone had to be converted to the corresponding 3-one-4-en form by cholesterol oxidase, to be detectable at 240 nm during HPLC analysis. Therefore, cholesterol oxidase was added to the boiled reaction mixture and incubated for 40 min at 37°C according to Yamato [33]. Cortisol was added as internal standard. The reaction was stopped by adding 1 reaction volume ethylacetate. Extraction of steroids was performed twice with ethylacetate and the ethylacetate phase was evaporated. The steroids were resuspended in 20% acetonitrile for subsequent HPLC analysis. K_m and k_{cat} values were determined by plotting the substrate conversion velocities versus the corresponding substrate concentrations and by using Michaelis–Menten kinetics (hyperbolic fit) utilizing the program OriginPro 8.6G.

HPLC analysis

Steroids were separated on a Jasco reversed phase HPLC system LC2000 using a 4.6 mm×125 mm NucleoDur C18 Isis Reversed Phase column (Macherey-Nagel) with an acetonitril/water gradient and a flow rate gradient of 1 ml/min –2 ml/min. Detection of the steroids was performed at 240 nm within 25 min at 40°C.

Optical biosensor measurements

The interaction of Adx and CYP11A1, was assayed with a Biacore3000 system as described previously [27]. The formation of

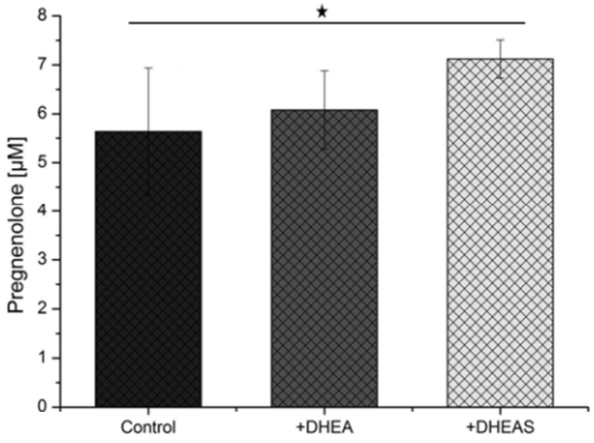

Figure 4. Comparison of pregnenolone formation by CYP 11A1 in the presence of 5-fold excess of DHEA or DHEAS (n = 5 for each group, asterisk: p<0.05).
doi:10.1371/journal.pone.0089727.g004

the CYP11A1-Adx complex was analyzed under three different conditions: in absence of cholesterol, in the presence of cholesterol (CYP11A1concentration: cholesterol concentration, 1:10) and in the presence of cholesterol and DHEAS (CYP11A1 concentration: cholesterol concentration: DHEAS concentration, 1:10:50). CYP11A1 was injected in concentrations between 5 nM and 7.5 nM in HBS-EP buffer at least three times for each concentration. Removal of bound CYP11A1 utilizing 2 mM NaOH was done as described elsewhere [34]. Biaeval 4.1 software was used for determination of K_d values.

Statistical evaluation- To determine the distribution of the samples Kolmogorov-Smirnov-test was used. To determine statistically significant differences between control samples and samples incubated with DHEA or DHEAS, Mann-Whitney *U*-test was applied. One asterisk symbolizes $p<0.05$, and two asterisks $p<0.01$.

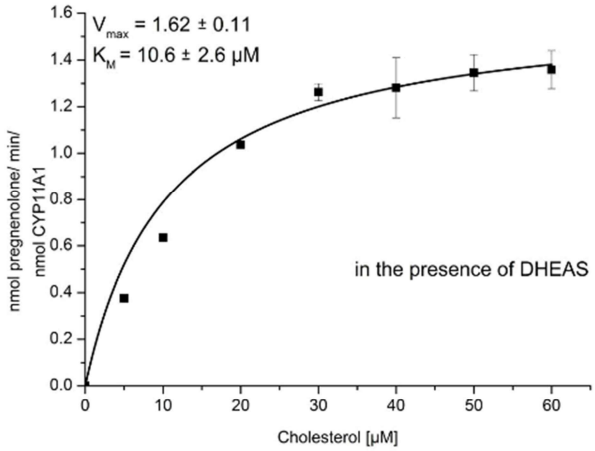

Figure 5. Kinetics of CYP11A1. Determination of kinetic parameters for the conversion of cholesterol to pregnenolone catalyzed by CYP11A1 with Adx and AdR as redox partners in the presence of DHEAS. The product formation analyzed by HPLC is represented as mean ± standard deviation of four individual experiments.
doi:10.1371/journal.pone.0089727.g005

Results

Optimization of the expression of CYP11A1 in *E. coli*

The heterologous expression of CYP11A1 in *E coli* has been reported to be in the range between 45–55 nmol l^{-1} culture [27,36], which is rather low. Harnastai et al. were able to enhance recombinant CYP11A1 expression up to 430 nmol l^{-1} culture co-expressing HemA [37]. In order to further improve the expression level of CYP11A1 we utilized the C43DE3 *E. coli* strain as expression host, which was shown to be adequate for other membrane-bound P450s, as previous results demonstrated [32,34,35]. The expressed His-tagged protein was purified by IMAC Ni-NTA followed by an ion exchange SP-sepharose. The purity of the enzyme was determined via SDS gelelectrophoresis (Fig. 2a), in which a single band at 55 kDa was obtained. The enzyme shows a typical P450 CO-difference spectrum with a major peak at 450 nm and a minor one at 420 nm (not shown). The expression levels using *E. coli* strain C43DE3 achieved here were 640 nmol per liter culture after the two purification steps, which is a great improvement compared to the published results. The UV/Vis spectrum classifies the expressed CYP11A1 as a low-spin protein with the typical cytochrome P450 absorption spectrum: the Q bands at 569 nm (α-band) and 541 nm (β-band), the Soret band at 418 nm, the UV band at 360 nm and the protein-band at 278 nm (Fig. 2b).

CYP11A1 dependent pregnenolone formation in the presence of sulfonated DHEA

CYP11A1 catalyzes the first reaction step in human steroidogenesis, the conversion of cholesterol to pregnenolone with a three step hydroxylation preceding the side-chain cleavage between C20 and C22. In this study, we investigated the influence of sulfonated DHEA on the CYP11A1 catalyzed reaction on a molecular level.

For detection of the product at 240 nm, pregnenolone was transformed to progesterone by using cholesterol oxidase reaction. The kinetic parameters of pregnenolone formation were determined to be $K_m = 14.1 \pm 2.8$ µM and $k_{cat} = 1.23 \pm 0.08$ min^{-1} (Fig. 3). In a first series of experiments, it was checked whether DHEAS can bind to CYP11A1 causing spectral changes of the protein. It was shown that DHEAS up to concentrations of 500 µM did not cause any spectral changes excluding its binding as type I or type II substrate (data not shown).

For further investigation of the DHEAS induced effect on the first step in steroidogenesis, we studied the activity of CYP11A1-dependent cholesterol side chain cleavage in the presence of 75 µM DHEA or DHEAS at a cholesterol concentration of 15 µM, which is around the K_m value determined (Fig. 3). The evaluation of the HPLC data is shown in Figure 4. The amount of pregnenolone formed was 5.6 ± 1.3 µM for the control experiment without DHEAS or DHEA and 6 ± 0.8 µM for the sample incubated with a 5-fold excess of DHEA. In contrast, the CYP11A1 dependent activity in the presence of DHEAS significantly increased by 26% forming 7.1 ± 0.4 µM pregnenolone.

After observing an increased product formation of the CYP11A1 catalyzed reaction in the presence of DHEAS, it was interesting to investigate the influence of DHEAS on the kinetics of this reaction. As shown in Figure 5 and Table 1, in the presence of DHEAS the K_m value for cholesterol decreased while the k_{cat} value increased being 10.6 ± 2.6 µM and 1.62 ± 0.1 min^{-1}, respectively. This leads to a nearly two fold increase of the catalytic efficiency of CYP11A1 in the presence of DHEAS being 87 ($min^{-1}mM^{-1}$) in absence and 153 ($min^{-1}mM^{-1}$) in the presence of DHEAS.

Table 1. Kinetic parameters of CYP11A1, metabolizing cholesterol with or without the addition of DHEAS.

− DHEAS			+ DHEAS		
K_m (mM)	k_{cat} (min^{-1})	k_{cat}/K_m ($min^{-1}mM^{-1}$)	K_m (mM)	k_{cat} (min^{-1})	k_{cat}/K_m ($min^{-1}mM^{-1}$)
0.0142±0.0028	1.23±0.08	86.6	0.0106±0.0026	1.62±0.11	152.8

doi:10.1371/journal.pone.0089727.t001

Analysis of the molecular mechanism of DHEAS action on CYP11A1

To investigate in more detail, which reaction step is being affected by DHEAS, we studied the binding of the substrate and the redox partner, Adx, in absence and in the presence of DHEAS. As shown in Figure 6, the K_d value of CYP11A1 and cholesterol is 40±2.7 µM in absence and 24.8±0.5 µM in the presence of DHEAS.

This indicates that the affinity of cholesterol for CYP11A1 is increased about 2-fold in the presence of DHEAS.

For the determination of the dissociation constant of CYP11A1 and Adx, surface plasmon resonance measurements were conducted (Fig. 7). Binding of CYP11A1 and Adx is essential for the correct function of the side-chain cleavage, since 6 electrons have to be transported from NADPH via AdR and Adx to CYP11A1. Surface plasmon resonance measurements using CYP11A1 and Adx revealed K_d values of 3.8±0.55 nM, when the interaction was measured without substrate, of 3.0±0.35 nM with addition of cholesterol and of 2.4±0.05 nM in the presence of cholesterol and DHEAS (Fig. 7). Comparing the interaction of CYP11A1 and Adx in the presence of cholesterol and DHEAS with the interaction of CYP11A1 and Adx in the presence of only cholesterol, a decrease of the K_d value by 20% is achieved, while a decrease of the K_d by 36% can be observed when the K_d values without substrate and with substrate and DHEAS are compared. As demonstrated in Table 2, changes in the interaction between CYP11A1 and Adx by DHEAS are mainly caused by changes in the k_{on} values. In the presence of cholesterol DHEAS increases the k_{on} value for the binding of Adx to CYP11A1 by 48%, whereas the k_{on} value is increased by 110% compared with the sample in absence of cholesterol. Both results display statistical significance with $p<0.01$. The k_{off} values do not differ in a statistically significant manner.

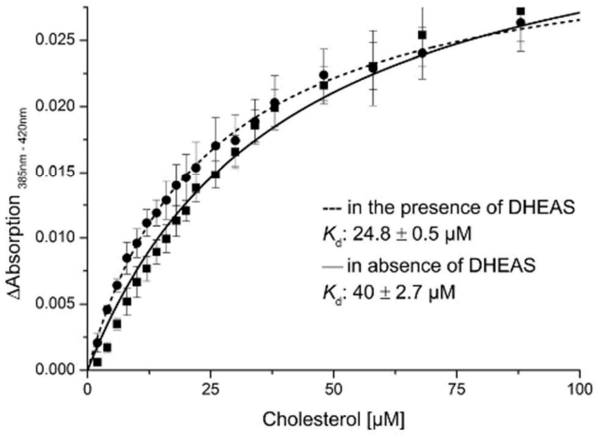

Figure 6. Determination of substrate affinity to CYP11A1. K_d values of CYP11A1 for cholesterol in absence (n = 5) and in the presence of a 5-fold excess of DHEAS (n = 5).
doi:10.1371/journal.pone.0089727.g006

Discussion

In human organism, 99% of DHEA circulates in its sulfonated form, DHEAS [38]. The concentration of circulating DHEAS reaches up to 10 µM in young adults [19] and decreases afterwards with age with concentrations of DHEAS between 20–30% in 70–80 year old people compared with the value of young adults [39]. These characteristics are unique for DHEA or DHEAS and in contrast to other steroid hormones like aldosterone or cortisol, whose serum concentrations stay constant during life. Hence, DHEAS is regarded as "fountain of youth", leading to uncontrolled use in Western countries [38]. In the last decades a huge number of publications concerning the effect of DHEAS on health appeared and the results were really conflicting, reporting about insignificant activity and even harmful effects up to life extending properties of DHEA or DHEAS. Long-term studies about the effect of DHEAS on health are very scarce and the existing ones concern elderly people, where the intake of DHEA is limited to amounts necessary to establish DHEAS concentrations that people have in younger age. This DHEAS replacement therapy in elderly people seems to have beneficial effects concerning bone turnover, skin hydration and libido, increasing the well-being of aging persons [22]. However, since DHEAS reaches major significance as dietary supplement, this requires further research on the effect of high DHEAS concentrations on metabolism. So far, research was mainly focused on the effect of DHEA and DHEAS on the production of androgens and estrogens. The effect of DHEA or DHEAS on the whole steroid hormone biosynthesis, especially on the enzymes involved in the first steps is not investigated so far. The rate-limiting step of the steroid hormone biosynthesis is realized by CYP11A1 catalyzing the side chain cleavage of cholesterol to yield pregnenolone. Thus, CYP11A1 represents an adequate target for regulation, on which the effect of DHEAS was studied here in a reconstituted *in vitro* system. In the presence of DHEAS, CYP11A1 displayed a 26% increased pregnenolone formation compared to the control, while in the presence of DHEA no significant difference from the control

Table 2. Binding parameters for CYP11A1 and Adx without cholesterol (n = 8), with cholesterol (n = 8) and with cholesterol and in the presence of DHEAS (n = 8) determined from measurements with a Biacore3000 system.

− Chol		+ Chol		+Chol +DHEAS	
k_{on} (M^{-1} s^{-1})	k_{off} (s^{-1})	k_{on} (M^{-1} s^{-1})	k_{off} (s^{-1})	k_{on} (M^{-1} s^{-1})	k_{off} (s^{-1})
6.4±1.84	2.4±0.99	8.9±0.79	2.8±0.09	13.2±2.29	3.0±0.14

doi:10.1371/journal.pone.0089727.t002

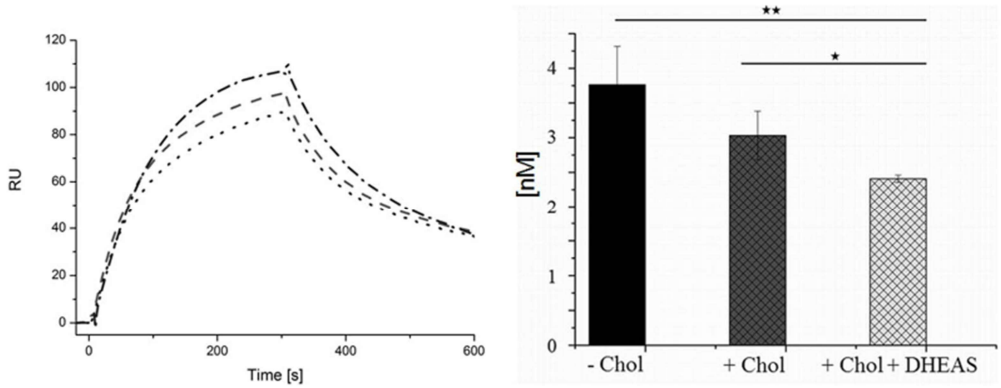

Figure 7. Binding affinity of Adx and CYP11A1. a) Overlay of Biacore3000 sensograms of measurements with 7.5 nM CYP11A1 in absence of cholesterol, in the presence of cholesterol and in the presence of cholesterol and DHEAS (CYP11A1: cholesterol: DHEAS, 1:15:75), b) Comparison of K_d values for the interaction between CYP11A1 and Adx without cholesterol (n = 8), with cholesterol (n = 8, CYP11A1: cholesterol, 1:15) and with cholesterol in the presence of DHEAS (n = 8, CYP11A1: cholesterol: DHEAS, 1:15:75).
doi:10.1371/journal.pone.0089727.g007

could be observed. Thus, the negatively charged sulfate group of DHEAS seems to be essential for the increase of the CYP11A1 activity. Interestingly, it was previously shown that polycationic natural polyamines interact through electrostatic forces with negatively charged spots at protein interfaces of the CYP11A1-Adx system. This interaction of the positively charged polyamines with the CYP11A1-Adx interface leads to an inhibition of the CYP11A1 activity [40]. This indicates that the type of charge of the compounds (DHEAS or polyamines) determines whether it displays an activatory (DHEAS) or inhibitory (polyamines) effect on the CYP11A1-dependent reaction, with an anionic compound stimulating and a cationic compound inhibiting CYP11A1 activity. To examine the stimulatory effect of DHEAS at the molecular level, we investigated the individual steps of the reaction cycle. It was demonstrated that the binding of the CYP11A1 substrate cholesterol was improved (Fig. 5) by the presence of DHEAS. Likewise, the interaction with the redox partner, Adx, was promoted by DHEAS. Together with the observation that DHEAS increases the catalytic efficiency of CYP11A1 nearly two-fold, this indicates that improved substrate and Adx binding to CYP11A1 cause higher activity and product formation.

Interestingly, the dissociation of the CYP11A1-Adx complex was not influenced when DHEAS was added similar to the situation with polyamines [40], as the similar k_{off} values between the samples incubated with only cholesterol and the samples incubated with cholesterol in the presence of DHEAS showed. This demonstrates that the interaction between CYP11A1 and Adx is facilitated as the k_{on} values display, probably through slight conformational changes of CYP11A1 and/or Adx induced by the presence of DHEAS.

As the crystal structures of CYP11A1 and of the CYP11A1-Adx complex are available, docking studies with DHEAS were performed to get a deeper insight concerning the structure- and function- relationships (data not shown). In fact, several amino groups of the CYP11A1-Adx complex seem to be able to establish contacts to DHEAS due to its negatively charged sulfate group, leading to various putative binding sites for DHEAS. This fact makes it impossible to postulate a certain binding position of DHEAS which could explain the obtained results by a reasonable way without further experiments.

Whether the stimulatory effect of DHEAS on the CYP11A1-system might possess physiological meaning and displays a novel putative regulation of the steroid hormone biosynthesis on the cellular level, needs to be investigated. It has to be mentioned, that the concentration of DHEAS used in this work (75 μM) exceeds the plasma concentration in humans (10 μM). However, it is not known whether DHEAS is enriched in tissues. In addition, elevated DHEAS concentrations up to 10-fold might occur due to adrenocortical disorders or the additional dietary intake of DHEA or DHEAS and do not only increase the level of steroids designated for the production of sexual hormones, but also might affect the steroid biosynthesis through an increased production of pregnenolone, which represents the precursor for mineralocorticoids, glucocorticoids and sexual hormones. As a consequence, the level of the end products of the steroid hormone biosynthesis might also increase, which could cause unwanted effects on health. Elevated production of the mineralocorticoid aldosterone leads to increasing blood pressure while an increase in the production of the glucocorticoid cortisol leads to Cushing's syndrome. Thus, besides all the beneficial effects ascribed to DHEAS, intake of high amounts of DHEAS might cause undesired side effects.

Taken together, our results clearly demonstrate that the catalytic efficiency of the side-chain cleavage of cholesterol can be up-regulated by 75% in the presence of DHEAS but not DHEA. The molecular mechanism of this increase was shown to be due to improved binding of the substrate cholesterol and the redox partner, Adx.

Author Contributions

Conceived and designed the experiments: JN RB. Wrote the paper: JN RB.

References

1. Lisurek M, Bernhardt R (2004) Modulation of aldosterone and cortisol synthesis on the molecular level. Molecular and cellular endocrinology 215, 149–159.
2. Bernhardt R, Waterman MR (2007) Cytochrome P450 and Steroid Hormone Biosynthesis. The Ubiquitous Roles of Cytochrome P450 Proteins, John Wiley & Sons, Ltd. 361–396.
3. Hannemann F, Bichet A, Ewen KM, Bernhardt R (2007) Cytochrome P450 systems – biological variations of electron transport chains. Biochim Biophys Acta. 1770, 330–344. Epub 2006 Aug 2002.
4. Strott CA (1996) Steroid sulfotransferases. Endocrine reviews 17, 670–697.

5. Janowski T, Zdunczyk S, Ras A, Mwaanga ES (1999) Use of estrone sulfate determination in goat blood for the detection of pregnancy and prediction of fetal number. Tierarztliche Praxis. Ausgabe G, Grosstiere/Nutztiere 27, 107–109.
6. Claus R, Hoffmann B (1980) Oestrogens, compared to other steroids of testicular origin, in blood plasma of boars. Acta Endocrinol (Copenh) 94, 404–411.
7. Hoffmann B, Landeck A (1999) Testicular endocrine function, seasonality and semen quality of the stallion. Anim Reprod Sci. 57, 89–98.
8. Pasqualini JR, Chetrite GS (2005) Recent insight on the control of enzymes involved in estrogen formation and transformation in human breast cancer. J Steroid Biochem Mol Biol. 93, 221–236.
9. Strott CA, Higashi Y (2003) Cholesterol sulfate in human physiology: what's it all about? J Lipid Res. 44, 1268–1278.
10. Tuckey RC (1990) Side-chain cleavage of cholesterol sulfate by ovarian mitochondria. The Journal of steroid biochemistry and molecular biology 37, 121–127.
11. Korte K, Hemsell PG, Mason JI (1982) Sterol sulfate metabolism in the adrenals of the human fetus, anencephalic newborn, and adult. The Journal of clinical endocrinology and metabolism 55, 671–675.
12. Lambeth JD, Xu XX, Glover M (1987) Cholesterol sulfate inhibits adrenal mitochondrial cholesterol side chain cleavage at a site distinct from cytochrome P-450scc. Evidence for an intramitochondrial cholesterol translocator. The Journal of biological chemistry 262, 9181–9188.
13. Tsutsumi R, Hiroi H, Momoeda M, Hosokawa Y, Nakazawa F, et al. (2008) Inhibitory effects of cholesterol sulfate on progesterone production in human granulosa-like tumor cell line, KGN. Endocrine journal 55, 575–581.
14. Schuler G, Greven H, Kowalewski MP, Doring B, Ozalp GR, et al. (2008) Placental steroids in cattle: hormones, placental growth factors or by-products of trophoblast giant cell differentiation? Exp Clin Endocrinol Diabetes. 116, 429–436.
15. Geyer J, Godoy JR, Petzinger E (2004) Identification of a sodium-dependent organic anion transporter from rat adrenal gland. Biochem Biophys Res Commun. 316, 300–306.
16. Xu XX, Lambeth JD (1989) Cholesterol sulfate is a naturally occurring inhibitor of steroidogenesis in isolated rat adrenal mitochondria. The Journal of biological chemistry 264, 7222–7227.
17. Montanini V, Simoni M, Chiossi G, Baraghini GF, Velardo A, et al. (1988) Age-related changes in plasma dehydroepiandrosterone sulphate, cortisol, testosterone and free testosterone circadian rhythms in adult men. Hormone research 29, 1–6.
18. Nieschlag E, Loriaux DL, Ruder HJ, Zucker IR, Kirschner MA, et al. (1973) The secretion of dehydroepiandrosterone and dehydroepiandrosterone sulphate in man. The Journal of endocrinology 57, 123–134.
19. Baulieu EE (1996) Dehydroepiandrosterone (DHEA): a fountain of youth? The Journal of clinical endocrinology and metabolism 81, 3147–3151.
20. Sekihara H, Osawa N, Ibayashi H (1972) A radioimmunoassay for serum dehydroepiandrosterone sulfate. Steroids 20, 813–824.
21. Nawata H, Yanase T, Goto K, Okabe T, Ashida K (2002) Mechanism of action of anti-aging DHEA-S and the replacement of DHEA-S. Mechanisms of ageing and development 123, 1101–1106.
22. Baulieu EE, Thomas G, Legrain S, Lahlou N, Roger M, et al. (2000) Dehydroepiandrosterone (DHEA), DHEA sulfate, and aging: contribution of the DHEAge Study to a sociobiomedical issue. Proceedings of the National Academy of Sciences of the United States of America 97, 4279–4284.
23. Vacheron-Trystram MN, Cheref S, Gauillard J, Plas J (2002) A case report of mania precipitated by use of DHEA. Encephale. 28, 563–566.
24. Uhlmann H, Beckert V, Schwarz D, Bernhardt R (1992) Expression of bovine adrenodoxin in E. coli and site-directed mutagenesis of/2 Fe-2S/cluster ligands. Biochemical and biophysical research communications 188, 1131–1138.
25. Sagara Y, Barnes HJ, Waterman MR (1993) Expression in Escherichia coli of functional cytochrome P450c17 lacking its hydrophobic amino-terminal signal anchor. Archives of biochemistry and biophysics 304, 272–278.
26. Nishihara K, Kanemori M, Kitagawa M, Yanagi H, Yura T (1998) Chaperone coexpression plasmids: differential and synergistic roles of DnaK-DnaJ-GrpE and GroEL-GroES in assisting folding of an allergen of Japanese cedar pollen, Cryj2, in Escherichia coli. Applied and environmental microbiology 64, 1694–1699.
27. Janocha S, Bichet A, Zollner A, Bernhardt R (2011) Substitution of lysine with glutamic acid at position 193 in bovine CYP11A1 significantly affects protein oligomerization and solubility but not enzymatic activity. Biochimica et biophysica acta 1814, 126–131.
28. Kimura T, Ono H (1968) Preparation of testis non-heme iron protein and substitution for adrenodoxin by various non-heme iron proteins in steroid 11-beta-hydroxylation. Journal of biochemistry 63, 716–724.
29. Hiwatashi A, Ichikawa Y, Maruya N, Yamano T, Aki K (1976) Properties of crystalline reduced nicotinamide adenine dinucleotide phosphate-adrenodoxin reductase from bovine adrenocortical mitochonria. I. Physicochemical properties of holo- and apo-NADPH-adrenodoxin reductase and interaction between non-heme iron proteins and the reductase. Biochemistry 15, 3082–3090.
30. Omura T, Sato R (1964) The Carbon Monoxide-Binding Pigment of Liver Microsomes. Ii. Solubilization, Purification, and Properties. The Journal of biological chemistry 239, 2379–2385.
31. Schenkman JB (1970) Studies on the nature of the type I and type II spectral changes in liver microsomes. Biochemistry 9, 2081–2091.
32. Hobler A, Kagawa N, Hutter MC, Hartmann MF, Wudy SA, et al. (2012) Human aldosterone synthase: recombinant expression in E. coli and purification enables a detailed biochemical analysis of the protein on the molecular level. The Journal of steroid biochemistry and molecular biology 132, 57–65.
33. Yamato S, Nakagawa S, Yamazaki N, Aketo T, Tachikawa E (2010) Simultaneous determination of pregnenolone and 17alpha-hydroxypregnenolone by semi-micro high-performance liquid chromatography with an immobilized cholesterol oxidase as a pre-column reactor: application to bovine adrenal fasciculata cells. Journal of chromatography. B, Analytical technologies in the biomedical and life sciences 878, 3358–3362.
34. Zollner A, Kagawa N, Waterman MR, Nonaka Y, Takio K, et al. (2008) Purification and functional characterization of human 11beta hydroxylase expressed in Escherichia coli. The FEBS journal 275, 799–810.
35. Kagawa N (2011) Efficient expression of human aromatase (CYP19) in E. coli. Methods Mol Biol. 705, 109–122.
36. Wada A, Mathew PA, Barnes HJ, Sanders D, Estabrook RW, et al. (1991) Expression of functional bovine cholesterol side chain cleavage cytochrome P450 (P450scc) in Escherichia coli. Archives of biochemistry and biophysics 290, 376–380.
37. Harnastai IN, Gilep AA, Usanov SA (2006) The development of an efficient system for heterologous expression of cytochrome P450s in Escherichia coli using hemA gene co-expression. Protein expression and purification 46, 47–55.
38. Leowattana W (2004) DHEAS as a new diagnostic tool. Clinica chimica acta; international journal of clinical chemistry 341, 1–15.
39. Kroboth PD, Salek FS, Pittenger AL, Fabian TJ, Frye RF (1999) DHEA and DHEA-S: a review. Journal of clinical pharmacology 39, 327–348.
40. Berwanger A, Eyrisch S, Schuster I, Helms V, Bernhardt R (2010) Polyamines: naturally occurring small molecule modulators of electrostatic protein-protein interactions. Journal of inorganic biochemistry 104, 118–125.

2.2 NEUNZIG ET AL., 2014

A STEROIDOGENIC PATHWAY FOR SULFONATED STEROIDS: THE METABOLISM OF PREGNENOLONE SULFATE

J. Neunzig, A. Sánchez-Guijo, A. Mosa, M.F. Hartmann, J. Geyer, S.A. Wudy, R. Bernhardt

J Steroid Biochem Mol Biol. 2014 Jul 16. pii: S0960-0760(14)00129-0. doi: 10.1016/j.jsbmb.2014.07.005

Journal of Steroid Biochemistry & Molecular Biology 144 (2014) 324–333

Contents lists available at ScienceDirect

Journal of Steroid Biochemistry & Molecular Biology

journal homepage: www.elsevier.com/locate/jsbmb

A steroidogenic pathway for sulfonated steroids: The metabolism of pregnenolone sulfate

J. Neunzig [a], A. Sánchez-Guijo [b], A. Mosa [a], M.F. Hartmann [b], J. Geyer [c], S.A. Wudy [b], R. Bernhardt [a,*]

[a] Department of Biochemistry, Faculty of Technical and Natural Sciences III, Saarland University, 66123 Saarbrücken, Germany
[b] Steroid Research & Mass Spectrometry Unit, Division of Pediatric Endocrinology & Diabetology, Center of Child and Adolescent Medicine, Justus-Liebig University, 35392 Giessen, Germany
[c] Institute of Pharmacology and Toxicology, Justus-Liebig University of Giessen, 35392 Giessen, Germany

ARTICLE INFO

Article history:
Received 7 May 2014
Received in revised form 11 July 2014
Accepted 14 July 2014
Available online 16 July 2014

Keywords:
CYP17A1
Steroidogenesis
Sulfonated steroids
Pregnenolone sulfate
Mass spectrometry

ABSTRACT

In many tissues sulfonated steroids exceed the concentration of free steroids and recently they were also shown to fulfill important physiological functions. While it was previously demonstrated that cholesterol sulfate (CS) is converted by CYP11A1 to pregnenolone sulfate (PregS), further conversion of PregS has not been studied in detail. To investigate whether a steroidogenic pathway for sulfonated steroids exists similar to the one described for free steroids, we examined the interaction of PregS with CYP17A1 in a reconstituted *in-vitro* system. Difference spectroscopy revealed a K_d-value of 74.8 ± 4.2 μM for the CYP17A1–PregS complex, which is 2.5-fold higher compared to the CYP17A1–pregnenolone (Preg) complex. Mass spectrometry experiments proved for the first time that PregS is hydroxylated by CYP17A1 at position C17, identically to pregnenolone. A higher K_m- and a lower k_{cat}-value for CYP17A1 using PregS compared with Preg were observed, indicating a 40% reduced catalytic efficiency when using the sulfonated steroid. Furthermore, we analyzed whether the presence of cytochrome b_5 (b_5) has an influence on the CYP17A1 dependent conversion of PregS, as was demonstrated for Preg. Interestingly, with 17OH-PregS no scission of the 17,20-carbon–carbon bond occurs, when b_5 is added to the reconstituted *in-vitro* system, while b_5 promotes the formation of DHEA from 17OH-Preg. When using human SOAT-HEK293 cells expressing CYP17A1 and CPR, we could confirm that PregS is metabolized to 17OH-PregS, strengthening the potential physiological meaning of a pathway for sulfonated steroids.

1. Introduction

CYP11A1 initiates steroid hormone biosynthesis (Fig. 1) through a side-chain cleavage reaction on cholesterol yielding pregnenolone [1,2] which represents the precursor of all steroid hormones. In a series of reactions where six different cytochromes P450 (CYPs) and three hydroxysteroid dehydrogenases (HSD) participate, mineralocorticoids, glucocorticoids and sex hormones are formed.

In order to induce a biological response, steroid hormones interact with their corresponding receptor and thus e.g., regulation of blood pressure, provision of carbon hydrates or development of secondary sexual characteristics take place in mammalian organisms. Interestingly, sulfonated steroids or sulfated steroids [3] often circulate in mammals in considerably higher concentrations than unconjugated steroids [4–6]. Dehydroepiandrosterone (DHEA) for example, one of the most abundant steroid in humans, occurs to 99% in its sulfonated form [7], reaching concentrations of up to 10 μM in young adults [8]. Steroid sulfates are generated by sulfonation of free steroids by three different sulfotransferases (SULT1E1, SULT2B1, SULT2A1). These enzymes are widely distributed in mammalian organism, as NCBI EST profiles indicate. Sulfonation of unconjugated steroids seems to contribute to the modulation of the genomic action of steroids. For instance, SULT1E1 is highly active in cultured normal breast epithelial cells compared to tumor cell lines [9]. Since it is known that increased exposure of estrogens increases breast cancer development, sulfonation of estrogens might be a crucial mechanism to impede the danger of excessive estrogenic exposure [9]. In addition, alterations of steroid sulfonation have a severe impact on the development in mammals. DHEA is mainly produced in the adrenals and the gonads. In the gonads DHEA is further metabolized to sex hormones, but in the adrenals, due to the presence of SULT2A1, most of the DHEA is sulfonated. In case of

* Corresponding author. Tel.: +49 681 302 3005; fax: +49 681 302 4739.
E-mail address: ritabern@mx.uni-saarland.de (R. Bernhardt).

http://dx.doi.org/10.1016/j.jsbmb.2014.07.005
0960-0760/

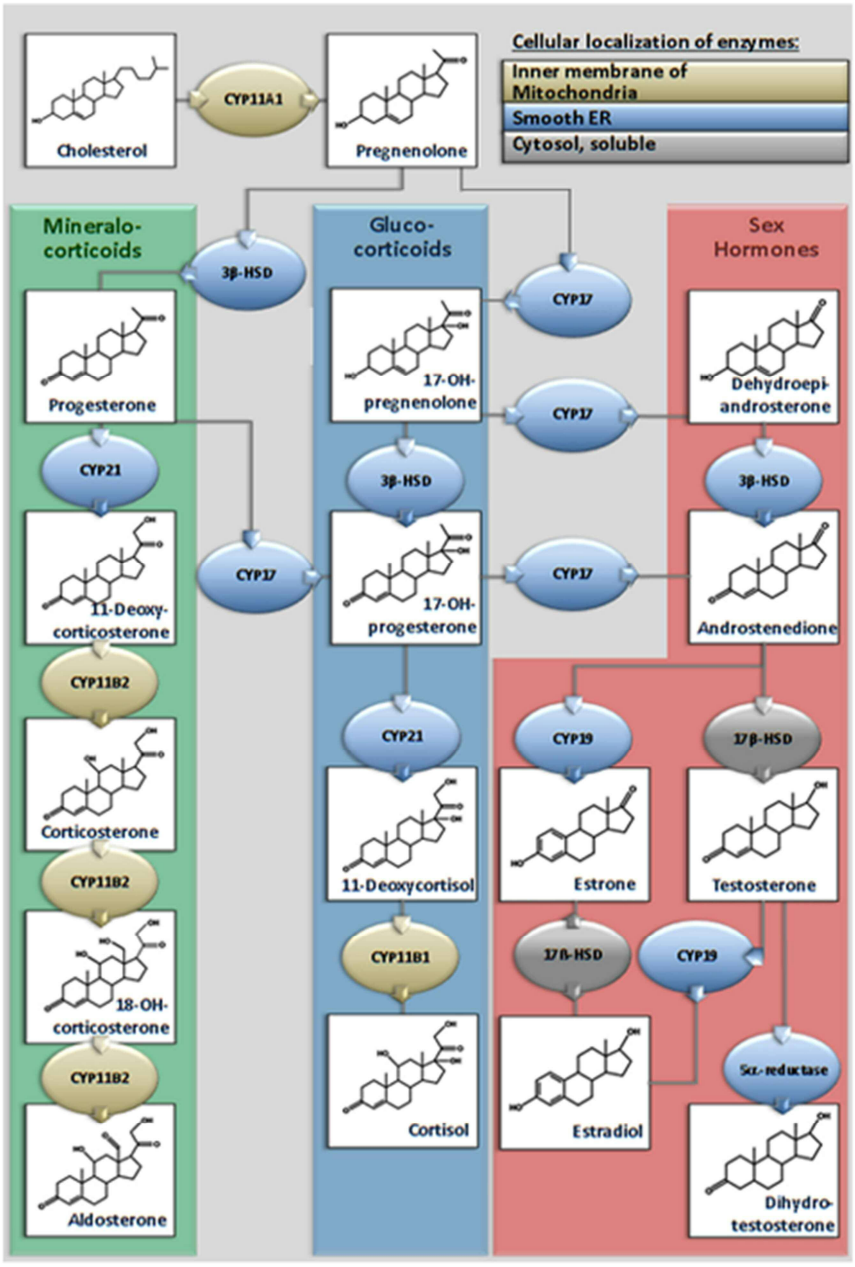

Fig. 1. Steroid hormone biosynthesis involving six cytochromes P450 and three hydroxysteroid dehydrogenases.

altered DHEA sulfonation, unconjugated DHEA accumulates, yielding to an excess of androgens and thus, virilization occurs in women [10].

On the other hand, excess of sulfonated steroids can lead to diseases, like the X-linked ichtiosis, which is caused by the accumulation of cholesterol sulfate in the epidermis [11].

Cell uptake of steroid sulfates depends on transporters of the SLC or SLCO family [12–14] as their hydrophilicity caused by the sulfate moiety hinders a passive passage. These transporters are expressed in many tissues, like liver, ovary, adrenal gland and hippocampus [15].

Sulfonated steroids have been regarded for a long time either as an end-product of xenobiotic metabolism designated for renal clearance [16] or as an inactive reservoir for unconjugated, active steroids [17]. Although the knowledge about the physiological role of steroid sulfates is still scarce, investigations about their biological function increased in the last decade. Recent studies showed that sulfonated steroid metabolites are involved in many different processes in mammalian organisms. Cholesterol sulfate (CS) possesses a stabilizing function in cell membranes; it is involved in the regulation of serine proteases and, moreover, in the differentiation of keratinocytes [18]. Recently, DHEAS was shown to induce a non-classical signaling pathway in spermatogenic cells [19]. Pregnenolone sulfate (PregS), on the other hand, represents a reservoir for pregnenolone (Preg), the precursor of mineralo-, and glucocorticoids, as well as sex hormones and it is described to act as neurosteroid modulating a big variety of ion channels, transporters, and enzymes [15]. For example, PregS was demonstrated to inhibit GABA-receptors [20], which play a crucial role in the neuronal network and to modulate *N*-methyl-D-aspartate (NMDA)-receptors. These receptors, which are essential for neuronal development and synapse formation, are heterodimers formed by several subunits (NR1, NR2A–D, NR3A–B). PregS modulates these receptors by enhancing the generation of

NR1/NR2A and NR1/NR2B receptors and inhibiting the formation of NR1/NR2C and NR1/NR2D receptors [21]. Further studies revealed that PregS promotes NMDA-receptor insertion in the cell surface [22] and thus, enhances the function of NMDA-receptors.

Moreover, PregS seems to play an essential role in reproduction as extremely increased concentrations during birth, pregnancy and parturition indicate [15].

It was demonstrated that PregS can be formed from CS through a side-chain cleavage reaction catalyzed by CYP11A1 [23] and seems to be metabolized to further sulfonated steroids as Korte et al. showed using tissue from human adrenals [24]. These findings inevitably lead to the question, whether a steroidogenic pathway for sulfonated steroids exists similar to the one described for free steroids. Trying to elucidate this question, we decided to investigate whether PregS serves as substrate for CYP17A1, a microsomal cytochrome P450 involved in the steroid hormone biosynthesis. CYP17A1 catalyzes the hydroxylation at position C17 of Preg or progesterone (Prog) yielding 17OH-Preg and 17OH-Prog, respectively, and subsequently catalyzes a 17,20-lyase reaction yielding dehydroepiandrosterone (DHEA) and androstenedione (andro) [25] (Fig. 2). In human and bovidae families (sheep, goat, bovine, bison), CYP17A1 exhibits lyase activity only toward delta5-steroids, like Preg and 17OH-Preg [26]. In these mammalian species CYP17A1 hydroxylates Prog at position C17 but 17OH-Prog is not further converted to androstenedione. Compared to the 17-hydroxylase activity, the 17,20-lyase reaction using 17OH-Preg as substrate is weak, but it is strongly enhanced in the presence of cytochrome b_5 (b_5) [27] or through phosphorylation of CYP17A1 at position 258 of its amino acid chain [28].

Here, we investigated the reaction of CYP17A1 with PregS as substrate in a reconstituted *in-vitro* system, consisting of recombinantly expressed and purified CYP17A1 and its electron transfer partner CPR, and were able to demonstrate for the first time its conversion to 17OH-PregS, but not to DHEAS.

2. Materials

Steroids were obtained from Sigma–Aldrich (Taufkirchen, Germany) or from C/D/N Isotopes Inc. (Quebec, Canada). 1,2-Dilauroyl-*sn*-glycero-3-phosphocholine (DLPC), kanamycin sulfate, arabinose, magnesium chloride, sodium hydroxide, sulfur trioxide triethylamine, sulfatase from *Helix pomatia* Type H-1 and HPLC-grade acetonitrile were from Sigma–Aldrich (Taufkirchen, Germany). Yeast extract, technical was from Becton, Dickinson and Company (Heidelberg, Germany). Pepton, pancreatically digested and Na-acetate were from Merck (Darmstadt, Germany). LCMS grade water and ammonium hydroxide were purchased from Fluka (Taufkirchen, Germany). Methanol, pyridine and ethanol were obtained from Merck (Darmstadt, Germany). SepPak C18 (360 mg) columns were from Waters Corporation (Milford, MA, USA). DMEM/F12 cell culture media and fetal calf serum were from Gibco by Life Technologies (California, USA). Imidazole and ampicillin were from CarlRoth (Karlsruhe, Germany). NADPH was from Carbolution (Saarbrücken, Germany). Glucose-6-phosphate and glucose-6-phosphate dehydrogenase were purchased from Roche (Basel, Switzerland). Protino Ni-NTA was obtained from Macherey-Nagel (Düren, Germany). 17OH-PregS was synthesized in the Steroid Research & Mass Spectrometry Unit, Division of Pediatric Endocrinology & Diabetology, Center of Child and Adolescent Medicine, Justus-Liebig University. All other chemicals were of highest purity available.

3. Experimental

3.1. Construction of recombinant expression plasmids in E. coli

The plasmid pET-17b was utilized to express bovine CYP17A1, b_5 and CPR in *E. coli*. Each cDNA was cloned via the restriction sites NdeI and BamHI into the vector. The cDNAs of b_5 and CPR were obtained through amplification from a cDNA library of bovine liver (Zyagen, California, USA). CYP17A1 cDNA was kindly provided by Prof. M. Waterman (Vanderbilt University, Nashville, USA). The amino acid sequence of CYP17A1 is lacking its N-terminal hydrophobic anchor [29] and is extended at the C-terminus by a hexa-histidine-tag to facilitate purification. The CPR amino acid sequence is extended at the C-terminus by three glycines and six histidines and at the N-terminus has a lack of the first 27 amino acids [30]. Cytochrome b_5 is extended at the C-terminus by a hexa-histidine-tag. For human cell culture studies, the plasmid pVITRO1-neo-mcs (Invivogen) was used to express CYP17A1 and CPR. The cDNAs of CYP17A1 and CPR were cloned via the restriction sites AgeI and BsrGI (CYP17A1) and BspEI and AvrII (CPR) into the vector. Both cDNAs were obtained from a cDNA library of bovine adrenal (CYP17A1) and bovine liver (CPR).

3.2. Protein expression and purification

Bovine CYP17A1 was co-expressed with chaperones GroEL and GroES similar to CYP21 expression [31]. As host *E. coli* strain C43DE3 was used. The expression was performed in 2 L baffled flasks containing 400 ml TB medium supplemented with 100 μg/ml ampicillin and 50 μg/ml kanamycin. The expression culture was inoculated from an overnight culture and grown at 37 °C and 120 rpm. Protein expression was induced at OD_{600} = 0.6 with 1 mM IPTG, 4 mg/ml arabinose, 1 mM δ-ALA and 50 μg/ml ampicillin. Afterwards, temperature was decreased to 26 °C and the cells incubated at 95 rpm for 48 h. Cells were harvested and sonicated as described elsewhere [32]. The purification was performed as described for CYP11B1 [33].

Bovine CPR was expressed in *E. coli* strain C43DE3 using similar conditions as described for bovine CYP17A1 with slight modifications: 2 L baffled flasks containing 300 ml TB medium were used and after induction of protein expression temperature was reduced to 30 °C and incubated at 100 rpm for 30 h. Cells were harvested and sonicated as described elsewhere [32]. CPR was purified via IMAC as described elsewhere [33] with 40 mM imidazole in the washing buffer and 200 mM imidazole in the elution buffer.

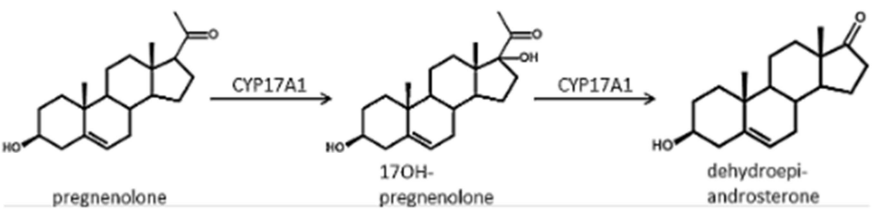

Fig. 2. Reaction catalyzed by CYP17A1. Pregnolone is hydroxylated at position C17 yielding 17OH-pregnenolone, and subsequently the 17,20-carbon–carbon bond scission takes place yielding DHEA.

Bovine b_5 was expressed according to Mulrooney et al. [34] using *E. coli* strain C43DE3. Purification was done as described for bovine CPR.

3.3. UV–vis spectroscopy

The protein concentration of the CPR was determined using a molar extinction coefficient $\varepsilon_{585} = 2.4\,mM^{-1}\,cm^{-1}$ [35]. Cytochrome b_5 concentration was calculated by using a difference extinction coefficient of $185\,mM^{-1}\,cm^{-1}$ for the absorbance change at 424–409 nm [34]. CYP17A1 concentration was calculated from a reduced carbon-monoxide difference spectroscopy according to Omura and Sato [36] with $\varepsilon_{448} = 91\,mM\,cm^{-1}$. Binding of Preg and PregS was investigated using difference spectroscopy, which was carried out in tandem cuvettes according to Schenkman [37]. Preg and PregS were dissolved in DMSO. The buffer utilized was composed of 50 mM HEPES (pH 7.4), 20% glycerol, and 100 μM dilauroyl phosphatidylcholin (DLPC). Difference spectra were recorded from 370 to 450 nm. To determine the dissociation constant (K_d), the values from three titrations were averaged and the resulting plots were fitted with hyperbolic regression.

3.4. Enzyme activity assay

In-vitro substrate conversion assays were done as described elsewhere [38] with slight modifications. The conversion buffer (50 mM HEPES, pH 7.4, 20% glycerol, 100 μM DLPC) contained 1 μM CYP17A1, 1 μM CPR, 1 mM $MgCl_2$, 5 mM glucose-6-phosphate, 1 U glucose-6-phosphate dehydrogenase for NADPH regeneration and varying concentrations of Preg or PregS as substrate. When substrate conversion assays were performed to investigate the influence of b_5, 4 μM of b_5 were added to the conversion buffer. After starting the reaction with 1 mM NADPH at 37 °C for 40, 50 and 60 min, the conversion was stopped in a boiling water bath for 5 min. Preg and the resulting product 17OH-Preg had to be converted to the corresponding 3-one-4-en form by cholesterol oxidase, to be detectable at 240 nm during HPLC analysis. Therefore, cholesterol oxidase was added to the boiled reaction mixture and incubated for 40 min at 37 °C according to Yamato [39]. Cortisol was added as internal standard. The reaction was stopped by addition of one reaction volume of ethylacetate. Extraction of steroids was performed twice with ethylacetate and the ethylacetate phase was evaporated. The steroids were resuspended in 20% acetonitrile for subsequent HPLC analysis. Steroids were separated on a Jasco reversed phase HPLC system LC2000 using a 4 mm × 125 mm Nucleodur C18 reversed phase column (Macherey-Nagel) with an acetonitrile/water gradient and a flow rate of 1 ml/min. Detection of the steroids was performed at 240 nm within 30 min at 40 °C. For analysis of sulfonated steroids mass spectrometry and liquid chromatography were utilized.

3.5. Substrate conversion in SOAT-HEK293 cells

For substrate conversion studies, 6-well plates were coated with poly-D-lysine for better attachment of the cells as described elsewhere [40]. 3×10^5 cells/well were plated and maintained in DMEM/F-12 (Invitrogen) medium with 10% fetal calf serum (Sigma), L-glutamine (4 mM), penicillin (100 units/ml) and tetracycline (1 μg/ml) (for SOAT expression). The cells were grown for 16 h at 37 °C and 5% CO_2 until they reached a confluency of 70%. Afterwards, they were transiently transfected with a plasmid containing the cDNAs of CYP17A1 and CPR with the Effectene Transfection Kit of Qiagen. After 5 h of incubation (37 °C and 5% CO_2), PregS (10 and 20 μM) was added and the cells were further incubated for 70 h, 37 °C and 5% CO_2. Subsequently, samples of 1 ml/well were collected and prepared for LC/MS-analysis.

3.6. Sample analysis by liquid chromatography-tandem mass spectroscopy (LC-MS/MS)

The studies were performed using a triple quadrupole mass spectrometer (TSQ, Quantum Ultra, Thermo Fisher Scientific, Dreieich, Germany) with electrospray ionization (ESI) in negative mode. Mass spectrometric parameters for sulfonated steroids were as described elsewhere [41]. For the in-house synthesized compound, 17OH-PregS, the collision energy and tube lens values were calculated, being similar to other sulfonated steroids. The selected quantifier transition was 411 →97. The collision energy was 32 eV and the tube lens value was 180 V. A C18 reverse phase column was used for the chromatographic method (Hypersil Gold column 50 × 2.1 mm, 5 μm, Thermo Fisher Scientific, Dreieich, Germany), mounted within a HPLC system (Agilent 1200SL, Waldbronn, Germany). Different concentrations of pure water and pure methanol (MeOH) were applied to achieve the separation of the compounds (Table 1). The retention time for both the enzymatically obtained 17OH-PregS and for the synthetic 17OH-PregS were the same.

3.7. Sample preparation and calibrations

The samples were always diluted due to the high concentrations of the analytes, and of the presence of buffer components that may affect the ionization process. At least two dilutions had to be used for each sample, as the concentrations of PregS and 17OH-PregS after enzymatic conversion were very different (high concentrations of PregS when compared to 17OH-PregS concentrations). The dilutions were made in a mixture containing MeOH, water and ammonia to facilitate dissolution and to improve the ionization of the analytes in negative mode (90.00% MeOH, 9.95% H_2O and 0.05% NH_3). In case a precipitate was observed, the samples were centrifuged and the clear supernatant was analyzed. The dilution was usually performed in glass vials which were first vortexed and later shaked for 30 min to allow equilibration with the internal standards. The calibration points for the calibration curve were prepared adding the same amount of buffer and internal standards (IS). d6DHEAS was used as IS for 17OH-PregS and d4PregS for PregS. Calibrations showed values always higher than 0.99 for R^2. Data analysis was performed with Thermo Xcalibur 2.1 software (Thermo Fisher Scientific, Dreieich, Germany).

3.8. Determination of kinetic parameters

K_m and k_{cat}-values were determined by plotting the substrate conversion velocities versus the corresponding substrate concentrations and by using Michaelis–Menten kinetics (hyperbolic fit) for Preg or Hill kinetics (sigmoidal fit) for PregS utilizing the program OriginPro 8.6G.

Table 1
LC Table-flows and gradients.

Start	Seconds	Flow	% H_2O	% MeOH
0.00	60	0.45	70	30
1.00	60	0.50	55	45
2.00	20	0.50	40	60
2.33	80	0.50	5	95
3.67	60	0.50	40	60
4.67	30	0.50	55	45
5.17	30	0.45	70	30

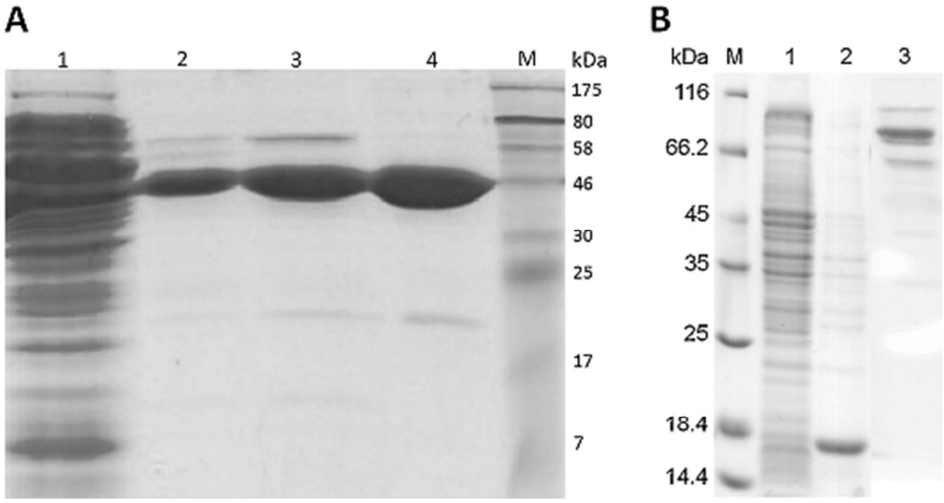

Fig. 3. SDS-polyacrylamide gel electrophoresis. (A) Lane 1: supernatant; lane 2: CYP17A1 after purification via IMAC; lane 3: CYP17A1 after purification via IMAC and DEAE-sepharose; lane 4: CYP17A1 after purification via IMAC, DEAE-sepharose and SP-sepharose; lane M: marker. (B) Lane M: marker; lane 1: supernatant; lane 2: b_5 after IMAC purification; lane 3: CPR after IMAC purification.

3.9. Synthesis and purification of 17OH-PregS

The method is based on Dusza et al. [42], with some modifications. Briefly, 1 mg of 17OH-Preg and 0.85 mg of triethylamine sulfur trioxide were mixed in 100 μl of anhydrous pyridine, in a 2 ml glass vial. The mixture was shaked at low speed during 3 h at room temperature, and consecutively evaporated. The residue was redissolved in 500 μl of ethanol. Then, 500 μl of NaOH 0.2 M in methanol were added, and a white precipitate was observed. After evaporation, the precipitate was washed twice with methanol.

Several HPLC-MS/MS analyses were performed to assess the purity of the reaction product. An aliquot of the solution was dissolved in a mixture of water:MeOH (1:1 v/v) and analyzed in positive full scan mode as previously described [41]. The product was free of 17OH-Preg, as no peak was present at 4.2 min, whereas a peak with *m/z* 297.2 at 0.75 min was observed. This mass-to-charge ratio value is identical to that of 17OH-Preg, and it is due to $(M - H_2O - H_2SO_4 + H)^+$.

The same chromatographic method was applied to ESI negative mode. The *m/z* value of the peak at 0.75 min was 411, molecular ion. A minority peak at 0.18 min was then found in negative mode. This peak corresponded to the disulfate fraction of 17OH-Preg, with *m/z* of 245, $(M - 2H)^{-2}$. Sulfonation of the hydroxyl group in position 3beta is favored over the sterically hindered 17alpha position.

Next, the mixture was purified with a solid phase extraction step. The precipitate was re-dissolved in a water:MeOH solution (70:30 v/v) and loaded onto a Sep-Pak column after activation. A gradient of MeOH was then applied (0–100%) and the fractions corresponding to 40–50% of MeOH were collected, discarding the rest. Those fractions were free of disulfate component, showing a clear single peak in the same chromatographic conditions described before.

The fractions collected after purification step were evaporated under nitrogen flow and weighed. A standard working solution was then prepared (250 μg/mL in MeOH).

In order to calculate the purity of the final solution, two aliquots, of 20 μl and 40 μl, were treated with 75 units of sulfatase at 37 °C during 6 h. The reaction products were then quantified using the aforementioned procedure described in Galuska et al. [41] for 17OH-Preg quantification. The analysis in negative mode proved that they were free of 17OH-PregS. The calculated purity was 90%.

4. Results and discussion

The levels of sulfonated steroids exceed in many species and tissues considerably the levels of the corresponding unconjugated steroids. In human, the plasma level of PregS varies significantly during life. The highest level is reached after birth with concentrations between 2–3 μM, depending on the gender, and afterwards rapidly decreases in the first year up to concentrations of about 30–50 nM [43]. During and after adrenarche, the PregS

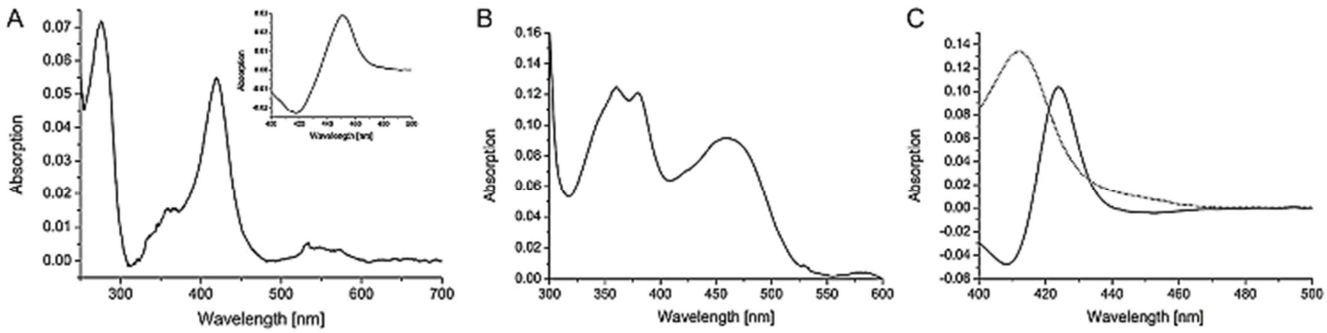

Fig. 4. Spectra of purified recombinant CYP17A1 (A), CPR (B) and b_5 (C). (A) Full spectrum of purified CYP17A1 recorded from 700 nm to 260 nm. The inset shows the CO-difference spectrum from 500 nm to 400 nm. (B) Spectrum of purified CPR recorded from 600 nm to 300 nm. (C) Spectrum of purified b_5 in its oxidized form (dotted line) and difference spectrum (reduced–oxidized) (solid line).

Table 2
Amount of heterologously expressed CPR, b_5 and CYP17A1.

	Yield of purified protein (mg/l)
CPR	34
b_5	22
CYP17A1	73

level in plasma again increases, achieving concentrations of 130–140 nM [43]. Although PregS represents a steroid hormone displaying high abundance in human and other mammalian organism [44] and exceeding its unconjugated form (0.9–6 nM [45]) by several folds, its influence on steroid hormone biosynthesis is poorly investigated. Moreover, it was already demonstrated that CS is converted to PregS through a CYP11A1 dependent reaction [23] leading necessarily to the issue whether also other sulfonated steroids are converted by enzymes involved in the steroid hormone biosynthesis, equally to free steroids. Korte et al. [24] suggested that CS is converted to PregS and afterwards to dehydroepiandrosterone sulfate (DHEAS), based on their observation that the fetal plasma contains very high levels of PregS and DHEAS. However, experiments to support this assumption were not performed in this early study. The conversion of PregS to sulfonated products was demonstrated by Jaffe et al. [46] and Lamont et al. [47] in the early 70 s, but, they did not identify the enzyme involved in this reaction. Therefore, it was the aim of our study to investigate, whether CYP17A1 is able to convert PregS.

4.1. Expression and purification of CPR, b_5 and CYP17A1

The three proteins necessary to perform *in-vitro* conversions of PregS were expressed in bacteria and purified from there.

For expression of the three proteins, *E. coli* C43DE3 were chosen as host, as this strain was described to display high expression yields for membrane-bound cytochrome P450's [33,38,48] and other membrane-bound proteins [49].

CPR and b_5 were purified by IMAC NTA, whereas CYP17A1 was purified at first by IMAC NTA followed by an anion exchange DEAE-sepharose and, in a last step, by an ion exchange SP-sepharose. The purity of the proteins was determined via SDS-gel electrophoresis (Fig. 3), in which a single band was obtained for CYP17A1 at 45 kDa and for b_5 at 17 kDa. CPR showed a main band at 70 kDa and two unknown bands located above and below the band corresponding to CPR. Further experiments, like

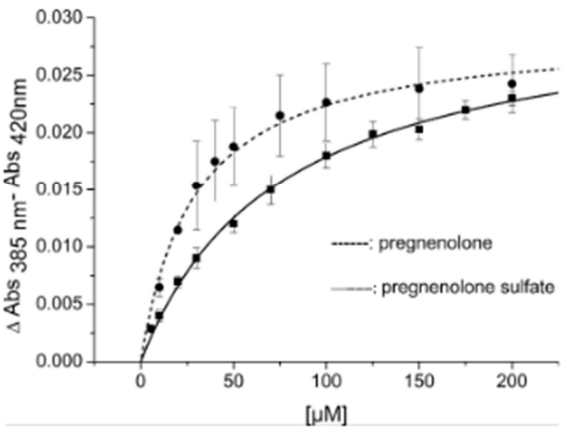

Fig. 5. Determination of substrate binding affinity to CYP17A1. The enzyme (1 μM) was titrated with increasing concentrations of Preg (dotted line) and PregS (solid line) dissolved in DMSO. The absorbance changes were plotted against the substrate concentration and fitted as described; R^2: 0.99; $n = 3$.

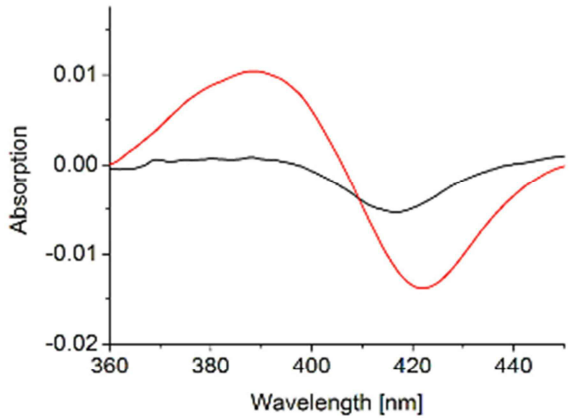

Fig. 6. Difference spectroscopy of CYP17A1 titrated with 150 μM PregS (red) and 150 μM 17OH-PregS (black). (For interpretation of the references to colour in this figure legend, the reader is referred to the web version of this article.)

the cytochrome c test (data not shown), spectral characterization (Fig. 4B) and substrate conversion experiments with CYP17A1 suggested an undisturbed catalytic function of CPR.

The UV–vis spectrum categorizes the expressed CYP17A1 as a low-spin protein with the characteristic cytochrome P450 absorption spectrum: the Q bands at 569 nm (α-band) and 541 nm (β-band), the Soret band at 418 nm, the UV band at 360 nm and the protein-band at 278 nm (Fig. 4A). Moreover, the enzyme displays a typical CO-difference spectrum, with a major peak at 450 nm and a minor peak at 420 nm (Fig. 4A inset). Spectral analysis of CPR also reveals its typical absorption spectrum: the enzyme shows its major peaks at 360 nm, 380 nm, and at 453 nm, indicating its air-stable semiquinone (FMNH·, FAD) form [50] (Fig. 4B). Cytochrome b_5 exhibits a major peak at 412 nm in its oxidized state, as well as a major peak at 424 nm and a minor peak at 409 nm in the difference (reduced–oxidized) spectrum [34] (Fig. 4C).

The amounts of CPR, b_5 and CYP17A1, respectively, obtained after purification are listed in Table 2.

Using *E. coli* C43DE3 as host, the expression yield of b_5 is similar to literature data [51], that of CYP17A1 achieved 73 mg/l, which is a great improvement compared to published data [29]. The expression yield of bovine CPR described here for the first time was 34 mg/l.

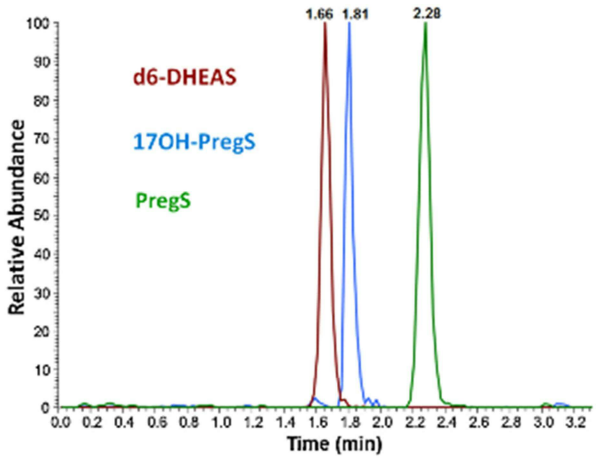

Fig. 7. Merged chromatogram of the analytes obtained from a conversion sample, as detected by ID-LC-MS/MS (peak at 1.66 min is d6-DHEAS, peak at 1.91 min is 17OH-PregS whereas peak at 2.28 min is PregS).

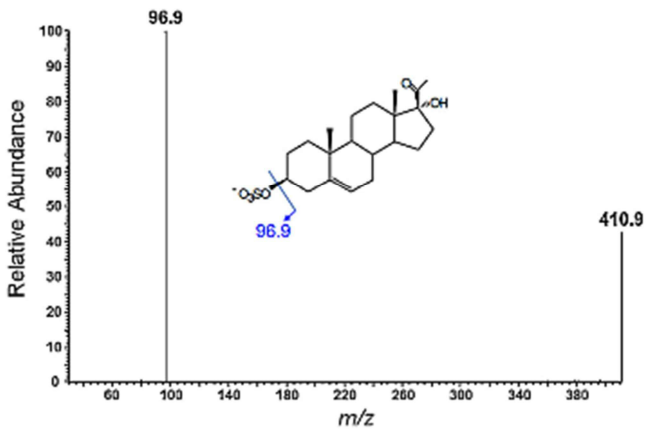

Fig. 8. Product-ion mass spectra of the molecular ion of 17OH-PregS (collision energy 32 eV). The predominant fragment ion at *m/z* 96.9 is due to the hydrogensulfate anion (HSO_4^-).

4.2. Determination of dissociation constants of CYP17A1 with pregnenolone and pregnenolone sulfate

In order to investigate the binding affinity of Preg and PregS with CYP17A1 in detail, we performed spectroscopic studies to determine dissociation constants (K_d). The experiments revealed a K_d-value for CYP17A1 and Preg of 28.9 ± 3.1 μM and for CYP17A1 and PregS of 74.8 ± 4.2 μM (Fig. 5), indicating a higher affinity of CYP17A1 toward the unconjugated pregnenolone.

Moreover, we aimed to compare the affinity of CYP17A1 toward PregS and its product 17OH-PregS. As the spectral change of CYP17A1 in the presence of 17OH-PregS was too low to determine the K_d-value, we compared the spectral change of CYP17A1 in the presence of 150 μM PregS and 150 μM 17OH-PregS (Fig. 6). In contrast to PregS, which induces a type I shift typical for substrates, 17OH-PregS does not, or only to a very low extend, influence the spectral properties of CYP17A1. This is an indication that 17OH-PregS might not be in a binding position suitable for further conversion.

4.3. Sample analysis by liquid chromatography-tandem mass spectrometry (LC-MS/MS)

In order to analyze the conversion of sulfonated steroids, we established a new LC-MS/MS method. This is the first time, to our knowledge, that 17OH-PregS has been quantified by LC-MS/MS, which represents the technique of choice to analyze sulfonated steroids [41]. In Fig. 7 a merged chromatogram for PregS, 17OH-PregS and DHEAS is displayed (detection by multiple reaction monitoring). All three steroid sulfates are baseline-resolved.

Fig. 8 shows the product-ion mass spectra of 17OH-PregS (molecular ion with *m/z* value of 411). This methodological development facilitates the analytical basis for the PregS metabolism in our reconstituted *in-vitro* system.

4.4. CYP17A1 dependent 17OH-pregnenolone and 17OH-pregnenolone sulfate conversion

Since we could clearly demonstrate that PregS efficiently interacts with CYP17A1, the next step was to evaluate whether the sulfonated steroid can be converted by CYP17A1. In mammalian steroidogenesis, CYP17A1 catalyzes the conversion of Preg to 17OH-Preg and DHEA. In our reconstituted *in-vitro* system nearly no lyase reaction and thus very little DHEA formation could be observed, because of the absence of b_5. Using PregS, we could demonstrate that it serves as a substrate for CYP17A1 and is converted to a considerable amount to 17OH-PregS. The kinetic parameters were determined to be K_m = 30.00 ± 3.31 μM and k_{cat} = 0.60 ± 0.02 (min^{-1}) for 17OH-Preg formation using Preg as substrate and K_m = 36.72 ± 3.22 μM and k_{cat} = 0.44 ± 0.03 (min^{-1}) for 17OH-PregS formation when PregS was utilized as substrate (Fig. 9). Comparing the curve shapes of the kinetics of CYP17A1 with Preg or with PregS a significant difference can be observed: in contrast to the hyperbolic shape of CYP17A1 with Preg (Fig. 9A), the kinetics of CYP17A1 with PregS display a sigmoidal form (Fig. 9B). When considering the surface of the CYP17A1 crystal structure [52], several positively charged regions that might act as potential interaction sites with the negatively charged sulfate moiety of PregS are found. This could lead to a decreased conversion rate at low substrate concentrations until these unspecific binding sites are saturated and could thus explain the sigmoidal character of the kinetics of CYP17A1 with PregS.

In Table 3, the kinetic parameters are summarized, revealing a catalytic efficiency k_{cat}/K_m for CYP17A1 toward Preg of 20.0 (min^{-1} mM^{-1}), which is two-fold higher compared to the catalytic efficiency toward PregS with k_{cat}/K_m = 11.9 (min^{-1} mM^{-1}).

Consequently, the nearly 2-fold increased catalytic efficiency of CYP17A1 converting Preg in comparison with PregS seems to be due to a higher affinity, as the K_d- and K_m-values indicate and to an higher k_{cat}-value. The K_d-value for CYP17A1 and PregS is about 2.5-fold higher compared with Preg (Fig. 5). Thus, PregS possesses less affinity to CYP17A1. By favoring Preg as a substrate, CYP17A1 might be able to compensate for the lower concentration

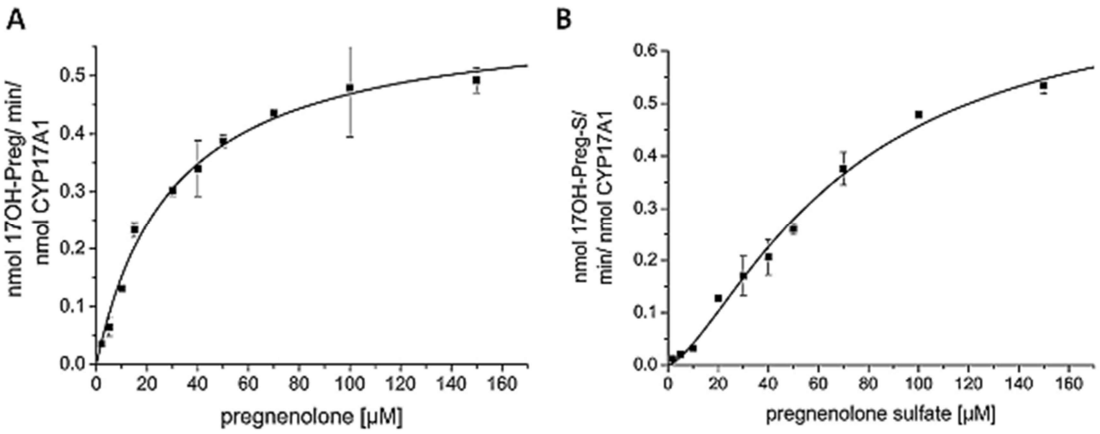

Fig. 9. (A) Kinetics of Preg to 17OH-Preg conversion catalyzed by CYP17A1 using CPR as redox partner; R^2: 0.99. (B) Kinetics of PregS to 17OH-PregS conversion catalyzed by CYP17A1 utilizing CPR as redox partner; R^2: 0.98.

Table 3
Kinetic parameters of CYP17A1 metabolizing Preg and PregS, respectively.

Pregnenolone			Pregnenolone sulfate		
K_m (mM)	k_{cat} (min^{-1})	k_{cat}/K_m (min^{-1} mM^{-1})	K_m (mM)	k_{cat} (min^{-1})	k_{cat}/K_m (min^{-1} mM^{-1})
0.030 ± 0.003	0.60 ± 0.02	20.00	0.036 ± 0.003	0.44 ± 0.03	11.98

of Preg in the plasma. However, since concentrations of Preg and PregS in tissues expressing CYP17A1 are unknown, the physiological importance of this observation is not clear yet.

4.5. Effect of b_5 on CYP17A1 dependent substrate conversions

The first reaction step of CYP17A1 consists of a 17-hydroxylation of Preg and is followed by a 17,20-carbon–carbon bond scission yielding DHEA, as shown in Fig. 2. The augmentation by several folds of the lyase of CYP17A1 in the presence of b_5 is well reported [53,54]. It is postulated that the effect of b_5 on this second reaction step of CYP17A1 is based on an allosteric interaction of b_5 with CYP17A1, enhancing the alignment of the iron–oxygen complex onto the C20 rather than the C17 atom of the steroid, hence augmenting the lyase reaction [27]. Further studies are necessary to confirm this hypothesis. Very recently, Scott and co-workers [55] demonstrated that structural changes occur at the proximal surface of CYP17A1 depending on the substrate binding. In reverse, they claim that binding of b_5 to the proximal surface of CYP17A1 induces changes in the active site of CYP17A1, leading to an enhanced lyase activity.

For this reason, we investigated the effect of b_5 on CYP17A1 dependent conversion of Preg and PregS. In our reconstituted *in-vitro* system, the lyase reaction was nearly absent without addition of b_5. Using 30 μM Preg as substrate for CYP17A1, 0.08 ± 0.02 μM DHEA is formed. In contrast, in the presence of b_5 the CYP17A1 dependent conversion of Preg to DHEA is strongly increased, forming 1.02 ± 0.07 μM DHEA, thus augmenting the lyase activity about 10-fold (Fig. 10). The relatively low lyase activity is in accordance with previous studies of Barnes et al. [56] demonstrating that the formation of DHEA is time-depending and starts after accumulation of the intermediate 17OH-Preg. Studies using 17OH-Preg instead of Preg as substrate also show higher levels of DHEA formation [57].

To our surprise, the conversion of PregS was not influenced by addition of b_5. Whether or not b_5 was present, no scission of the 17,20-carbon–carbon bond took place and, consequently, no DHEAS was formed. It seems that the sulfate moiety hinders the alignment of the iron–oxygen complex onto the C20 atom of 17OH-PregS, possibly due to the increased size of the molecule and/or to the negative charge of the sulfate, which finally prevents the lyase reaction of CYP17A1 on 17OH-PregS. As discussed before and shown in Fig. 6, difference spectroscopy performed with CYP17A1 in the presence of 17OH-PregS showed that this metabolite might not to be capable to enter in the active site of CYP17A1, as nearly no spectral change of CYP17A1 was induced. This means that DHEAS seems to be produced solely by sulfonation of DHEA catalyzed by sulfotransferases, whereas PregS and 17OH-PregS can either be synthesized by sulfonation of unconjugated Preg and 17OH-Preg or by further conversion of CS or PregS.

4.6. CYP17A1 dependent substrate conversion in SOAT-HEK293 cells

To investigate whether the results concerning the conversion of PregS observed in our reconstituted *in-vitro* system may possess potential physiological meaning, we performed conversion experiments in SOAT-HEK293 cells. This cell line exhibits an integrative gene encoding for the human sodium-dependent organic anion transporter (SOAT), which was shown to display high specificity toward PregS [40]. SOAT-HEK293 cells were transiently transfected with a plasmid containing genes encoding for CYP17A1 and its electron transfer partner, CPR. LC-MS/MS analysis after three days of incubation with PregS could clearly confirm the formation of reasonable amounts of 17OH-PregS. As shown in Fig. 11, 2.30 ± 0.30 μM 17OH-PregS was synthesized when 20 μM PregS was used as substrate. Also in this case, no DHEAS could be detected, confirming our *in-vitro* results, where no 17,20-lyase activity could be attributed to CYP17A1 using PregS as substrate. In contrast, when using 20 μM Preg as substrate, 5.30 ± 0.35 μM 17OH-Preg, as well as 0.86 ± 0.2 μM DHEA are formed (Fig. 11).

The utilized cell line exhibits RNA expression of b_5 and MAPK14 as "The Human Protein Atlas" indicates. MAPK14 (p38alpha) is a kinase that phosphorylates CYP17A1 at position 258 of the amino acid chain [58]. This post-translational modification of CYP17A1 is described to enhance the lyase reaction of CYP17A1, similar to the effect of b_5 [28]. The presence of these two proteins (b_5, MAPK14) obviously supports the formation to 17OH-Preg and DHEA using Preg as substrate. However, the lyase reaction of CYP17A1 does not take place in these cells with PregS as substrate. In cell culture as well as in the reconstituted *in-vitro* system 17OH-PregS represents the end product of the CYP17A1 catalyzed reaction using PregS as substrate.

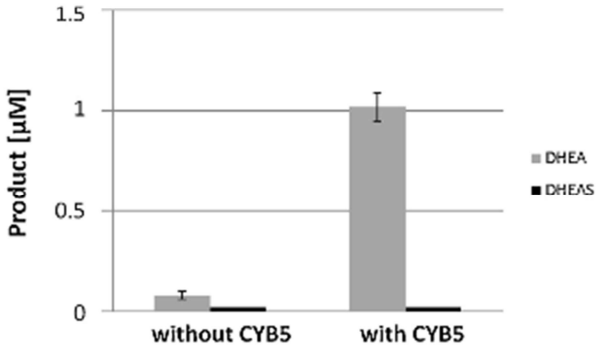

Fig. 10. Comparison of DHEA and DHEAS formation by CYP17A1 in absence and in the presence of b_5 using Preg and PregS, respectively, as substrate ($n = 5$).

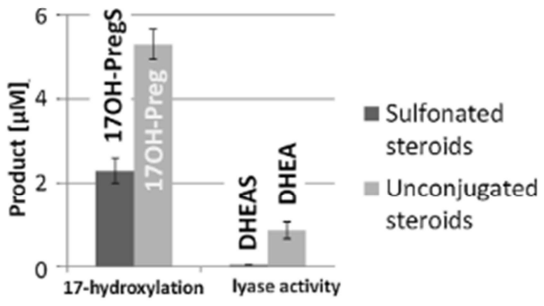

Fig. 11. Conversion of 20 μM PregS (black) and 20 μM Preg (grey) in SOAT-HEK293 cells. The product formation analyzed by LC-MS/MS (black) and HPLC (grey) is represented as mean ± standard deviation of five (black) and three (grey) individual experiments.

5. Summary

In this work we could clearly demonstrate that PregS serves as a substrate for CYP17A1, being converted to 17OH-PregS. Summarizing, we demonstrated for the first time that CYP17A1, which is involved in the steroid hormone biosynthesis, can convert sulfonated steroids in a similar manner as free steroids indicating a potential alternative steroidogenic pathway for sulfonated steroids. As already described, this pathway is initiated by the side-chain cleavage of CS by CYP11A1, yielding PregS [23]. Subsequently, PregS is metabolized in a CYP17A1 dependent hydroxylation reaction to 17OH-PregS, but not to DHEAS. At this point the steroidogenic pathway for sulfonated steroids differs from the one for free steroids yielding DHEA in large quantities. The k_{cat}- and K_m-values, as well as the K_d-value were determined for CYP17A1 with PregS. Moreover, we showed that b_5 does not enhance the 17,20-lyase activity of CYP17A1 when PregS was used as substrate, highlighting fundamental differences between the metabolism of free Preg and sulfonated Preg by CYP17A1. Utilizing a SOAT-HEK293 whole cell system, expressing SOAT, CYP17A1 and CPR, we confirmed the conversion of PregS into 17OH-PregS and the absence of the CYP17A1 dependent lyase reaction, indicating a potential physiological relevance of our findings.

Acknowledgement

The financial support of the Deutsche Forschungsgemeinschaft DFGFOR1369 is gratefully acknowledged.

References

[1] M. Lisurek, R. Bernhardt, Modulation of aldosterone and cortisol synthesis on the molecular level, Mol. Cell Endocrinol. 215 (2004) 149–159.
[2] R. Bernhardt, M.R. Waterman, Cytochrome P450 and steroid hormone biosynthesis, The Ubiquitous Roles of Cytochrome P450 Proteins, John Wiley & Sons, Ltd., Chichester, UK, 2007, pp. 361–396.
[3] D. Fietz, K. Bakhaus, B. Wapelhorst, G. Grosser, S. Gunther, et al., Membrane transporters for sulfated steroids in the human testis – cellular localization, expression pattern and functional analysis, PLoS One 8 (2013) e62638.
[4] T. Janowski, S. Zdunczyk, A. Ras, E.S. Mwaanga, Use of estrone sulfate determination in goat blood for the detection of pregnancy and prediction of fetal number, Tierarztl. Prax. Ausg. G Grosstiere Nutztiere 27 (1999) 107–109.
[5] R. Claus, B. Hoffmann, Oestrogens, compared to other steroids of testicular origin, in blood plasma of boars, Acta Endocrinol. (Copenhagen) 94 (1980) 404–411.
[6] B. Hoffmann, A. Landeck, Testicular endocrine function, seasonality and semen quality of the stallion, Anim. Reprod. Sci. 57 (1999) 89–98.
[7] W. Leowattana, DHEAS as a new diagnostic tool, Clin. Chim. Acta 341 (2004) 1–15.
[8] E.E. Baulieu, Dehydroepiandrosterone (DHEA): a fountain of youth? J. Clin. Endocrinol. Metab. 81 (1996) 3147–3151.
[9] E. Anderson, A. Howell, Oestrogen sulphotransferases in malignant and normal human breast tissue, Endocr. Relat. Cancer 2 (1995) 227–233.
[10] C. Noordam, V. Dhir, J.C. McNelis, F. Schlereth, N.A. Hanley, et al., Inactivating PAPSS2 mutations in a patient with premature pubarche, N. Eng. J. Med. 360 (2009) 2310–2318.
[11] P.M. Elias, D. Crumrine, U. Rassner, J.P. Hachem, G.K. Menon, et al., Basis for abnormal desquamation and permeability barrier dysfunction in RXLI, J. Invest. Dermatol. 122 (2004) 314–319.
[12] J. Geyer, B. Doring, K. Meerkamp, B. Ugele, N. Bakhiya, et al., Cloning and functional characterization of human sodium-dependent organic anion transporter (SLC10A6), J. Biol. Chem. 282 (2007) 19728–19741.
[13] G. Grosser, D. Fietz, S. Gunther, K. Bakhaus, H. Schweigmann, et al., Cloning and functional characterization of the mouse sodium-dependent organic anion transporter Soat (Slc10a6), J. Steroid Biochem. Mol. Biol. 138 (2013) 90–99.
[14] M.V. St-Pierre, B. Hagenbuch, B. Ugele, P.J. Meier, T. Stallmach, Characterization of an organic anion-transporting polypeptide (OATP-B) in human placenta, J. Clin. Endocrinol. Metab. 87 (2002) 1856–1863.
[15] C. Harteneck, Pregnenolone sulfate: from steroid metabolite to TRP channel ligand, Molecules 18 (2013) 12012–12028.
[16] C.A. Strott, Steroid sulfotransferases, Endocr. Rev. 17 (1996) 670–697.
[17] J.R. Pasqualini, G.S. Chetrite, Recent insight on the control of enzymes involved in estrogen formation and transformation in human breast cancer, J. Steroid Biochem. Mol. Biol. 93 (2005) 221–236.
[18] C.A. Strott, Y. Higashi, Cholesterol sulfate in human physiology: what's it all about? J. Lipid Res. 44 (2003) 1268–1278 Epub 2003 May 1261.
[19] M. Shihan, U. Kirch, G. Scheiner-Bobis, Dehydroepiandrosterone sulfate mediates activation of transcription factors CREB and ATF-1 via a Galpha11-coupled receptor in the spermatogenic cell line GC-2, Biochim. Biophys. Acta 1833 (2013) 3064–3075.
[20] M.D. Majewska, J.M. Mienville, S. Vicini, Neurosteroid pregnenolone sulfate antagonizes electrophysiological responses to GABA in neurons, Neurosci. Lett. 90 (1988) 279–284.
[21] M. Horak, K. Vlcek, H. Chodounska, L. Vyklicky Jr., Subtype-dependence of *N*-methyl-D-aspartate receptor modulation by pregnenolone sulfate, Neuroscience 137 (2006) 93–102.
[22] E. Kostakis, C. Smith, M.K. Jang, S.C. Martin, K.G. Richards, et al., The neuroactive steroid pregnenolone sulfate stimulates trafficking of functional *N*-methyl-D-aspartate receptors to the cell surface via a noncanonical, G-protein, and Ca^{2+}-dependent mechanism, Mol. Pharmacol. 84 (2013) 261–274.
[23] R.C. Tuckey, Side-chain cleavage of cholesterol sulfate by ovarian mitochondria, J. Steroid Biochem. Mol. Biol. 37 (1990) 121–127.
[24] K. Korte, P.G. Hemsell, J.I. Mason, Sterol sulfate metabolism in the adrenals of the human fetus, anencephalic newborn, and adult, J. Clin. Endocrinol. Metab. 55 (1982) 671–675.
[25] T. Imai, H. Globerman, J.M. Gertner, N. Kagawa, M.R. Waterman, Expression and purification of functional human 17alpha-hydroxylase/17,20-lyase (P450c17) in *Escherichia coli*. Use of this system for study of a novel form of combined 17alpha-hydroxylase/17,20-lyase deficiency, J. Biol. Chem. 268 (1993) 19681–19689.
[26] A.A. Gilep, T.A. Sushko, S.A. Usanov, At the crossroads of steroid hormone biosynthesis: the role, substrate specificity and evolutionary development of CYP17, Biochim. Biophys. Acta 1814 (2011) 200–209.
[27] M.K. Akhtar, S.L. Kelly, M.A. Kaderbhai, Cytochrome b_5 modulation of 17alpha hydroxylase and 17,20-lyase (CYP17) activities in steroidogenesis, J. Endocrinol. 187 (2005) 267–274.
[28] Y.H. Wang, M.K. Tee, W.L. Miller, Human cytochrome p450c17: single step purification and phosphorylation of serine 258 by protein kinase a, Endocrinology 151 (2010) 1677–1684.
[29] Y. Sagara, H.J. Barnes, M.R. Waterman, Expression in *Escherichia coli* of functional cytochrome P450c17 lacking its hydrophobic amino-terminal signal anchor, Arch. Biochem. Biophys. 304 (1993) 272–278.
[30] D. Sandee, W.L. Miller, High-yield expression of a catalytically active membrane-bound protein: human P450 oxidoreductase, Endocrinology 152 (2011) 2904–2908.
[31] M. Arase, M.R. Waterman, N. Kagawa, Purification and characterization of bovine steroid 21-hydroxylase (P450 c21) efficiently expressed in *Escherichia coli*, Biochem. Biophys. Res. Commun. 344 (2006) 400–405.
[32] J. Neunzig, R. Bernhardt, Dehydroepiandrosterone sulfate (DHEAS) stimulates the first step in the biosynthesis of steroid hormones, PLoS One 9 (2014) e89727.
[33] A. Zollner, N. Kagawa, M.R. Waterman, Y. Nonaka, K. Takio, et al., Purification and functional characterization of human 11beta hydroxylase expressed in *Escherichia coli*, FEBS J. 275 (2008) 799–810.
[34] S.B. Mulrooney, L. Waskell, High-level expression in *Escherichia coli* and purification of the membrane-bound form of cytochrome b_5, Protein Expr. Purif. 19 (2000) 173–178.
[35] J.L. Vermilion, M.J. Coon, Purified liver microsomal NADPH-cytochrome P450 reductase Spectral characterization of oxidation–reduction states, J. Biol. Chem. 253 (1978) 2694–2704.
[36] T. Omura, R. Sato, The carbon monoxide-binding pigment of liver microsomes II. Solubilization, purification, and properties, J. Biol. Chem. 239 (1964) 2379–2385.
[37] J.B. Schenkman, Studies on the nature of the type I and type II spectral changes in liver microsomes, Biochemistry 9 (1970) 2081–2091.
[38] A. Hobler, N. Kagawa, M.C. Hutter, M.F. Hartmann, S.A. Wudy, et al., Human aldosterone synthase: recombinant expression in *E. coli* and purification enables a detailed biochemical analysis of the protein on the molecular level, J. Steroid Biochem. Mol. Biol. 132 (2012) 57–65.
[39] S. Yamato, S. Nakagawa, N. Yamazaki, T. Aketo, E. Tachikawa, Simultaneous determination of pregnenolone and 17alpha-hydroxypregnenolone by semi-micro high-performance liquid chromatography with an immobilized cholesterol oxidase as a pre-column reactor: application to bovine adrenal fasciculata cells, J. Chromatogr. B Analyt. Technol. Biomed. Life Sci. 878 (2010) 3358–3362.
[40] J. Geyer, T. Wilke, E. Petzinger, The solute carrier family SLC10: more than a family of bile acid transporters regarding function and phylogenetic relationships, Naunyn. Schmiedebergs. Arch. Pharmacol. 372 (2006) 413–431.
[41] C.E. Galuska, M.F. Hartmann, A. Sanchez-Guijo, K. Bakhaus, J. Geyer, et al., Profiling intact steroid sulfates and unconjugated steroids in biological fluids by liquid chromatography-tandem mass spectrometry (LC–MS–MS), Analyst 138 (2013) 3792–3801.
[42] J.P. Dusza, J.P. Joseph, S. Bernstein, Steroid conjugates IV. The preparation of steroid sulfates with triethylamine-sulfur trioxide, Steroids 12 (1968) 49–61.
[43] E. de Peretti, E. Mappus, Pattern of plasma pregnenolone sulfate levels in humans from birth to adulthood, J. Clin. Endocrinol. Metab. 57 (1983) 550–556.
[44] A. Ruokonen, Steroid metabolism in testis tissue: the metabolism of pregnenolone, pregnenolone sulfate, dehydroepiandrosterone and

dehydroepiandrosterone sulfate in human and boar testes in vitro, J. Steroid Biochem. 9 (1978) 939–946.
[45] T.J. McKenna, R.D. Brown, Pregnenolone in man: plasma levels in states of normal and abnormal steroidogenesis, J. Clin. Endocrinol. Metab. 38 (1974) 480–485.
[46] R.B. Jaffe, G. Perez-Palacios, E. Dizzfalusy, Conversion of pregnenolone and pregnenolone sulfate to other steroid sulfates by the human fetus perfused at midgestation, J. Clin. Endocrinol. Metab. 35 (1972) 646–654.
[47] K.G. Lamont, G. Perez-Palacios, A.E. Perez, R.B. Jaffe, Pregnenolone and pregnenolone sulfate metabolism by human fetal testes in vitro, Steroids 16 (1970) 127–140.
[48] N. Kagawa, Efficient expression of human aromatase (CYP19) in *E. coli*, Methods Mol. Biol. 705 (2011) 109–122.
[49] B. Miroux, J.E. Walker, Over-production of proteins in *Escherichia coli*: mutant hosts that allow synthesis of some membrane proteins and globular proteins at high levels, J. Mol. Biol. 260 (1996) 289–298.
[50] D.D. Oprian, M.J. Coon, Oxidation–reduction states of FMN and FAD in NADPH-cytochrome P450 reductase during reduction by NADPH, J. Biol. Chem. 257 (1982) 8935–8944.
[51] R. Hewson, R.J. Newbold, D. Whitford, The expression of bovine microsomal cytochrome b_5 in *Escherichia coli* and a study of the solution structure and stability of variant proteins, Protein Eng. 6 (1993) 953–964.
[52] N.M. DeVore, E.E. Scott, Structures of cytochrome P450 17A1 with prostate cancer drugs abiraterone and TOK-001, Nature 482 (2012) 116–119.
[53] Y. Khatri, M.C. Gregory, Y.V. Grinkova, I.G. Denisov, S.G. Sligar, Active site proton delivery and the lyase activity of human CYP17A1, Biochem. Biophys. Res. Commun. 443 (2014) 179–184.
[54] M. Katagiri, N. Kagawa, M.R. Waterman, The role of cytochrome b_5 in the biosynthesis of androgens by human P450c17, Arch. Biochem. Biophys. 317 (1995) 343–347.
[55] D.F. Estrada, J.S. Laurence, E.E. Scott, Substrate-modulated cytochrome P450 17A1 and cytochrome b5 interactions revealed by NMR, J. Biol. Chem. 288 (2013) 17008–17018.
[56] H.J. Barnes, M.P. Arlotto, M.R. Waterman, Expression and enzymatic activity of recombinant cytochrome P450 17alpha-hydroxylase in *Escherichia coli*, Proc. Natl. Acad. Sci. U. S. A. 88 (1991) 5597–5601.
[57] T.A. Pechurskaya, O.P. Lukashevich, A.A. Gilep, S.A. Usanov, Engineering, expression, and purification of soluble human cytochrome P450 17alpha and its functional characterization, Biochemistry (Mosc) 73 (2008) 806–811.
[58] M.K. Tee, W.L. Miller, Phosphorylation of human cytochrome P450c17 by p38alpha selectively increases 17,20-lyase activity and androgen biosynthesis, J. Biol. Chem. 288 (2013) 23903–23913.

2.3 SHANMUGASUNDARARAJ ET AL., 2013

CARBOETOMIDATE: AN ANALOG OF ETOMIDATE THAT INTERACTS WEAKLY WITH 11B-HYDROXYLASE

S. Shanmugasundararaj, X. Zhou, **J. Neunzig**, R. Bernhardt, J.F. Cotten, R. Ge, K.W. Miller, D.E. Raines

Anesthesia & Analgesia, June 2013, Volume 116, Issue 6, p 1249–1256, doi: 10.1213/ANE.0b013e31828b3637

Anesthetic Pharmacology and Preclinical Pharmacology Section Editor: Marcel E. Durieux
Clinical Pharmacology Section Editor: Tony Gin

Carboetomidate: An Analog of Etomidate That Interacts Weakly with 11β-Hydroxylase

Sivananthaperumal Shanmugasundararaj, PhD,* Xiaojuan Zhou, BS,* Jens Neunzig, MA,† Rita Bernhardt, PhD,† Joseph F. Cotten, MD, PhD,* Rile Ge, MD, PhD,* Keith W. Miller, DPhil,* and Douglas E. Raines, MD*

BACKGROUND: Carboetomidate is a pyrrole etomidate analog that is 3 orders of magnitude less potent an inhibitor of in vitro cortisol synthesis than etomidate (an imidazole) and does not inhibit in vivo steroid production. Although carboetomidate's reduced functional effect on steroid synthesis is thought to reflect lower binding affinity to 11β-hydroxylase, differential binding to this enzyme has never been experimentally demonstrated. In the current study, we tested the hypothesis that carboetomidate and etomidate bind with differential affinity to 11β-hydroxylase by comparing their abilities to inhibit photoaffinity labeling of purified enzyme by a photoactivatable etomidate analog and to modify the enzyme's absorption spectrum in a way that is indicative of ligand binding. In addition, we made a preliminary exploration of the manner in which etomidate and carboetomidate might differentially interact with this site using spectroscopic methods as well as molecular modeling techniques to better understand the structural basis for their selectivity.

METHODS: The ability of azi-etomidate to inhibit cortisol synthesis was tested by assessing its ability to inhibit cortisol synthesis by H295R cells. The binding affinities of etomidate and carboetomidate to 11β-hydroxylase were compared by assessing their abilities to (1) inhibit photoincorporation of the photolabile etomidate analog [^{3}H]azi-etomidate into the enzyme and (2) modify the absorption spectrum of the enzyme's heme group. In silico docking studies of etomidate, carboetomidate, and azi-etomidate binding to 11β-hydroxylase were performed using the computer software GOLD.

RESULTS: Similar to etomidate, azi-etomidate potently inhibits in vitro cortisol synthesis. Etomidate inhibited [^{3}H]azi-etomidate photolabeling of 11β-hydroxylase in a concentration-dependent manner. At a concentration of 40 μM, etomidate reduced photoincorporation of [^{3}H] azi-etomidate by 96% ± 1% whereas carboetomidate had no experimentally detectable effect. On addition of etomidate to 11β-hydroxylase, a type 2 difference spectrum was produced indicative of etomidate complexation with the enzyme's heme iron; carboetomidate had no effect whereas azi-etomidate produced a reverse type 1 spectrum. Computer modeling studies predicted that etomidate, carboetomidate, and azi-etomidate can fit into the heme-containing pocket that forms 11β-hydroxylase's active site and pose with their carbonyl oxygens interacting with the heme iron and their phenyl rings stacking with phenylalanine-80. However, additional unique poses were identified for etomidate and azi-etomidate that likely account for their higher affinities.

CONCLUSIONS: Carboetomidate's reduced ability to suppress in vitro and in vivo steroid synthesis as compared with etomidate reflects its lower binding affinity to 11β-hydroxylase and may be attributed to carboetomidate's inability to form a coordination bond with the heme iron located at the enzyme's active site. (Anesth Analg 2013;116:1249–56)

Etomidate is an imidazole-based sedative hypnotic that has minimal effects on respiratory and cardiovascular function.[1–3] Unfortunately, it potently suppresses the synthesis of adrenocortical steroids that are necessary for a wide range of biological functions including glucose homeostasis, electrolyte, and water balance, and the stress response to trauma and infection.[4–6] This side effect restricts etomidate use to single bolus administration for the induction of anesthesia and requires that other drugs be used to maintain anesthesia during surgery.[7,8]

Etomidate is thought to inhibit adrenocortical steroid synthesis by binding with high affinity to the active site of the cytochrome P450 (CYP) enzyme 11β-hydroxylase.[9] Based on the hypothesis that such high affinity binding requires an interaction (coordination bond) between the basic nitrogen in etomidate's imidazole ring and the heme iron at 11β-hydroxylase's active site, we developed carboetomidate as a pyrrole etomidate analog and predicted that it would not bind with high affinity to 11β-hydroxylase;[10] carboetomidate is structurally identical to etomidate (and is a potent hypnotic) but lacks the basic nitrogen necessary to form a

From the *Department of Anesthesia, Critical Care, and Pain Medicine, Massachusetts General Hospital, Boston, Massachusetts; and †Institut für Biochemie, Universität des Saarlandes, Saarbrücken, Germany.

Accepted for publication January 16, 2013

This research was supported by grants to D.E.R. (R01-GM087316 and R21-DA029253 from the National Institutes of Health, Bethesda, MD), R.B. (FOR 13698 from the Deutsche Forschungsgemeinschaft), J.F.C. (K08-GM083216), and by the Department of Anesthesia, Critical Care, and Pain Medicine, Massachusetts General Hospital.

See Disclosures at end of article for Author Conflicts of Interest.

Reprints will not be available from the authors.

Address correspondence to Douglas E. Raines, MD, Department of Anesthesia, Critical Care, and Pain Medicine, Massachusetts General Hospital, 55 Fruit St., Boston, MA 02114-2621. Address e-mail to draines@partners.org.

DOI: 10.1213/ANE.0b013e31828b3637

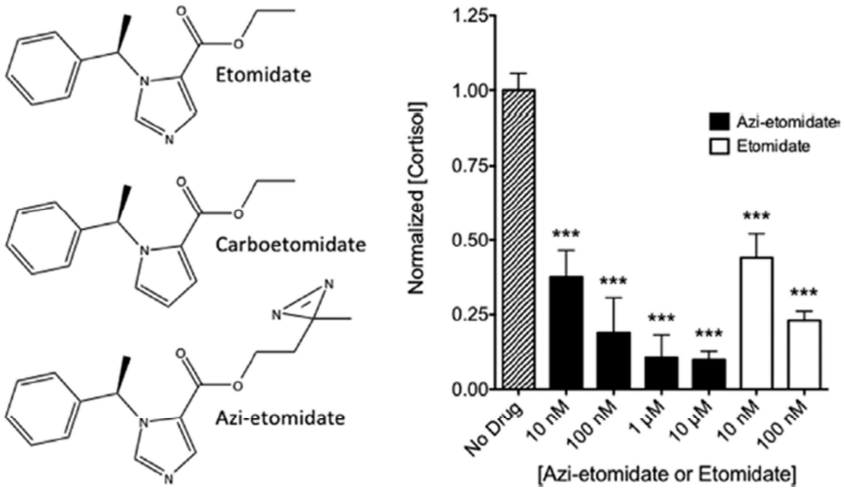

Figure 1. A, Chemical structures of etomidate, carboetomidate, and azi-etomidate. B, Inhibition of cortisol synthesis by azi-etomidate and etomidate. At all concentrations studied, azi-etomidate and etomidate reduced cortisol concentrations in wells containing H295R cells 24 hours after simulation with forskolin. Control (no drug) cortisol concentrations were 1.86 ± 0.10 ng/mL. ***$P < 0.001$ versus control value; 1-way analysis of variance followed by a Dunnett multiple comparison post-test. Each column shows the mean ± SD from 4 to 8 wells.

coordination bond (Fig. 1). Functional studies generally support this hypothesis as carboetomidate is 3 orders of magnitude less potent an inhibitor of cortisol synthesis in vitro[10] and does not suppress adrenocorticotropic hormone-stimulated steroid production in vivo.[10,11]

In the present study, we sought to test the hypothesis that etomidate and carboetomidate bind with different affinities to 11β-hydroxylase by comparing their abilities to inhibit photoincorporation of a photolabile etomidate analog into 11β-hydroxylase and to modify the absorption spectrum of 11β-hydroxylase in a way that is indicative of ligand binding to the enzyme's heme group. In addition, we made a preliminary exploration of the manner in which etomidate and carboetomidate might differentially interact with this site using molecular modeling techniques to better understand the structural basis for their selectivity.

METHODS

[^{3}H]azi-etomidate (12 Ci/mmol in methanol) was synthesized as previously described.[12] Etomidate was obtained from Bachem (Torrance, CA), and carboetomidate was synthesized by Aberjonia Laboratories (Beverly, MA) as previously described.[10] They were prepared as stock solutions in methanol. Buffer A contained: 50 mM K_2HPO_4, 20% glycerol, 500 mM Na acetate, 0.1 mM dithiothreitol, 0.1 mM EDTA, 1% Na cholate, and 1% Tween 20, at pH 7.4. Gel-counting buffer consisted of 90% toluene plus 10% tissue solubilizer (TS-2, from Research Products International, Mount Prospect, IL) containing 2.8 g/L of 2,5-diphenyloxazole and 0.28 g/L of 1,4-bis(5-phenyloxazol-2-yl)benzene. IRB approval for these studies was not sought because neither animals nor humans were used.

Inhibition of In Vitro Cortisol Synthesis

The abilities of azi-etomidate and etomidate to inhibit cortisol synthesis were assessed using the adrenocortical cell line H295R as previously described. Cortisol concentrations in culture plate wells were measured 24 hours after forskolin stimulation using a commercially available enzyme-linked immunosorbent assay (R&D Systems, Minneapolis, MN, no. KGE008).[10]

Preparation and Purification of Human 11β-Hydroxylase

Human 11β-hydroxylase was expressed in *Escherichia coli* as a mature form with N- and C-terminal modifications as described.[13] The 11β-hydroxylase expression plasmid was introduced into *E coli* strain BL21(DE3)pLys along with a GroES/GroEL expression vector pGro12.

Expression and purification were performed as described by Zöllner et al.[13] The protein was purified to apparent homogeneity. Its ultraviolet/visible absorption spectrum in the substrate-free form showed an absorption maximum at 392 nm indicating a high-spin form of this P450 enzyme.

Photolabeling of 11β-Hydroxylase with [^{3}H] Azi-Etomidate in the Presence of Etomidate or Carboetomidate

[^{3}H]azi-etomidate (10 nM) along with either etomidate or carboetomidate from the stock solutions was added to the wells of a glass 96-well plate and the methanol evaporated. The ligands were dissolved in 136 μL of buffer A, and 14 μL of human 11β-hydroxylase (2 mg/mL) in buffer A was added. Samples were then irradiated at 365 nm for 45 minutes on ice to induce photoincorporation of the radioactive ligand into the enzyme as previously described.[12] After irradiation, samples were loaded on separate lanes of an 8% sodium dodecyl sulfate gel and run overnight. A single protein band at approximately 50 kDa was identified by Coomassie blue staining and excised for scintillation counting in the gel-counting buffer after destaining. Blank sections of the gel were also treated similarly, and the counts in these blanks were subtracted from those containing 11β-hydroxylase.

Spectroscopic Studies of Etomidate and Carboetomidate Interactions with 11β-Hydroxylase

Spectrophotometric analysis was performed using a model V-630 spectrophotometer from Jasco (Easton, MD). Difference spectroscopy was performed in tandem cuvettes as generally described by Schenkman.[14] Each tandem cuvette contained 2 chambers. The first chamber of the "test" cuvette was filled with 2 μM of

11β-hydroxylase in buffer, whereas the second chamber was filled only with buffer. For reference, a second tandem cuvette was used. The chambers in the reference cuvette were identically filled with 11β-hydroxylase and buffer. Etomidate or carboetomidate (40 μM final concentration from dimethyl sulfoxide stocks) was added to the first chamber of the test cuvette and to the second chamber of the reference cuvette. An equal volume of dimethyl sulfoxide was added to the remaining 2 chambers of the cuvettes. Difference spectra were recorded from 370 to 450 nm. The buffer was composed of 50 mM potassium phosphate (pH 7.4), 20% glycerol, 0.5% sodium cholate, and 0.05% Tween 20.

Absorption spectra of etomidate and carboetomidate were recorded in quartz cuvettes. The final concentration of each compound was 40 μM in Milli-Q water (Millipore Corp., Billerica, MA). These spectra were recorded from 230 to 300 nm.

In Silico Docking Studies of Etomidate and Carboetomidate Binding to 11β-Hydroxylase

Ligands were docked to the homology model developed by Roumen et al.[15] and based primarily on the known structure of CYP101 (pdb: 2CPP)[16] with the structure of CYP2C5 (pdb: 1NR6)[17] inserted where there are gaps in the amino acid alignment between 11β-hydroxylase and CYP101 (B′–C loop, F–G–H region, J–K loop, K–L loop). The first 50 N-terminal residues, the membrane-binding region, were excluded because there is no known structural template. In addition to sequence alignment, they carefully considered where the steroid might dock in relation to its proximity to iron for the oxidation reaction.

Molecular docking calculations were performed with the program GOLD 4.1 (Cambridge Crystallographic Data Center, Cambridge, United Kingdom; http://www.ccdc.cam.ac.uk/products/life_sciences/gold/) using the default settings. The program was run under the slow mode for improved accuracy, and for efficiency, the ligand was confined to a sphere of 20 Å radius centered on the heme iron. Each ligand was docked for a maximum of 25 poses. The ligands to be docked were prepared using the PRODRG server (http://davapc1.bioch.dundee.ac.uk/prodrg/). The homology model (presented earlier) was loaded into the Hermes (Cambridge Cystallographic Data Center, Cambridge, UK) program, and hydrogen atoms were added and included in the calculation. The algorithm exhaustively searches the entire rotational and translational space of the ligand with respect to the protein. It considers hydrogen bonding and van der Waals interactions between the ligand and the protein, as well as the ligand's internal van der Waals and intramolecular hydrogen bonding interactions. All the calculations were performed in the absence of water molecules.

RESULTS

Azi-Etomidate Inhibits In Vitro Cortisol Synthesis at Nanomolar Concentrations

Azi-etomidate reduced forskolin-stimulated cortisol concentrations in culture plate wells to 37% ± 9%, 19% ± 12%, 11% ± 8%, and 10% ± 3% (n = 4 replicates, mean ± SD) of the control concentrations measured in the absence of hypnotic at respective concentrations of 10 nM, 100 nM, 1 μM, and 10 μM (Fig. 1B). For comparison, Figure 1B also shows the quantitatively similar inhibitory actions of etomidate determined in the same cell batch (44% ± 8% and 23% ± 3% at 10 and 100 nM, respectively; n = 4–8, mean ± SD).

Etomidate Inhibits [^{3}H]Azi-Etomidate Photolabeling of 11β-Hydroxylase Whereas Carboetomidate Does Not

Because of the predicted nanomolar affinity of etomidate and the experimental need to maintain the 11β-hydroxylase concentration in the micromolar range (ligand depletion conditions), we compared the ability of 40 μM etomidate and carboetomidate (near its aqueous solubility limit) to protect against photoincorporation of 10 nM [^{3}H]azi-etomidate (Table 1). Etomidate's inhibition of [^{3}H]azi-etomidate photolabeling was nearly complete, with just 4.1% ± 1.1% of the photolabeling remaining (n = 3 replicates, mean ± SD, $P < 0.0001$, 1-way analysis of variance with Dunnett multiple comparison post-test versus control). Conversely, carboetomidate had no experimentally detectable inhibitory effect, as 102% ± 8.2% (n = 3 replicates, mean ± SD) of the photolabeling remained.

Spectroscopy of the 11β-Hydroxylase Interacting with Ligands

Etomidate, carboetomidate, and azi-etomidate showed absorption maxima at 243, 272.5, and 220 nm, respectively. The difference spectrum of 11β-hydroxylase titrated with etomidate displayed a maximum at 424.5 nm and a minimum at 410 nm (Fig. 2). This is consistent with a type 2 spectral interaction, indicating that the hypnotic binds to the

Table 1. Protection Against [3H]Azi-Etomidate Photolabeling of 11β-Hydroxylase[a]

Competing ligand	Normalized photoincorporation		
	Average (95% CI)	±SD	*n*
Control	100 (92–109)	7.5	3
Carboetomidate[b]	102 (92–110)	8.2	3
Etomidate[b]	4.1 (2.8–5.3)	1.1	3

n = number of replicates in the experiment.
[a]6 μM 11β-hydroxylase.
[b]40 μM drug.

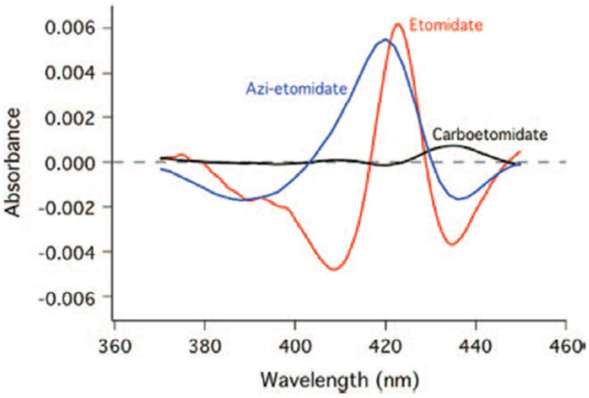

Figure 2. Spectral change induced by addition of etomidate (red curve), carboetomidate (black curve), or azi-etomidate (blue), all at 40 μM, to purified human 11β-hydroxylase.

heme iron to form a low-spin complex.[14,18,19] The difference spectrum of 11β-hydroxylase titrated with azi-etomidate displayed a maximum at 420 nm and a minimum at 388 nm, consistent with a reverse type 1 spectrum (sometimes also termed a modified type 2 spectrum) and also suggesting an interaction between the ligand and the heme iron. In contrast to etomidate and azi-etomidate, carboetomidate induced essentially no spectral change.

In Silico Docking Within the 11β-Hydroxylase Active Site

The docking algorithm that we used seeks different arrangements of the ligand in the binding pocket (called poses) that are consistent with the geometry and surface composition of the binding pocket. Because of the complexity of force fields within proteins, it is has been optimized for the prediction of ligand-binding positions rather than the prediction of binding affinities. Thus, our exploration was designed to ask whether the specific homology model might aid our understanding of the interactions underlying the clear specificity of action of these 2 ligands on 11β-hydroxylase. Our strategy had 2 parts. First, we sought poses that were unique to etomidate and thus might be the ones responsible for its observed higher affinity as an inhibitor. Second, we analyzed situations in which the 2 ligands adopted identical (i.e., isosteric or superimposable) poses to assess the role of imidazole in contributing additional binding energy.

Overview of Poses: Etomidate Versus Carboetomidate

The structural differences between etomidate and carboetomidate (Fig. 1) are minor and cause essentially no change in volume. It is not surprising that the docking routine showed that both agents were able to fit in the heme-containing pocket of 11β-hydroxylase. Thus, steric constraints do not seem to play a role in specificity. The docking routine found 11 different poses for etomidate and 6 different poses for carboetomidate within the heme-containing cavity of the 11β-hydroxylase homology model. For etomidate, these 11 poses were in 2 categories based on their interaction with the enzyme's heme iron. In 5 poses, the iron interacted with etomidate's imidazole nitrogen, whereas in the other 6 poses, the iron interacted with etomidate's carbonyl group. For carboetomidate, only the latter (i.e., carbonyl–iron) interactions were found.

Heme–Imidazole Interactions

Of the 5 predicted etomidate poses in which the iron interacted with the imidazole nitrogen, in 4 cases the imidazole ring was approximately perpendicular to the heme ring, and in 1, it lay nearly parallel to it. One representative of the 5 poses is shown in Figure 3. The docking algorithm predicted nitrogen–iron distances of 1.7 to 2.0 Å, which are comparable with, but generally shorter than, those found in a number of moderately high resolution CYP structures. For example, in the CYP 2B4 structure, 3 different imidazole-containing ligands all exhibit a nitrogen–iron distance of 2.1 Å (pdb, resolution [Å]: 1SUO, 1.9; 2BDM, 2.3; 2Q6N, 2.5).[20–22] In a much higher resolution structure of human oxyhemoglobin (2DN1, 1.25 Å), the imidazole of His-92 is 2.06 Å from the iron.[23] In addition to the nitrogen–iron interaction, a common finding was that the aromatic ring of

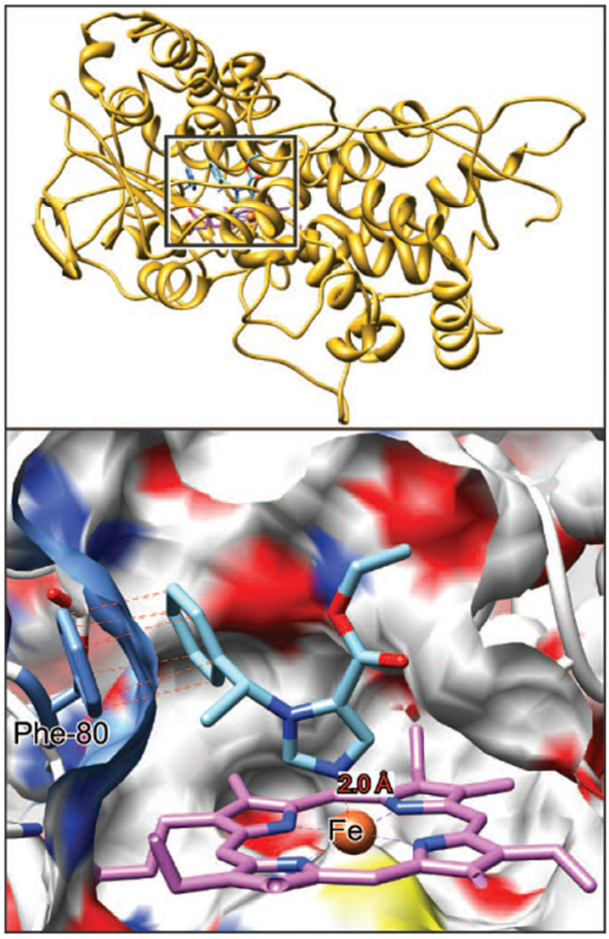

Figure 3. Top panel: Etomidate docked in the substrate-binding pocket of 11β-hydroxylase. Bottom panel: A cross-section through the surface of the binding cavity is shown. The surface is colored according to the atoms behind it: white is carbon, blue nitrogen, red oxygen, and yellow sulfur. Etomidate is depicted in stick representation with blue nitrogens, red oxygens, and sky blue carbons. In the heme system, purple is carbon, blue is nitrogen, and iron is rust. The heme iron atom is coordinated to Cys-400 below the ring and etomidate's imidazole nitrogen above the ring.

etomidate was almost perfectly aligned with that of Phe-80 on the surface of the pocket. The carbon atoms of the rings were in register (dotted red lines in Fig. 3), and the distance between opposed carbons were in the range expected for strong van der Waals interactions, varying systematically around the ring from 3.4 to 3.8 Å. Such distances may be compared with values of 3.5 to 3.8 Å for the ring stacking of α-naphthoflavone with Phe-226 in cytochrome P4501A2.[24]

The carbonyl group had only a single interaction with the protein that was shorter than 5 Å, being 4.4 Å from the side chain of Phe-437. The ester oxygen faired slightly better, being 3.6 Å from Phe-437 and 3.7 Å from Thr-268's hydroxyl. Although this latter distance is too long for hydrogen bonding, it should be remembered that we did not allow the protein's structure to react to the presence of the ligand.

The single pose with the imidazole ring parallel to the heme ring (not shown) still maintained the aromatic ring stacking with Phe-80, albeit somewhat weaker with distances ranging from 3.0 to 4.3 Å. The iron–imidazole

distance was long (3.2 Å), but this lack of coordination is possibly offset by multiple interactions with the iron because the imidazole ring atoms and the carbonyl and ether oxygens were all within 2.6 to 4.0 Å of the iron.

Heme–Carbonyl Interactions

In the remaining 6 predicted etomidate poses, the carbonyl group interacted with the heme iron (e.g., Fig. 4). No poses with the ester oxygen interacting with iron were found. There were 2 main categories of pose, each with 3 poses that differed from each other in only minor ways. In 1 set of poses, the phenyl ring of etomidate lay close to Phe-80 in the surface of the binding pocket. In the other set, the phenyl ring was on the opposite side of the pocket near Phe-437. The 6 carboetomidate poses also were in 2 such sets, and they may be considered together with those of etomidate. The carbonyl oxygen–iron distances were all close to 1.9 Å.

For the first set of poses mentioned earlier, Figure 4 shows that etomidate and carboetomidate superimpose quite well, no equivalent atom in the 2 molecules being >0.2 Å apart. The carbonyl oxygens interact identically with the iron and the ring stacking with Phe-80 is also identical, with separation of carbons varying from 3.0 to 4.4 Å. Thus, the observed difference in affinity for 11β-hydroxylase is not accounted for by these interactions. However, the imidazole ring's interaction with the protein does provide 2 possible explanations. First, the free nitrogen is 3.3 Å from the backbone carbonyl of Gly-264 and 4.0 Å from the backbone amide nitrogen of Gly-264. Neither of these distances is consistent with strong hydrogen bonding, although some electrostatic interaction must occur. The equivalent carbon is a similar distance from these moieties, but it lacks the electronegativity of the nitrogen. Second, the imidazole ring lies above one of the pyrrole rings of the porphyrin ring system of the heme. The distance of the imidazole ring atoms to the nearest pyrrole ring atoms range from 3.3 to 3.9 Å, consistent with the 2 delocalized π-ring systems undergoing good van der Waals interactions. Because the carboetomidate ring lacks this aromatic quality, it will be less polarizable and should interact more weakly with the porphyrin ring system.

For the second set of poses mentioned earlier, the carbonyl–iron interaction is again very similar. In these poses, the aromatic rings of both agents interact with Phe-437, but they do not ring stack. Instead, they are tilted back so that the agents' aromatic ring is 130° to that of Phe-437 with their carbon atoms separated by 3.6 to 7.1 Å. This weakens the aromatic interaction but allows several other interactions. For example, Ala-263 and Met-180 interact strongly with the agents' aromatic ring. The imidazole nitrogen of etomidate makes a hydrogen bond with the backbone carbonyl of Glu-260 (2.8 Å) and van der Waals contact with the backbone amide of Gly-264 (3.5 Å) and the side chain of Glu-260 (4.7 Å).

An Additional Unique Pose for Azi-Etomidate

In addition to the 2 categories of poses described earlier for etomidate (i.e., heme–imidazole interactions and heme–carbonyl interactions), the docking routine identified an ensamble of azi-etomidate poses in which a diazerine moiety nitrogen interacts with the heme iron (Fig. 5). In these poses, the distance between the azi moiety's nitrogen and the iron ranged from 1.5 to 1.6 Å, and there were no apparent stacking interactions between azi-etomidate's phenyl ring and any of the aromatic residues in or near the binding pocket.

DISCUSSION

We have shown that etomidate interacts strongly and selectively with purified 11β-hydroxylase, whereas

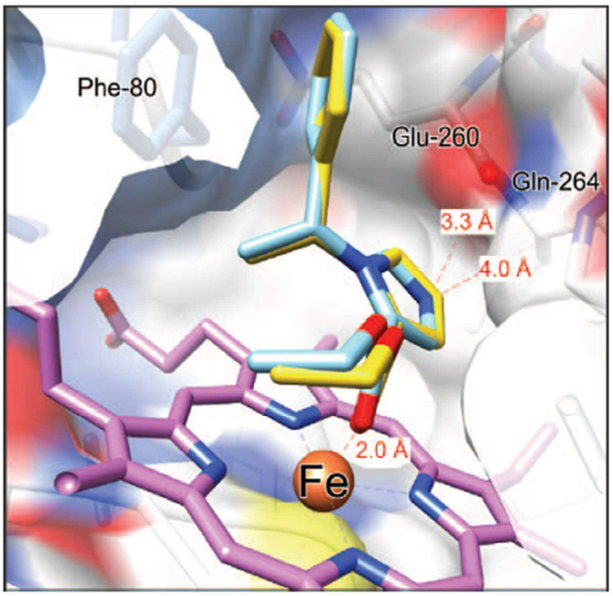

Figure 4. Superimposed structures of etomidate and carboetomidate docked in the substrate-binding pocket of 11β-hydroxylase. Carboetomidate is shown with gold carbons. Both agents adopt very similar poses with the heme iron coordinated to the ester carbonyl oxygen and the phenyl ring proximal to Phe-80.

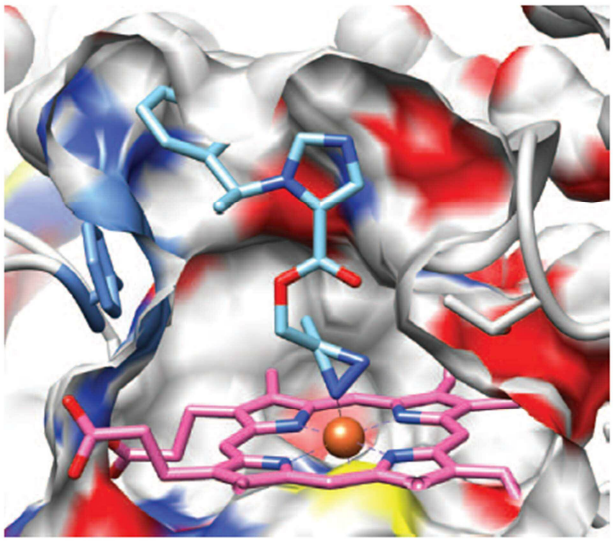

Figure 5. Representative pose showing azi-etomidate docked in the substrate-binding pocket of 11β-hydroxylase with its azi moiety interacting with the enzyme's heme iron. A cross-section through the surface of the binding cavity is shown. The surface is colored according to the atoms behind it; white is carbon, blue nitrogen, red oxygen and yellow sulfur. Azi-etomidate is depicted in stick representation with blue nitrogens, red oxygens, and sky blue carbons.

carboetomidate interacts weakly if at all. This conclusion rests on 2 distinct experimental methods. The first method was a kinetic competition assay between photolabeling and ligand binding. Even with competing azi-etomidate concentrations as low as 10 nM, a near-saturated solution of carboetomidate (40 μM) failed to protect effectively against photolabeling, whereas etomidate at the same concentration almost completely inhibited photolabeling. The second method supporting our conclusion was spectroscopic, and it added the additional information that etomidate interacted directly with the heme iron because the spectrum showed the classic type 2 behavior (Fig. 2), whereas carboetomidate did not cause spectral changes. The physiologic implications of carboetomidate's inability to interact with 11β-hydroxylase are of interest because the agent does inhibit in vitro cortisol synthesis defined using a human adrenocortical cell assay, although its potency is 2000-fold less than that of etomidate.[10]

We sought to gain a qualitative understanding of the origin of the difference in affinities of these 2 agents for 11β-hydroxylase by performing docking studies using a proven homology model of 11β-hydroxylase. Several points should be borne in mind when seeking the origin of difference in interaction strength. First, our understanding of the force fields within proteins is inadequate for precise prediction of ligand–protein interaction energies. Second, for a 1000-fold difference in dissociation constant the difference in free energy of binding is approximately 4 kcal/mol, equivalent to 1 to 2 hydrogen bonds. Third, the free energy for binding contains contributions from the energy of removing the agent from aqueous solution (desolvation) as well as those for insertion into the binding pocket. It seems likely that the free energy of desolvation for carboetomidate would be less than that for etomidate, because the imidazole ring will undergo polar interactions with water that are lost when the >N is replaced by >CH to give a pyrrole ring. The additional hydrophobicity introduced by this substitution would create an entropic driving force for desolvation. This would suggest that the etomidate–11β-hydroxylase interaction itself must be >4 kcal/mol stronger than that of carboetomidate to compensate for desolvation.

Our docking studies revealed that the major difference between the agents was the ability of the imidazole ring to coordinate the sixth position of the porphyrin ring iron atom, an interaction that carboetomidate is incapable of. Theoretical studies on simple models suggest that imidazole can displace water in $Fe(H_2O)_6^{2+}$ with a favorable free energy of some −20 kcal/mol. This is attributed to its large dipole (3.7 D) and high polarizability[25] that lead to favorable charge–dipole and charge-induced dipole interactions. In the pyrrole ring of carboetomidate, the ring dipole is smaller but in the same direction (the negative end pointing toward the iron), and the polarizability is comparable with that of imidazole. Free pyrroles interact via their nitrogen with the iron, but this is not possible in carboetomidate because of steric constraints. Binding to CYP-bound porphyrin–iron complexes is more complex than the aforementioned model system and contains terms from protein conformational changes; nonetheless, for 2 such similar molecules these terms are likely to be similar, and one may conclude that the high affinity of etomidate compared with carboetomidate very likely comes from the inability of the >CH in carboetomidate to coordinate strongly with the heme iron.

An alternative interaction with the iron was through the carbonyl oxygen, and both agents adopted similar poses when this interaction was present, so it is unlikely that the carbonyl–iron interaction itself is responsible for the experimentally observed difference in the 2 agents. Furthermore, our photolabeling and spectroscopic experiments indicate that the putative carbonyl–iron interaction is of insufficient strength to significantly stabilize binding of carboetomidate to 11β-hydroxylase.

Results with azi-etomidate were generally similar to etomidate; azi-etomidate is a very potent inhibitor of cortisol synthesis and adopts the same 2 categories of poses as etomidate. However, our docking studies identified an additional set of poses for azi-etomidate in which the photolabel's diazerine moiety interacts with the heme iron. It is unclear whether these poses explain the distinct spectral pattern (i.e., reverse type 1 spectrum) induced by azi-etomidate on purified 11β-hydroxylase. This pattern has been described for other inhibitors of CYP enzymes that do not contain a diazirine, but its precise origin is unknown.[26] Future photoaffinity labeling studies aimed at identifying the specific amino acid residues near this azi moiety may provide additional information regarding the orientation(s) of this ligand within the enzyme's active site.

In summary, we have shown that unlike etomidate, carboetomidate neither inhibits photoaffinity labeling of 11β-hydroxylase by azi-etomidate nor alters the enzyme's spectrum in a manner indicative of drug interacting with the enzyme's heme moiety. Using molecular modeling, we identified 11 predicted poses of etomidate in the active site of 11β-hydroxylase. Of these, 6 are shared with carboetomidate. The remaining poses of etomidate, none of which are emulated by carboetomidate, all include an iron–imidazole interaction. Thus, this interaction is most likely the dominant determinant of the high affinity binding of etomidate to 11β-hydroxylase. A secondary motif, the interaction between etomidate's phenyl ring and Phe-80 is a stabilizing factor, but it is not sufficient to confer stability because it is also present in some of the carboetomidate poses.

DISCLOSURES

Name: Sivananthaperumal Shanmugasundararaj, PhD.
Contribution: This author performed the computer modeling studies.
Attestation: Sivananthaperumal Shanmugasundararaj approved the final manuscript.
Conflicts of Interest: The author has no conflicts of interest to declare.
Name: Xiaojuan Zhou, BS.
Contribution: This author performed the competition experiments.
Attestation: Xiaojuan Zhou approved the final manuscript.
Conflicts of Interest: The author has no conflicts of interest to declare.
Name: Jens Neunzig, MA.
Contribution: This author performed the spectroscopic studies.
Attestation: Jens Neunzig approved the final manuscript.

Conflicts of Interest: The author has no conflicts of interest to declare.
Name: Rita Bernhardt, PhD.
Contribution: This author expressed and purified 11β-hydroxylase.
Attestation: Rita Bernhardt approved the final manuscript.
Conflicts of Interest: The author has no conflicts of interest to declare.
Name: Joseph F. Cotten, MD, PhD.
Contribution: This author helped design the experiment.
Attestation: Joseph F. Cotten approved the final manuscript.
Conflicts of Interest: Joseph F. Cotten is a coinventor on a patent application submitted by the Massachusetts General Hospital. He, his department, his laboratory, and his institution could receive royalties relating to the development of carboetomidate or related analogs.
Name: Rile Ge, MD, PhD.
Contribution: This author performed the H295R cell assays.
Attestation: Rile Ge approved the final manuscript.
Conflicts of Interest: The author has no conflicts of interest to declare.
Name: Keith W. Miller, DPhil.
Contribution: This author oversaw the binding and computer modeling studies and helped write the manuscript.
Attestation: Keith W. Miller approved the final manuscript and the integrity of the original data and the analysis reported in this manuscript. Keith W. Miller is the archival author.
Conflicts of Interest: Keith W. Miller is a coinventor on a patent application submitted by the Massachusetts General Hospital. He, his department, his laboratory, and his institution could receive royalties relating to the development of carboetomidate or related analogs.
Name: Douglas E. Raines, MD.
Contribution: This author designed the experiments and wrote the manuscript.
Attestation: Douglas E. Raines approved the final manuscript and the integrity of the original data and the analysis reported in this manuscript.
Conflicts of Interest: Douglas E. Raines is a coinventor on a patent application submitted by the Massachusetts General Hospital. He, his department, his laboratory, and his institution could receive royalties relating to the development of carboetomidate or related analogs. Douglas E. Raines is a consultant for and holds an equity position in Annovation BioPharma, a pharmaceutical company that seeks to develop technologies covered by that patent.
This manuscript was handled by: Marcel E. Durieux, MD, PhD.

ACKNOWLEDGMENTS

The authors thank Prof. Hermans (Department of Pharmacology and Toxicology, Cardiovascular Research Institute, University Maastricht, the Netherlands) for providing them with the published homology model and Wolfgang Reinle for preparation of the protein. Molecular graphics images were produced using the University of California, San Francisco Chimera package from the Resource for Biocomputing, Visualization, and Informatics at the University of California, San Francisco (supported by National Institutes of Health P41 RR-01081).

REFERENCES

1. Dubois-Primo J, Bastenier-Geens J, Genicot C, Rucquoi M. A comparative study of etomidate and methohexital as induction agents for analgesic anesthesia. Acta Anaesthesiol Belg 1976;27 suppl:187–95
2. Gooding JM, Corssen G. Effect of etomidate on the cardiovascular system. Anesth Analg 1977;56:717–9
3. Gooding JM, Weng JT, Smith RA, Berninger GT, Kirby RR. Cardiovascular and pulmonary responses following etomidate induction of anesthesia in patients with demonstrated cardiac disease. Anesth Analg 1979;58:40–1
4. de Jong FH, Mallios C, Jansen C, Scheck PA, Lamberts SW. Etomidate suppresses adrenocortical function by inhibition of 11 beta-hydroxylation. J Clin Endocrinol Metab 1984;59: 1143–7
5. Wagner RL, White PF. Etomidate inhibits adrenocortical function in surgical patients. Anesthesiology 1984;61:647–51
6. Wagner RL, White PF, Kan PB, Rosenthal MH, Feldman D. Inhibition of adrenal steroidogenesis by the anesthetic etomidate. N Engl J Med 1984;310:1415–21
7. Absalom A, Pledger D, Kong A. Adrenocortical function in critically ill patients 24 h after a single dose of etomidate. Anaesthesia 1999;54:861–7
8. Bloomfield R, Noble DW. Etomidate and fatal outcome–even a single bolus dose may be detrimental for some patients. Br J Anaesth 2006;97:116–7
9. Hahner S, Stuermer A, Kreissl M, Reiners C, Fassnacht M, Haenscheid H, Beuschlein F, Zink M, Lang K, Allolio B, Schirbel A. [123 I]Iodometomidate for molecular imaging of adrenocortical cytochrome P450 family 11B enzymes. J Clin Endocrinol Metab 2008;93:2358–65
10. Cotten JF, Forman SA, Laha JK, Cuny GD, Husain SS, Miller KW, Nguyen HH, Kelly EW, Stewart D, Liu A, Raines DE. Carboetomidate: a pyrrole analog of etomidate designed not to suppress adrenocortical function. Anesthesiology 2010;112: 637–44
11. Cotten JF, Le Ge R, Banacos N, Pejo E, Husain SS, Williams JH, Raines DE. Closed-loop continuous infusions of etomidate and etomidate analogs in rats: a comparative study of dosing and the impact on adrenocortical function. Anesthesiology 2011;115:764–73
12. Husain SS, Ziebell MR, Ruesch D, Hong F, Arevalo E, Kosterlitz JA, Olsen RW, Forman SA, Cohen JB, Miller KW. 2-(3-Methyl-3H-diaziren-3-yl)ethyl 1-(1-phenylethyl)-1H-imidazole-5-carboxylate: a derivative of the stereoselective general anesthetic etomidate for photolabeling ligand-gated ion channels. J Med Chem 2003;46:1257–65
13. Zöllner A, Kagawa N, Waterman MR, Nonaka Y, Takio K, Shiro Y, Hannemann F, Bernhardt R. Purification and functional characterization of human 11beta hydroxylase expressed in Escherichia coli. FEBS J 2008;275:799–810
14. Schenkman JB. Studies on the nature of the type I and type II spectral changes in liver microsomes. Biochemistry 1970;9:2081–91
15. Roumen L, Sanders MP, Pieterse K, Hilbers PA, Plate R, Custers E, de Gooyer M, Smits JF, Beugels I, Emmen J, Ottenheijm HC, Leysen D, Hermans JJ. Construction of 3D models of the CYP11B family as a tool to predict ligand binding characteristics. J Comput Aided Mol Des 2007;21:455–71
16. Poulos TL, Finzel BC, Howard AJ. High-resolution crystal structure of cytochrome P450cam. J Mol Biol 1987;195:687–700
17. Wester MR, Johnson EF, Marques-Soares C, Dijols S, Dansette PM, Mansuy D, Stout CD. Structure of mammalian cytochrome P450 2C5 complexed with diclofenac at 2.1 A resolution: evidence for an induced fit model of substrate binding. Biochemistry 2003;42:9335–45
18. Parker JE, Warrilow AG, Cools HJ, Martel CM, Nes WD, Fraaije BA, Lucas JA, Kelly DE, Kelly SL. Mechanism of binding of prothioconazole to Mycosphaerella graminicola CYP51 differs from that of other azole antifungals. Appl Environ Microbiol 2011;77:1460–5
19. Locuson CW, Hutzler JM, Tracy TS. Visible spectra of type II cytochrome P450-drug complexes: evidence that "incomplete" heme coordination is common. Drug Metab Dispos 2007;35:614–22
20. Scott EE, White MA, He YA, Johnson EF, Stout CD, Halpert JR. Structure of mammalian cytochrome P450 2B4 complexed with 4-(4-chlorophenyl)imidazole at 1.9-A resolution: insight into

the range of P450 conformations and the coordination of redox partner binding. J Biol Chem 2004;279:27294–301
21. Zhao Y, White MA, Muralidhara BK, Sun L, Halpert JR, Stout CD. Structure of microsomal cytochrome P450 2B4 complexed with the antifungal drug bifonazole: insight into P450 conformational plasticity and membrane interaction. J Biol Chem 2006;281:5973–81
22. Zhao Y, Sun L, Muralidhara BK, Kumar S, White MA, Stout CD, Halpert JR. Structural and thermodynamic consequences of 1-(4-chlorophenyl)imidazole binding to cytochrome P450 2B4. Biochemistry 2007;46:11559–67
23. Park SY, Yokoyama T, Shibayama N, Shiro Y, Tame JR. 1.25 A resolution crystal structures of human haemoglobin in the oxy, deoxy and carbonmonoxy forms. J Mol Biol 2006;360:690–701
24. Kassimi NE, Doerksen RJ, Thakkar AJ. Polarizabilities of aromatic five-membered rings: azoles. J Phys Chem A 1995;99:12790–6
25. Ricca A, Bauschlicher CW. Theoretical study of the interaction of water and imidazole with iron and nickel dications. J Phys Chem A 2002;106:3219–23
26. Berwanger A, Eyrisch S, Schuster I, Helms V, Bernhardt R. Polyamines: naturally occurring small molecule modulators of electrostatic protein-protein interactions. J Inorg Biochem 2010;104:118–25

3 DISCUSSION AND CONCLUSIONS

EFFECT AND ROLE OF SULFONATED STEROIDS ON STEROIDOGENIC CYPS

The studies comprising this work illustrate for the first time the influence of sulfonated DHEA and Preg on the biosynthesis of steroid hormones. The obtained results give insight into a crucial mechanism for the regulation of the steroidogenesis in mammals.

Many important steroid hormones are present in a sulfo-conjugated form, often in concentrations exceeding the unbound form by many folds. The sulfonation of unbound and hydrolysis of sulfonated steroids constitute an additional regulatory system of steroidogenesis, modulating the availability of unbound and thus active steroid hormones. The relevance of this mechanism can be observed in patients with a defect of the involved enzymes. Concerning the sulfonation, PAPS synthase deficiency manifests in an accumulation of unconjugated DHEA in the adrenal, leading to an increase of androgens and thus females are virilized, displaying advanced bone age, and suffer from amenorrhea. As a result of defects of a sulfatase, sulfonated steroids are enriched in skin, generating x-linked ichtiosis. However, this mechanism is not fully understood so far.

In the last decades, sulfonated steroids have been considered to mainly serve as reservoir for inactive steroids, without exerting a direct biological function. So far, the interaction of these compounds with enzymes involved in steroidogenesis and their influence on steroid hormone production have not been investigated. In the first two publications forming this work, evidence is provided for the vital role of sulfonated steroids in the mammalian steroidogenesis. In publication 2.1 a new regulatory role of sulfonated steroids in steroid hormone biosynthesis was elucidated, demonstrating that DHEAS directly increases CYP11A1 activity and, thus, modulates the production of steroid hormones. Moreover, it was shown that PregS was converted into 17OH-PregS by CYP17A1 giving new insights into the metabolism of sulfonated steroids by steroidogenic CYPs (publication 2.2). In mammals the steroid hormone biosynthesis displays interesting differences between species. For example, the absence of cortisol in the blood of mice is well known, whereas for human and other mammal´s health, a considerable cortisol concentration in blood is absolutely required. It seems that DOC fulfills the cortisol action in mice. Moreover, concerning the CYP17A1 activity, there are interspecies differences, with either the Δ^5-, or Δ^4-pathway being dominant. Human, bovine, bison, goat, sheep and cat only accept Δ^5 steroids for the formation of sex hormones, whereas guinea pig uses Δ^4 steroids for this purpose. Horse, hamster, pig and rat are able to utilize both Δ^5 and Δ^4 steroid for sex hormone synthesis [58]. In the first two publications, the experiments were performed using bovine proteins. Bovine proteins have been explored for a longer time compared with the human ones, and although the steroidogenic CYPs of bovine and human show differences in substrate affinities and catalytic efficiencies their molecular mechanism is well comparable, as both species undergo the Δ^5-pathway for sex hormone production. For these reasons, the bovine system was chosen as model organism.

It was demonstrated that under the influence of DHEAS the activity of CYP11A1 is significantly increased due to an enhanced interaction of CYP11A1 and Adx, as well as an elevated substrate affinity of CYP11A1 for cholesterol (Publication 2.1). Based on these results, additional experiments were performed to investigate whether DHEAS exhibits a regulatory effect on further steroidogenic CYPs (appendix). Its potential effects on CYP17A1, the crucial CYP for the production of sex hormones and glucocorticoids, as well as on CYP21A2, which is essential for mineralo- and glucocorticoid production, were examined. The obtained results showed a slight, but statistically not significant inhibitory effect of DHEAS on the 17-hydroxylation activity of CYP17A1 and no effect on CYP21A2. These findings suggest that the influence of DHEAS on steroidogenic CYPs might be highly selective. The main differences between the mitochondrial CYP11A1 and the microsomal CYP17A1 and CYP21A2 are their cellular localization and interaction with the respective electron transfer partners. Additional studies are required to explore, whether the impact of DHEAS might be restricted to mitochondrial CYPs, to CYP11A1 alone or if it depends on the redox partners. As Pechurskaya et al. showed, CYP17A1 is able to utilize the mitochondrial AdR and Adx as an electron transfer chain for its substrate conversion [59]. Therefore, it would be of interest to investigate whether DHEAS affects the activity of CYP17A1 with these redox partners. Additionally, *in-vitro* experiments with the mitochondrial CYP11B1 and CYP11B2 should be performed. If the activity would be influenced, DHEAS might act in a different manner on the different CYP classes. In the case of no effect, DHEAS might constitute a highly selective compound acting solely on CYP11A1.

In summary, the enhanced activity of CYP11A1 in the presence of DHEAS was clearly demonstrated at the molecular level, providing new insights about regulatory features of sulfonated steroids on steroidogenic CYPs.

To establish a physiological relevance of these findings, cell culture experiments on the effect of DHEAS were carried out using the SOAT-HEK293 cell line, expressing CYP11A1 and its redox partner, Adx. Due to the low uptake of the extremely unpolar cholesterol into the cells, 22(R)-OH-cholesterol, the first hydroxylated intermediate of the CYP11A1-dependent reaction was used as an alternative substrate and proved to be converted to pregnenolone to a high extent. Interestingly, the presence of DHEAS did not affect the activity of CYP11A1 regarding this reaction; neither in cell culture nor in the reconstituted *in-vitro* system. Although the previous findings with cholesterol as substrate could not be confirmed, these results give additional information about the mechanism of DHEAS action on CYP11A1 indicating that only the first of the three hydroxylation steps catalyzed by CYP11A1 is affected by DHEAS (Figure 11).

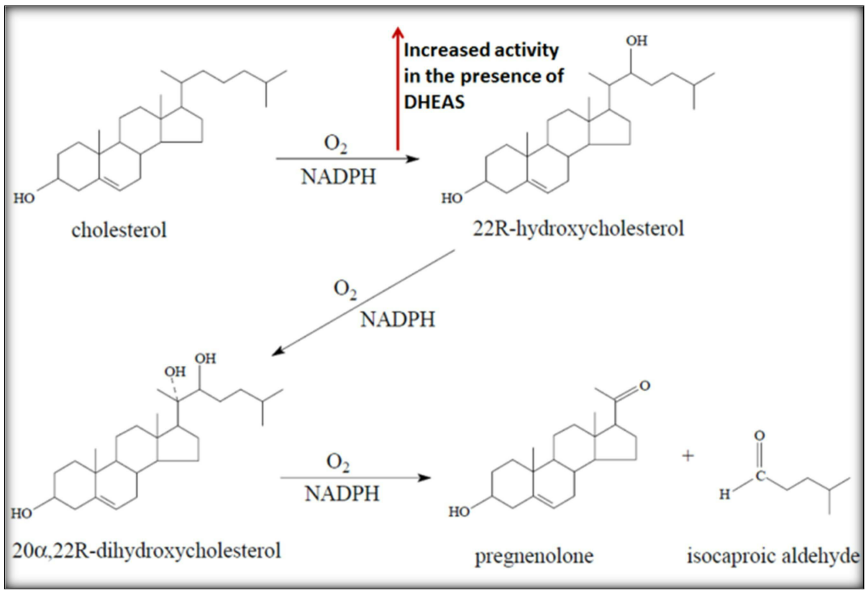

FIGURE 11: CONVERSION OF C INTO PREG BY CYP11A1, SHOWING ALL THREE HYDROXYLATION STEPS. DHEAS SEEMS TO HAVE AN EFFECT ONLY ON THE FIRST HYDROXYLATION STEP.

In order to explore whether the regulatory mechanism of DHEAS on the steroid hormone biosynthesis might have a physiological impact, further studies still have to be done using an *in-vivo* model that allows uptake of cholesterol, for instance through the expression of the steroidogenic acute regulatory protein StAR, responsible for cholesterol transport, at the cells' surface. Taken together, steroid hormone delivery underlies a complicated regulation at different levels to ensure the optimal dosage of required steroids, and these results demonstrate an additional regulatory mechanism at the cellular level. The findings show that, in the presence of DHEAS, the first step in the steroidogenesis is enhanced resulting in an increased Preg formation, whereas CYP17A1, which is crucial for glucocorticoid and sex hormones formation as well as CYP21A2, which is essential for gluco- and mineralocorticoid synthesis, are not affected. As a consequence DHEAS might promote the formation of all three steroid hormone classes: the mineralo- and glucocorticoids as well as the sex hormones. The dosage of DHEAS required in mammalian organism to prompt these effects is not possible to anticipate. Therefore, data obtained from animal or human studies are needed, showing the steroid profile before and after the intake of different concentrations of DHEAS.

Furthermore, from the biotechnological point of view, DHEAS might be an interesting compound for substrate conversions with CYP11A1, as its catalytic activity is strongly increased in the presence of this sulfonated steroid.

Besides the impact of sulfonated steroids on the natural substrate conversion of steroidogenic CYPs, the ability of PregS and 17OH-PregS to serve as substrates for CYP17A1 was assessed. So far, only CS was shown to be converted by CYP11A1 [57,60] and to be present in rat adrenal mitochondria [61]. Publication 2.2 focuses on the conversion of PregS in a reconstituted *in-vitro* system with purified CYP17A1 and CPR, as well as in a SOAT-HEK293 cell culture system. Binding studies were performed and the kinetic parameters of CYP17A1-dependent PregS conversion were elucidated, revealing PregS to be a substrate for CYP17A1, yielding 17OH-PregS. Moreover, it was demonstrated, that CYP17A1 only performs the 17-hydroxylation reaction using PregS, whereas the 17,20 lyase activity could not be

activated, even when cytochrome b_5 was added to the system. This finding implies that the metabolism of PregS does not contribute to the production of sex hormones. To elucidate whether 17OH-PregS is an end-product of the steroidogenic pathway for sulfonated steroids or it possibly undergoes the pathway for production of glucocorticoids, it was aimed to convert 17OH-PregS with purified CYP21A2. This steroidogenic CYP hydroxylates 17OH-Prog at position C21 yielding 11-deoxycortisol. Therefore, the expected product when using 17OH-PregS as substrate would be sulfonated 11-deoxycortisol. However, it was not possible to detect any product formation (not shown). Hence, we postulate an alternative steroidogenic pathway for sulfonated steroids, starting from CS and ending with 17OH-PregS.

The results obtained from the conversion of PregS, which circulates in large quantities with varying concentrations during the mammalian life cycle, lead to the conclusion that considerable amounts of 17OH-PregS may exist in mammalian organism. These concentrations might vary during life, similar to those of its substrate PregS. This speculation still needs to be proved, as there are no detailed studies about concentrations of 17OH-PregS in human or other mammals. In order to quantify the achieved concentrations of 17OH-PregS from the PregS conversion experiments, this work describes an analytical method to quantify this sulfonated steroid metabolite via LC/MS-MS for the first time. This method can be applied to determine 17OH-PregS levels in humans and other mammals.

Whether 17OH-PregS exhibits a physiological meaning in mammals still remains to be explored. On one hand, it might act as a reservoir for free 17OH-Preg, and, thus, constitute a precursor for glucocorticoids and sex hormones. In contrast, the desulfonation of PregS leads to Preg, which is a precursor for all three steroid hormone classes. This fact makes 17OH-PregS a more specific precursor compared with PregS. Taken the plasma concentrations of the steroid hormones into account, it might be reasonable to provide a precursor designated for the synthesis of glucocorticoids or sex hormones such as cortisol or testosterone, which achieve a plasma concentration of 12 µg/ 100 ml and 0.7 µg/ 100 ml, being many folds higher compared with the mineralocorticoid concentrations such as aldosterone (0.0068 µg /100 ml) [62]. On the other hand, 17OH-PregS might fulfill biological functions similar to the ones described for PregS, such as modulating ion channels or, more general, acting as a neurosteroid [27]. However, these assumption needs to be explored, as so far no studies have been published referring to the physiological impact of 17OH-PregS in mammals.

Taken together, the results achieved from the reconstituted *in-vitro* and from the cell culture experiments both showing an efficient conversion of PregS to 17OH-PregS, suggest that this reaction is not an artificial observation, but might be of physiological relevance.

EFFECT OF PHARMACEUTICAL COMPOUNDS ON CYP11B1

This work focuses on the effect of two anesthetic agents on CYP11B1, the cortisol producing cytochrome P450, and provides data about their mechanistic action.
Alterations of the regulatory system of steroid delivery can lead to a modified steroid profile deviating from normal range, with severe consequences for the affected organism. These changes can be generated by xenobiotics that directly interact with steroidogenic enzymes, influencing their catalytic properties. These types of substances are denominated endocrine disruptors, as they modulate the level of required steroids, mostly having a negative effect on the organism.
In terms of the development of new drugs it is of particular significance to minimalize side-effects, such as interferences with the endocrine system, without impairing their mode of action. Etomidate, an anesthetic compound acting on GABA-receptors, has been used as sedative for more than 25 years [63]. Due to its high affinity towards CYP11B1, suppressing cortisol synthesis and, thus, altering a wide range of biological functions such as stress response and immune defense, etomidate cannot be administrated for a long time period and has to be replaced by other sedatives. To elude these side-effects, Cotten and colleagues [64] designed an etomidate analog, carboetomidate, which exhibits similar anesthetic features without influencing the activity of CYP11B1. Using two different approaches, it was shown in our studies that etomidate and carboetomidate differentially bind to CYP11B1. At first, a kinetic competition assay between photolabeling and ligand binding was performed, demonstrating that etomidate, and not carboetomidate, inhibits photoincorporation of azi-etomidate. Secondly, spectroscopic studies showed the interaction of etomidate with the active site of CYP11B1, whereas carboetomidate did not induce any spectral change of CYP11B1, suggesting no interaction with the enzyme.
In summary, this work presents a novel experimental procedure to investigate whether pharmaceutical compounds influence the cortisol production. The methods established in this study could be applied to other steroidogenic CYPs such as CYP17A1 and CYP19A1, as all of them can be recombinantly expressed and purified, and constitute promising targets in anti-cancer treatments. Further, the spectroscopic studies of this work represent an efficient screening system for inhibitors or interacting compounds for CYPs. For example, in cases of congestive heart failure and myocardial fibrosis, it is of interest to develop CYP11B2 inhibitors to reduce the aldosterone level in humans, which do not interact with CYP11B1, and thus influence the cortisol level. In our study, the described experiments could serve to examine the cross reactivity with other steroidogenic CYPs and, thus determine their specificity in a simple and fast manner.

4 OUTLOOK

The findings obtained during this work demonstrate that sulfonated steroids actually do have a regulatory effect on CYP11A1 catalyzed reactions, especially on the interaction with the redox partner Adx. As the experiments were performed *in-vitro* with bovine enzymes expressed in bacteria and purified from there, these results are to be confirmed in an *in-vivo* system using mammalian cells. Therefore, some challenges have to be overcome, as preliminary experiments utilizing SOAT-HEK293 cells showed. So far, it is not possible to detect CYP11A1-dependent cholesterol conversion in this cell line, since no cholesterol is translocated into the mitochondria, where CYP11A1 is located. Nevertheless, this cell line can be used to study the effect of sulfonated steroids on other CYPs involved in steroid hormone biosynthesis, as it was shown in the second publication forming this work.

As the experiments were done using bovine enzymes, it would be of interest to switch to the human system. The bovine steroidogenic CYPs display a high homology with the human ones. Bovine CYP11A1 and CYP17A1 share 85 % and 86 % of their amino acid sequences with their human analogs, respectively. Moreover, the human and bovine steroidogenic CYPs both use the delta-5 pathway for the production of sex hormones, suggesting the bovine system to be a useful model system. Nevertheless, comparison of these systems will elucidate whether the bovine system serves as useful universal model or whether big differences between these species exist concerning the regulation of steroid hormone biosynthesis. Although the steroidogenic CYPs of bovine and human species are similar, differences in the activity and affinity of CYPs to their natural substrates were reported, suggesting differences of the bovine and the human system, when testing the influence of sulfonated steroids. To which extend this might occur has to be elucidated.

In this work, an alternative pathway for sulfonated steroids was postulated involving CYP11A1 and CYP17A1. It starts with the conversion of CS and ends with the formation of 17OH-PregS. As bovine enzymes and proteins were used for these experiments, the question arises, whether human CYPs behave similar or if 17OH-PregS is further metabolized.

Further, investigations on CYP19A1 are of great interest. CYP19A1 forms E1 and E2 in mammals and represents a target for inhibitors used in breast cancer therapy. How DHEAS and E1S influence this enzyme is not known and should be studied *in-vitro,* to reveal the effect on a molecular level as well as in cell culture to postulate a physiological relevance.

It was shown that the effect of DHEAS on CYP11A1, CYP17A1 and CYP21A2 differs. In the presence of DHEAS, CYP11A1 activity is enhanced, whereas CYP17A1- and CYP21A2-activities are not or only slightly inhibited. It would be interesting to analyze, whether sulfonated steroids have a regulatory effect on mitochondrial, but not on microsomal steroidogenic CYPs. For this reason, investigations of the role of DHEAS on mitochondrial CYP11B1 and CYP11B2, as well on microsomal CYP19A1 should be performed.

Furthermore, the effect of sulfonated steroids on human CYP11A1 mutants displaying replacements in putative interaction sites with the redox partner, Adx, should be studied by expressing them in the SOAT-HEK293 cell culture system to analyze the influence which the

sulfonated steroids may have on these interactions and by this way on the modulation of the disease.

In addition, it is conceivable to study, whether a correlation between phosphorylation of Adx and steroid sulfates exists. Adx can be phosphorylated by CK2, which introduces a negatively charged group and leads to an increased activity of CYP11A1 (similar to the effect of the negatively charged DHEAS). It would be interesting to see if steroid sulfates can further augment this activity.

Taken together, further examinations of sulfonated steroids and their impact on steroidogenesis are highly interesting and very promising, as the results obtained so far indicate.

5 ABBREVIATIONS

17OH-Preg(S)	**17OH-Pregnenolone (sulfate)**
17OH-Prog(S)	17OH-Progesterone (sulfate)
18OH-B	18OH-corticosterone
22(R)OH-C	22(R)OH-cholesterol
AdR	Adrenodoxin reductase
Adx	Adrenodoxin
Aldo	Aldosterone
Andro	Androstenedione
B	Corticosterone
b_5	Cytochrome b_5
C	Cholesterol
CAH	Congenital adrenal hyperplasia
CPR	NADPH-dependent oxidoreductase
CS	Cholesterol sulfate
CYP	Cytochrome P450
DHEA	Dehydroepiandrosterone
DHEAS	Dehydroepiandrosterone sulfate
DOC	11-Deoxycorticosterone
E1	Estrone
E1S	Estrone sulfate
E2	Estradiol
ER	Endoplasmatic reticulum
F	Cortisol
FAD	Flavin adenine dinucleotide
FGly(S)	Formylglycine (sulfate)
FMN	Flavin mononucleotide
PAPS	3'-phosphoadenosine-5'-phosphosulfate
Preg	Pregnenolone
PregS	Pregnenolone sulfate
Prog	Progesterone
RNA	ribonucleic acid
RSS	11-deoxycortisol
StS	Sulfatase
SULT	Sulfotransferase
T(S)	Testosterone (sulfate)

6 APPENDIX

CYP17A1-DEPENDENT PRODUCT FORMATION IN THE PRESENCE OF SULFONATED DHEA

CYP17A1 catalyzes the conversion of Preg to 17OH-Preg and DHEA. In our reconstituted *in-vitro* system CYP17A1 did not exhibit its lyase activity, because of the absence of b_5. Here, we investigated the effect of DHEAS on the CYP17A1 catalyzed reaction on a molecular level. We examined the activity of CYP17A1 dependent 17-hydroxylation in the presence of 50 µM DHEAS at a Preg concentration of 10 µM. The evaluation of the HPLC data is shown in Figure A1. The amount of 17OH-Preg formed was 8.1 ± 0.5 µM for the control without DHEAS, and 6.7 ± 0.9 µM for the sample incubated with 5-fold excess of DHEAS. Thus, DHEAS did not influence the activity of CYP17A1 in a significant manner.

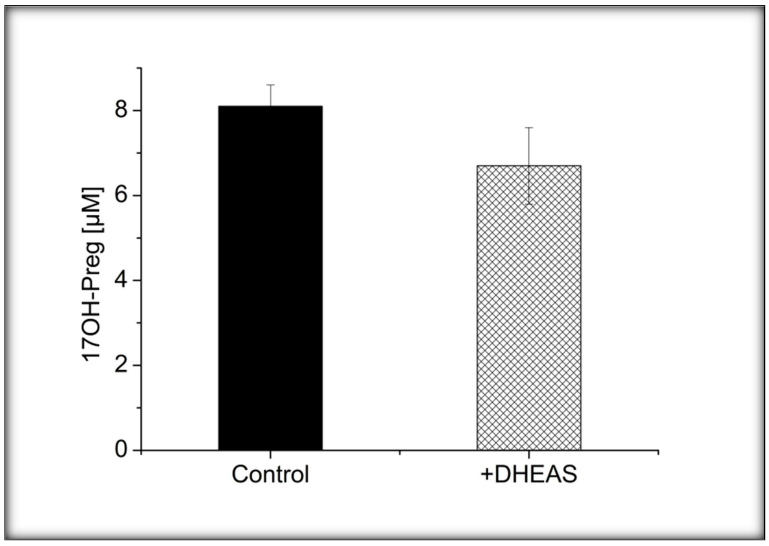

FIGURE A1: COMPARISON OF 17OH-PREG FORMATION BY CYP17A1 IN THE PRESENCE OF 5-FOLD EXCESS OF DHEA OR DHEAS (N=4 FOR EACH GROUP)

CYP21A2-DEPENDENT PRODUCT FORMATION IN THE PRESENCE OF SULFONATED DHEA

CYP21A2 hydroxylates Prog and 17OH-Prog at position C21. The activity of this reaction was explored in the presence of 50 µM DHEAS at a substrate concentration of 10 µM. In Figure A2 the evaluation of the HPLC data is displayed. Using Prog as substrate CYP21A2 formed 4.9 ± 0.7 µM DOC without DHEAS, and 4.8 ± 0.4 µM DOC when DHEAS was added to the system in a 5-fold excess. Utilizing 17OH-Prog CYP21A2 converted this substrate into 3.5 ± 0.1 µM RSS in the absence of DHEAS. When DHEAS was added to the system 3.2 ± 0.2 µM RSS were formed.

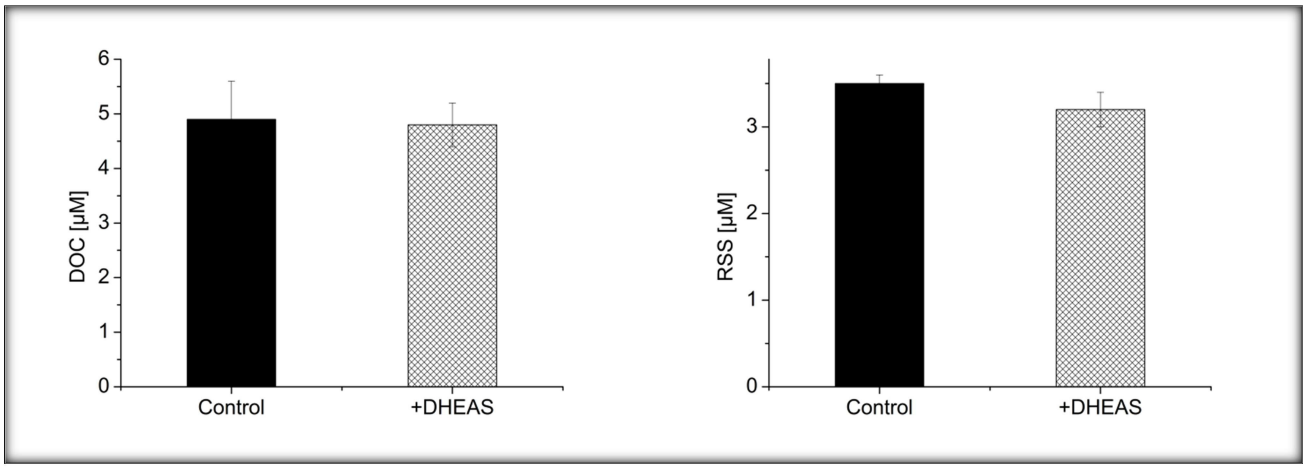

FIGURE A2: COMPARISON OF DOC AND RSS FORMATION BY CYP21A2 IN THE PRESENCE OF 5-FOLD EXCESS OF DHEA OR DHEAS (N=5 FOR EACH GROUP)

CYP11A1-DEPENDENT CONVERSION OF 22(R)OH-C TO PREG IN THE PRESENCE OF DHEAS

In the presence of DHEAS the catalytic efficiency of CYP11A1 is clearly enhanced as shown in the publication 2.1. In order to investigate whether the results obtained from these *in-vitro* studies might possess a potential physiological relevance, cell culture experiments were conducted with SOAT-HEK293 cells recombinantly expressing CYP11A1 and Adx. Because of the insoluble nature of the substrate C, which was not possible convert in this cell culture system, 22(R)OH-C was chosen to be the substrate. The results showed that DHEAS did not influence the activity of CYP11A1 (Figure A3). The amount of Preg formed was 8.1 ± 03 µM for the control without DHEAS and 7.6 ± 0.5 µM for the sample with 75 µM DHEAS.

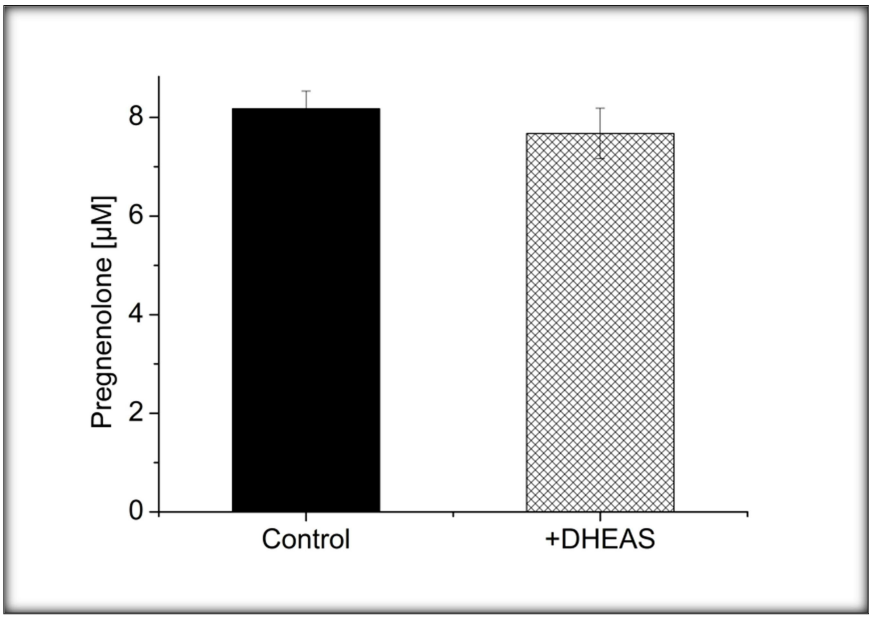

FIGURE A3: CONVERSION OF 15 µM 22(R)OH-C IN SOAT-HEK293 CELLS BY CYP11A1. THE PRODUCT FORMATION ANALYZED BY HPLC IS REPRESENTED AS MEAN ± STANDARD DEVIATION OF FIVE INDIVIDUAL EXPERIMENTS.

The next step was to explore whether the discrepancies between the *in-vitro* (publication 2.1) and the cell culture experiments were due to the different substrates. Therefore, reconstituted *in-vitro* experiments were performed utilizing 22(R)OH-C as substrate. The

evaluation of the HPLC data is displayed in Figure A4. The results showed that without DHEAS, 9.0 ±0.7 µM Preg were produced, which is similar to the product formation in the presence of DHEAS, where 9.0 ± 0.4 µM were obtained.

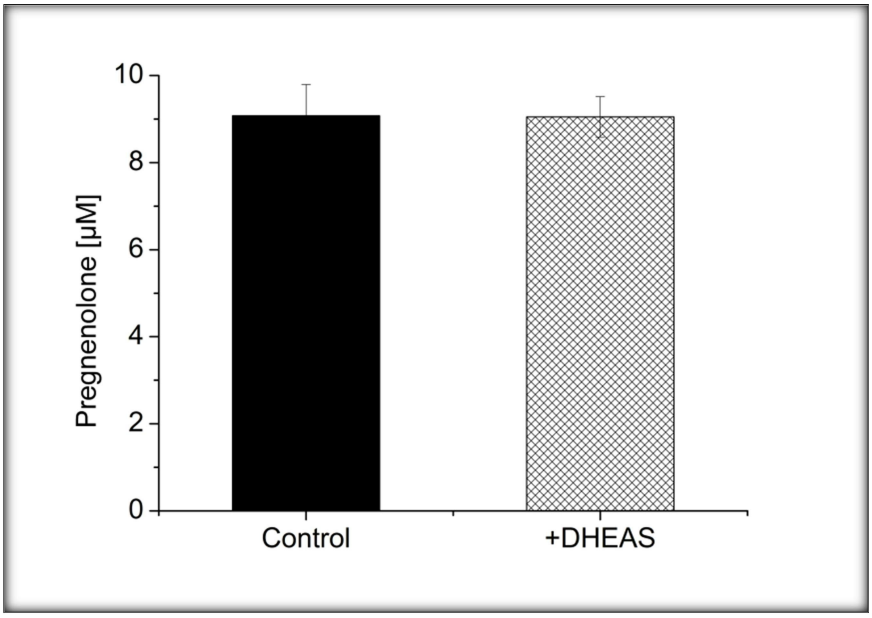

FIGURE A12: CONVERSION OF 15 µM 22(R)OH-C IN A RECONSTITUTED *IN-VITRO* SYSTEM BY CYP11A1. THE PRODUCT FORMATION ANALYZED BY HPLC IS REPRESENTED AS MEAN ± STANDARD DEVIATION OF FIVE INDIVIDUAL EXPERIMENTS.

7 REFERENCES

1. Bernhardt R (2006) Cytochromes P450 as versatile biocatalysts. J Biotechnol 124: 128-145. Epub 2006 Mar 2003.
2. Hannemann F, Bichet A, Ewen KM, Bernhardt R (2007) Cytochrome P450 systems--biological variations of electron transport chains. Biochim Biophys Acta 1770: 330-344. Epub 2006 Aug 2002.
3. Nebert DW, Nelson DR, Feyereisen R (1989) Evolution of the cytochrome P450 genes. Xenobiotica 19: 1149-1160.
4. Garfinkel D (1958) Studies on pig liver microsomes. I. Enzymic and pigment composition of different microsomal fractions. Arch Biochem Biophys 77: 493-509.
5. Klingenberg M (1958) Pigments of rat liver microsomes. Arch Biochem Biophys 75: 376-386.
6. Omura T, Sato R (1964) The Carbon Monoxide-Binding Pigment of Liver Microsomes. I. Evidence for Its Hemoprotein Nature. J Biol Chem 239: 2370-2378.
7. Ichikawa Y, Hiwatashi A, Yamano T (1978) Behaviors on NAD(P)H-reduction and their magnetic absorptions of multiple molecular forms of cytochromes P-450 and P-448. Med J Osaka Univ 28: 205-214.
8. Palmer G, Reedijk J (1991) Nomenclature Committee of the International Union of Biochemistry (NC-IUB). Nomenclature of electron-transfer proteins. Recommendations 1989. Biochim Biophys Acta 1060: 599-611.
9. Gotoh O (1992) Substrate recognition sites in cytochrome P450 family 2 (CYP2) proteins inferred from comparative analyses of amino acid and coding nucleotide sequences. J Biol Chem 267: 83-90.
10. Nguyen PT, Conley AJ, Sneyd J, Lee RS, Soboleva TK, et al. (2013) The role of enzyme compartmentalization on the regulation of steroid synthesis. J Theor Biol 332: 52-64.
11. Weber KT (2001) Aldosterone in congestive heart failure. N Engl J Med 345: 1689-1697.
12. Hanukoglu I, Feuchtwanger R, Hanukoglu A (1990) Mechanism of corticotropin and cAMP induction of mitochondrial cytochrome P450 system enzymes in adrenal cortex cells. J Biol Chem 265: 20602-20608.
13. Nawata H, Yanase T, Goto K, Okabe T, Ashida K (2002) Mechanism of action of anti-aging DHEA-S and the replacement of DHEA-S. Mech Ageing Dev 123: 1101-1106.
14. Lambard S, Carreau S (2005) Aromatase and oestrogens in human male germ cells. Int J Androl 28: 254-259.
15. Veldhuis JD, Keenan DM, Liu PY, Iranmanesh A, Takahashi PY, et al. (2009) The aging male hypothalamic-pituitary-gonadal axis: pulsatility and feedback. Mol Cell Endocrinol 299: 14-22.
16. Pikuleva IA, Waterman MR (2013) Cytochromes p450: roles in diseases. J Biol Chem 288: 17091-17098.
17. DeVore NM, Scott EE (2012) Structures of cytochrome P450 17A1 with prostate cancer drugs abiraterone and TOK-001. Nature 482: 116-119.
18. Ghosh D, Lo J, Morton D, Valette D, Xi J, et al. (2012) Novel aromatase inhibitors by structure-guided design. J Med Chem 55: 8464-8476.
19. Claus R, Hoffmann B (1980) Oestrogens, compared to other steroids of testicular origin, in blood plasma of boars. Acta Endocrinol (Copenh) 94: 404-411.
20. Janowski T, Zdunczyk S, Ras A, Mwaanga ES (1999) [Use of estrone sulfate determination in goat blood for the detection of pregnancy and prediction of fetal number]. Tierarztl Prax Ausg G Grosstiere Nutztiere 27: 107-109.

21. Hoffmann B, Landeck A (1999) Testicular endocrine function, seasonality and semen quality of the stallion. Anim Reprod Sci 57: 89-98.
22. Hahnel R, Twaddle E, Ratajczak T (1973) The specificity of the estrogen receptor of human uterus. J Steroid Biochem 4: 21-31.
23. Kuiper GG, Carlsson B, Grandien K, Enmark E, Haggblad J, et al. (1997) Comparison of the ligand binding specificity and transcript tissue distribution of estrogen receptors alpha and beta. Endocrinology 138: 863-870.
24. Strott CA (1996) Steroid sulfotransferases. Endocr Rev 17: 670-697.
25. Hum DW, Belanger A, Levesque E, Barbier O, Beaulieu M, et al. (1999) Characterization of UDP-glucuronosyltransferases active on steroid hormones. J Steroid Biochem Mol Biol 69: 413-423.
26. Chapman E, Best MD, Hanson SR, Wong CH (2004) Sulfotransferases: structure, mechanism, biological activity, inhibition, and synthetic utility. Angew Chem Int Ed Engl 43: 3526-3548.
27. Harteneck C (2013) Pregnenolone sulfate: from steroid metabolite to TRP channel ligand. Molecules 18: 12012-12028.
28. Reed MJ, Purohit A, Woo LW, Newman SP, Potter BV (2005) Steroid sulfatase: molecular biology, regulation, and inhibition. Endocr Rev 26: 171-202.
29. Schuler G, Greven H, Kowalewski MP, Doring B, Ozalp GR, et al. (2008) Placental steroids in cattle: hormones, placental growth factors or by-products of trophoblast giant cell differentiation? Exp Clin Endocrinol Diabetes 116: 429-436.
30. Geyer J, Doring B, Meerkamp K, Ugele B, Bakhiya N, et al. (2007) Cloning and functional characterization of human sodium-dependent organic anion transporter (SLC10A6). J Biol Chem 282: 19728-19741.
31. Grosser G, Fietz D, Gunther S, Bakhaus K, Schweigmann H, et al. (2013) Cloning and functional characterization of the mouse sodium-dependent organic anion transporter Soat (Slc10a6). J Steroid Biochem Mol Biol 138: 90-99.
32. St-Pierre MV, Hagenbuch B, Ugele B, Meier PJ, Stallmach T (2002) Characterization of an organic anion-transporting polypeptide (OATP-B) in human placenta. J Clin Endocrinol Metab 87: 1856-1863.
33. Kawabe S, Ikuta T, Ohba M, Chida K, Ueda E, et al. (1998) Cholesterol sulfate activates transcription of transglutaminase 1 gene in normal human keratinocytes. J Invest Dermatol 111: 1098-1102.
34. Denning MF, Kazanietz MG, Blumberg PM, Yuspa SH (1995) Cholesterol sulfate activates multiple protein kinase C isoenzymes and induces granular cell differentiation in cultured murine keratinocytes. Cell Growth Differ 6: 1619-1626.
35. Bertoni A, Rastoldo A, Sarasso C, Di Vito C, Sampietro S, et al. (2012) Dehydroepiandrosterone-sulfate inhibits thrombin-induced platelet aggregation. Steroids 77: 260-268.
36. Sicard F, Ehrhart-Bornstein M, Corbeil D, Sperber S, Krug AW, et al. (2007) Age-dependent regulation of chromaffin cell proliferation by growth factors, dehydroepiandrosterone (DHEA), and DHEA sulfate. Proc Natl Acad Sci U S A 104: 2007-2012.
37. Shihan M, Kirch U, Scheiner-Bobis G (2013) Dehydroepiandrosterone sulfate mediates activation of transcription factors CREB and ATF-1 via a Galpha11-coupled receptor in the spermatogenic cell line GC-2. Biochim Biophys Acta 1833: 3064-3075.
38. Strott CA (2002) Sulfonation and molecular action. Endocr Rev 23: 703-732.
39. Zhang H, Varlamova O, Vargas FM, Falany CN, Leyh TS (1998) Sulfuryl transfer: the catalytic mechanism of human estrogen sulfotransferase. J Biol Chem 273: 10888-10892.

40. Falany CN (1997) Enzymology of human cytosolic sulfotransferases. FASEB J 11: 206-216.
41. Forbes-Bamforth KJ, Coughtrie MW (1994) Identification of a new adult human liver sulfotransferase with specificity for endogenous and xenobiotic estrogens. Biochem Biophys Res Commun 198: 707-711.
42. Her C, Szumlanski C, Aksoy IA, Weinshilboum RM (1996) Human jejunal estrogen sulfotransferase and dehydroepiandrosterone sulfotransferase: immunochemical characterization of individual variation. Drug Metab Dispos 24: 1328-1335.
43. Falany JL, Falany CN (1996) Regulation of estrogen sulfotransferase in human endometrial adenocarcinoma cells by progesterone. Endocrinology 137: 1395-1401.
44. Her C, Wood TC, Eichler EE, Mohrenweiser HW, Ramagli LS, et al. (1998) Human hydroxysteroid sulfotransferase SULT2B1: two enzymes encoded by a single chromosome 19 gene. Genomics 53: 284-295.
45. Dooley TP, Haldeman-Cahill R, Joiner J, Wilborn TW (2000) Expression profiling of human sulfotransferase and sulfatase gene superfamilies in epithelial tissues and cultured cells. Biochem Biophys Res Commun 277: 236-245.
46. Kong AN, Yang L, Ma M, Tao D, Bjornsson TD (1992) Molecular cloning of the alcohol/hydroxysteroid form (hSTa) of sulfotransferase from human liver. Biochem Biophys Res Commun 187: 448-454.
47. Otterness DM, Wieben ED, Wood TC, Watson WG, Madden BJ, et al. (1992) Human liver dehydroepiandrosterone sulfotransferase: molecular cloning and expression of cDNA. Mol Pharmacol 41: 865-872.
48. Comer KA, Falany CN (1992) Immunological characterization of dehydroepiandrosterone sulfotransferase from human liver and adrenal. Mol Pharmacol 41: 645-651.
49. Luu-The V, Dufort I, Paquet N, Reimnitz G, Labrie F (1995) Structural characterization and expression of the human dehydroepiandrosterone sulfotransferase gene. DNA Cell Biol 14: 511-518.
50. Schmidt B, Selmer T, Ingendoh A, von Figura K (1995) A novel amino acid modification in sulfatases that is defective in multiple sulfatase deficiency. Cell 82: 271-278.
51. Pechurskaya TA, Lukashevich OP, Gilep AA, Usanov SA (2008) Engineering, expression, and purification of "soluble" human cytochrome P45017alpha and its functional characterization. Biochemistry (Mosc) 73: 806-811.
52. Kagawa N (2011) Efficient expression of human aromatase (CYP19) in E. coli. Methods Mol Biol 705: 109-122.
53. Hobler A, Kagawa N, Hutter MC, Hartmann MF, Wudy SA, et al. (2012) Human aldosterone synthase: recombinant expression in E. coli and purification enables a detailed biochemical analysis of the protein on the molecular level. J Steroid Biochem Mol Biol 132: 57-65.
54. Zollner A, Kagawa N, Waterman MR, Nonaka Y, Takio K, et al. (2008) Purification and functional characterization of human 11beta hydroxylase expressed in Escherichia coli. FEBS J 275: 799-810.
55. Arase M, Waterman MR, Kagawa N (2006) Purification and characterization of bovine steroid 21-hydroxylase (P450c21) efficiently expressed in Escherichia coli. Biochem Biophys Res Commun 344: 400-405.
56. Woods ST, Sadleir J, Downs T, Triantopoulos T, Headlam MJ, et al. (1998) Expression of catalytically active human cytochrome p450scc in Escherichia coli and mutagenesis of isoleucine-462. Arch Biochem Biophys 353: 109-115.
57. Tuckey RC (1990) Side-chain cleavage of cholesterol sulfate by ovarian mitochondria. J Steroid Biochem Mol Biol 37: 121-127.

58. Gilep AA, Sushko TA, Usanov SA (2011) At the crossroads of steroid hormone biosynthesis: the role, substrate specificity and evolutionary development of CYP17. Biochim Biophys Acta 1814: 200-209.
59. Pechurskaya TA, Harnastai IN, Grabovec IP, Gilep AA, Usanov SA (2007) Adrenodoxin supports reactions catalyzed by microsomal steroidogenic cytochrome P450s. Biochem Biophys Res Commun 353: 598-604.
60. Tuckey RC, Kostadinovic Z, Cameron KJ (1994) Cytochrome P-450scc activity and substrate supply in human placental trophoblasts. Mol Cell Endocrinol 105: 103-109.
61. Xu XX, Lambeth JD (1989) Cholesterol sulfate is a naturally occurring inhibitor of steroidogenesis in isolated rat adrenal mitochondria. J Biol Chem 264: 7222-7227.
62. Anthony W. Norman GL (1997) Hormones: Academic Press.
63. Vinson DR, Bradbury DR (2002) Etomidate for procedural sedation in emergency medicine. Ann Emerg Med 39: 592-598.
64. Cotten JF, Forman SA, Laha JK, Cuny GD, Husain SS, et al. (2010) Carboetomidate: a pyrrole analog of etomidate designed not to suppress adrenocortical function. Anesthesiology 112: 637-644.